A dissimilar non-matching HDG discretization for Stokes flows

Jaime Manríquez * Ngoc-Cuong Nguyen † Manuel Solano ‡

January 27, 2022

Abstract

In this work we propose and analyze an HDG method for the Stokes equation whose domain is discretized by two independent polygonal subdomains with different meshsizes. This causes a non-conformity at the intersection of the subdomains or leaves a gap (unmeshed region) between them. In order to appropriately couple these two different discretizations, we propose suitable transmission conditions to preserve the high order convergence of the scheme. Furthermore, stability estimates are established in order to show the well-posedness of the method and the error estimates. In particular, for smooth enough solutions, the L^2 norm of the errors associated to the approximations of the velocity gradient, the velocity and the pressure are of order h^{k+1}, where h is the meshsize and k is the polynomial degree of the local approximation spaces. Moreover, the method presents superconvergence of the velocity trace and the divergence-free postprocessed velocity. Finally, we show numerical experiments that validate our theory and the capacities of the method.

Keywords: non-matching meshes, non-coincident meshes, dissimilar meshes, hybrid method, Stokes flows

1 Introduction.

In many different applications, interfaces divide the domain of interest $\Omega \subset \mathrm{R}^d$ $(d = 2, 3)$ into several subdomains on which the governing equations and/or the boundary conditions are different. For instance, in the case of solid-fluid interactions, the boundary of the solid corresponds to an interface where the equations of motion for the fluid are coupled with the elasticity equations of the former via appropiate transmission conditions, namely the no-slip condition (continuity of the velocities) and the balance of forces (or, more specifically, of the stresses). Nonetheless, as the geometrical complexity and the required spatial sampling of the subdomains increases, e.g. when the region occupied by the fluid requires a finer mesh compared to the meshsize of the discretization of the solid, it is not uncommon to mesh these regions separately, leading to a mismatch between the two discretizations as one can observe in Figure 1. As mentioned in [43], it is possible to identify in the literature two configurations where the domain is discretized by the union of different computational subdomains. In the first one, subdomains are independently meshed, originating a discretization of the domain made of *dissimilar meshes*, where the discrete interfaces of neighboring subdomains need to be properly "tied" (cf. [27]), as is the case in Figure 1 (left), which can lead to gaps and overlaps between the two meshes; in the second configuration, an interface is endowed with two different grids originating from *non-matching* interfaces as happens, for example, in the domain decomposition method like in [46]. An example of this can be seen in Figure 1 (right), where both grids follow a linear interpolation of the physical interface. We note that, while gaps can occur when that interface is not polygonal, overlaps between the domains are ruled out in this case.

In general, methods that deal with smooth boundaries and interfaces can be classified as *fitted* or *unfitted*, where the former adjusts the discretization to the not necessarily polygonal boundaries and interfaces

*Centre for Mathematical Sciences, Lund University, Lund, Sweden.
†Department of Aeronautics and Astronautics, Massachusetts Institute of Technology, Cambridge, Massachusetts, USA.
‡Departamento de Ingeniería Matemática, Facultad de Ciencias Físicas y Matemáticas and Centro de Investigación en Ingeniería Matemática (CI^{2}MA), Universidad de Concepción, Concepción, Chile.

(cf. [3], [4]), as is the case with isoparametric [2] or isogeometric [26] elements, while the latter considers discretizations that are relatively independent of the curved side (we refer the reader to [20, Sect. 1] for a thorough review of unfitted methods). Although fitted methods present easy implementation of previously known methods with high accuracy, the construction of such a mesh might result too difficult for complex geometries; in the case of isoparametric elements, the complexity relies on the computation of non-linear maps which result in the need of higher-order quadratures for the basis functions. Furthermore, the use of curvilinear maps might not eliminate the spatial mismatch of the discretizations unless the parametrization of the interface can be represented exactly by these mappings. On the other hand, unfitted methods present a more simple geometric approach, but at the cost of presenting a higher difficulty to devise high-order methods as the variational crime is much higher in this case. In the context of finite differences, the Immersed Boundary method (IB) has been shown to obtain first order accuracy for the velocity [36] and, in the case of Finite Element methods, Mortar methods have been used to impose the transmission conditions using Lagrange multipliers, but with sub-optimal convergence rates [28, 29]. Higher-order results have been obtained with the Cut Finite Element method (CutFEM) [5, 6], which uses a Nitsche-type approach by adding pressure stabilization and ghost penalty terms, although the results remain quasi-optimal as inf-sup stable spaces must still be chosen in this case. Fitted hybridizable discontinuous Galerkin (HDG) methods were proposed for elliptic interface problems [34] and for Stokes interface problems [47]. It was demonstrated that the interface conditions could be naturally incorporated into the standard HDG method with a judicious choice of the numerical flux, and that such treatment resulted in additional terms in the right-hand side of the global linear system, so the global matrix remains unchanged. With the aim of devising a high-order unfitted method to handle complex geometries, we present a unfitted HDG method for the Stokes problems on dissimilar and non-matching meshes.

In [11], a high order method for problems with curved interfaces is shown to be optimally convergent. It draws upon the ideas of the polynomial extension finite element method (PE-FEM), originally developed for problems with smooth boundaries [12], where instead of adjusting the mesh to the curved domain, a polynomial extrapolation of the approximate solution is used to match the prescribed Neumann or Dirichlet boundary condition. This approach has been successfully applied in the context of HDG methods during the last decade in works such as [20] and [41].

Let us briefly describe the historic perspective of the development of HDG methods. The main criticism of Discontinuous Galerkin (DG) methods is due to the fact that they have too many globally coupled degrees of freedom. In order to overcome this drawback, [16] introduced a unifying framework for hybridization of DG methods for diffusion problems, where the only globally coupled degrees of freedom are those of the numerical traces on the inter-element boundaries. The remaining unknowns are then obtained by solving local problems on each element. To be more precise, at the continuous level, the intra-element variables can be written in terms of the inter-element unknowns by solving local problems on each element. These problems, called local-solvers, can be discretized by a DG method, generating a family of methods named HDG methods. Furthermore, the analysis of general geometries and the estimates for meshes with hanging nodes for these methods is carried out in [9, 10].

We will now discuss the HDG method and its applications related to our context. In addition to diffusion equations, in the context of fluid mechanics, HDG methods have been developed for a wide variety of problems such as Stokes flow equations [15, 17, 19, 21, 37], quasi-Newtonian Stokes flow [31, 32], Stokes–Darcy coupling [33], Brinkman problem [1, 30] and Navier–Stokes equations [8, 38, 40, 42], just to name a few. In particular, we take note of [15], where a class of HDG methods for the Stokes problem considering a vorticity-velocity-pressure formulation was derived. Furthermore, it was shown that the method can be hybridized in four different ways including tangential velocity/pressure and velocity/average pressure hybridizations.

Hybridization for DG methods for Stokes was initially introduced in [7] as a technique that allowed the use of globally divergence-free velocity spaces without having to actually carry out their almost-impossible constructions. The technique was then further developed, with a similar intention, in the framework of mixed methods in [13, 14]. Later on, the analysis of an HDG method based on a velocity gradient-velocity-pressure formulation was analyzed in [17], where an element-by-element postprocess of the velocity was introduced in order to achieve a globally divergence-free condition.

This work is closely related to the technique developed in [18, 20, 23] to handle curved domains, which is based on transferring the boundary condition to the computational boundary using a line integration of the extrapolated approximation of the gradient. This technique has been successfully applied and analyzed in different contexts [22, 24, 41, 44]. Recently, we have developed in [43] an HDG method for dissimilar meshes for the Poisson's equation. In this direction, based on the scheme developed in [43], which extend the transferring technique of [20] from the curved boundary case to the curved interface one, and on the ideas presented in [44], this work proposes an extension to the context of a Stokes interface problem which, to the best of our knowledge, has not been introduced as of yet. To that end, we consider the following governing equations:

$$\mathrm{L} - \nabla \boldsymbol{u} = 0 \qquad \text{on } \Omega, \tag{1a}$$

$$-\nabla \cdot (\nu \mathrm{L} - p\mathrm{I}) = \boldsymbol{f} \qquad \text{on } \Omega, \tag{1b}$$

$$\nabla \cdot \boldsymbol{u} = 0 \qquad \text{on } \Omega, \tag{1c}$$

$$\boldsymbol{u} = \boldsymbol{g} \qquad \text{on } \Gamma, \tag{1d}$$

$$[\![\boldsymbol{u}]\!] = 0 \qquad \text{on } \mathcal{I}, \tag{1e}$$

$$[\![(\nu \mathrm{L} - p\mathrm{I})\boldsymbol{n}]\!] = 0 \qquad \text{on } \mathcal{I}, \tag{1f}$$

$$\int_\Omega p = 0, \tag{1g}$$

where $\Omega \subset \mathrm{R}^d$ will be a polygonal ($d = 2$) or polyhedral ($d = 3$) domain with boundary $\Gamma := \partial\Omega$; $\Omega^1, \Omega^2 \subset \Omega$ are two disjoint open subsets such that $\mathcal{I} := \overline{\Omega^1} \cap \overline{\Omega^2}$ is the interface that separates them, $\nu > 0$ is a constant viscosity, $\boldsymbol{f} \in \boldsymbol{L}^2(\Omega)$ is the volumetric force acting on the fluid, $\boldsymbol{g} \in \boldsymbol{H}^{1/2}(\Omega)$ is the boundary data that satisfies $\int_{\partial\Omega} \boldsymbol{g} \cdot \boldsymbol{n} = 0$ ($\boldsymbol{n}$ being the outward unit normal to Ω), and $[\![\star]\!] := \star \cdot \boldsymbol{n}^+ + \star \cdot \boldsymbol{n}^-$ is the usual jump operator. While the method presented in [44] allows us to deal with curved boundaries and thus removing the restriction for Ω to be polygonal or polyhedral, for the sake of simplicity we choose to avoid this in order to focus on the treatment of the transmission conditions on the interface.

The remainder of this work is organized as follows. In Section 2 we will present some preliminaries and definitions related to the computational domain, the approximation spaces, as well as the necessary notation related to the discretization and transferring segments. The HDG scheme along with a postprocess for the recovery of the pressure and the construction of a divergence-free approximation of the velocity will be introduced in Section 3. The analysis of the proposed HDG method will be presented in Section 4, where the main results will be stated in Section 4.5, whereas the proofs will be detailed in Section 4.4. Then, in Section 5 we will show numerical results to validate our theoretical estimates. Finally, will provide conclusions and further discussions in Section 6.

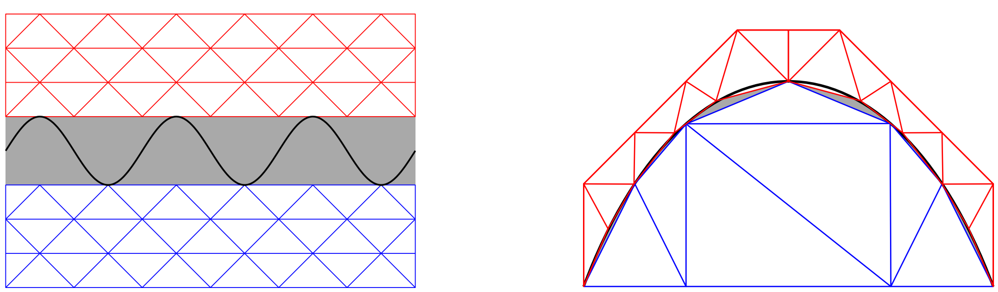

Figure 1: Example of dissimilar meshes (left) and non-matching meshes (right). In the first case, two independent meshes that approach the interface must be properly "tied", while in the latter the boundaries of each discretization respect the interface, leading to gaps in the non-polygonal case.

2 Preliminaries.

This section introduces notation related to the geometric discretization and the HDG scheme. For the former we will explain the terminology associated to the computational domain and to the family of segments that "tie" the dissimilar interfaces, whereas for the latter we will introduce the approximation spaces and the HDG projection. Although most of the notation have been introduced in several works, we include it here in order to make it self-contained.

2.1 Computational domain

Let $\Omega \subset \mathrm{R}^d$ be a domain with polyhedral boundary Γ. The domain is divided into two disjoint open subdomains Ω^1 and Ω^2, with the interface between the two denoted as $\mathcal{I} := \overline{\Omega^1} \cap \overline{\Omega^2}$. We now consider two polyhedral discretizations, $\Omega^1_{h_1}$ and $\Omega^2_{h_2}$, with mesh sizes $h_1, h_2 > 0$ and boundaries $\Gamma^1_{h_1}, \Gamma^2_{h_2}$, respectively. Without loss of generality we suppose $h_2 > h_1$ and drop the sub-index i when there is no confusion, for example, denoting the triangulations as Ω^1_h and Ω^2_h henceforth. We also denote the sets of all faces of each discretization as $\mathcal{E}^1_h$ and $\mathcal{E}^2_h$, respectively. Furthermore, since $\overline{\Omega^1_h} \cap \overline{\Omega^2_h}$ does not necessarily equal to $\mathcal{I}$, for $i \in \{1, 2\}$, we consider the discrete interfaces $\mathcal{I}^i_h := \Gamma^i_h \setminus \Gamma$.

For $i \in \{1, 2\}$, we assume that there exists a constant $\kappa_i > 0$ such that for all elements $K \in \Omega^i_h$ and all $h > 0$, $h_K/\rho_K \leq \kappa_i$, where h_K is the diameter of K and ρ_K is the diameter of the largest ball contained in K. For every element K, we will denote by $\boldsymbol{n}_K$ the outward unit normal vector to K, writing $\boldsymbol{n}$ instead of $\boldsymbol{n}_K$ when there is no confusion.

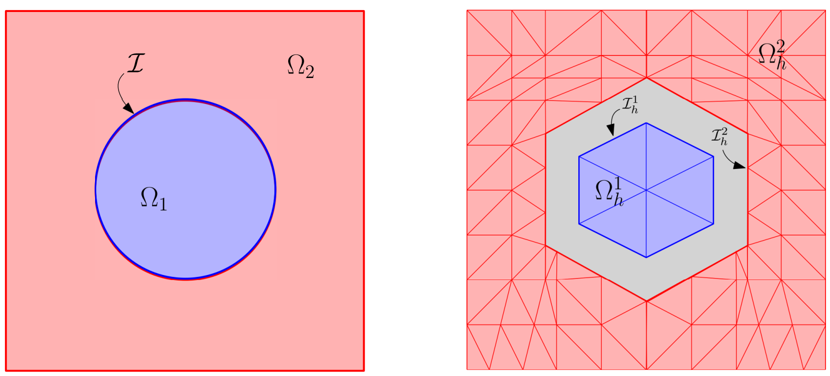

Figure 2: The physical domains (left) and the corresponding discretizations (right).

2.2 Connecting segments

We introduce a mapping $\boldsymbol{\varphi} : \mathcal{I}^2_h \to \mathcal{I}^1_h$ such that for each point $\boldsymbol{x}^2 \in \mathcal{I}^2_h$, we associate a point $\boldsymbol{x}^1 = \boldsymbol{\varphi}(\boldsymbol{x}^2) \in \mathcal{I}^2_h$ and denote by $\ell(\boldsymbol{x}^2)$ the segment joining these two points, with unit tangent vector $\boldsymbol{m}$ and length $\left|\ell(\boldsymbol{x}^2)\right|$. The segment $\ell(\boldsymbol{x}^2)$ is referred as the *connecting segment* associated to $\boldsymbol{x}^2$ and is assumed to satisfy two conditions: it does not intersect the interior of another segment and its length $\left|\ell(\boldsymbol{x}^2)\right|$ is of order at most $\max\{h_1, h_2\} = h_2$.

For every vertex $\boldsymbol{v}^2 \in \mathcal{I}^2_h$, we assume that its corresponding point $\boldsymbol{v}^1$ is also a vertex of $\mathcal{I}^1_h$. This induces a partition $\mathcal{F}^2_h = \{F\}$ of $\mathcal{I}^2_h$, where each face F is the opposite to some face $e \in \mathcal{I}^1_h$ given by $\boldsymbol{\varphi}(F) = e$. An example of such a partition can be seen in Figure 3, where each face on the bottom mesh is divided into two faces corresponding to the opposing side of some face in the upper mesh. This partition is induced by the connecting segments between the vertices (solid black arrows) and an example of the mapping $\boldsymbol{\varphi}$ for an arbitrary point $\boldsymbol{x}^2$ on the bottom interface (dashed arrow).

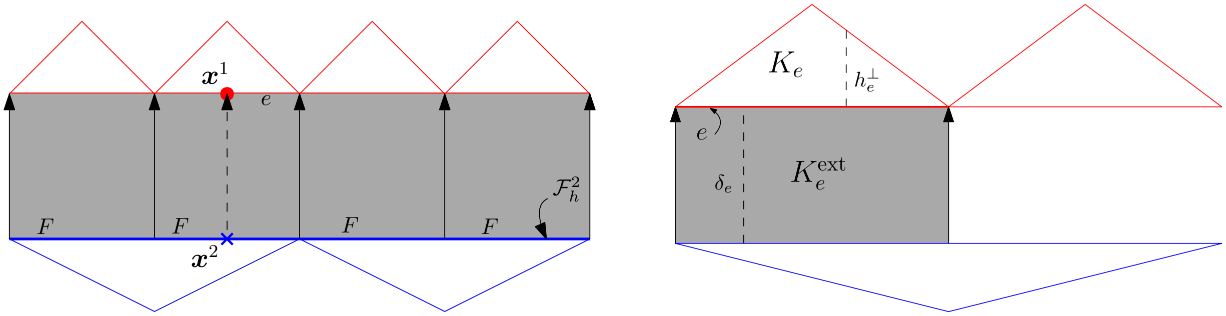

Figure 3: Partition $\mathcal{F}_h^2$ of $\mathcal{I}_h^2$ induced by $\mathcal{I}_h^1$ via $\boldsymbol{\varphi}$ (left). Extrapolation region and gap for the leftmost element of the upper mesh (right).

Let $i \in \{1,2\}$. Given a face $e \in \mathcal{I}_h^i$ belonging to the element $K_e \in \Omega_h^i$, we define the *extrapolation patch* as

$$K_e^{\text{ext}} := \{\boldsymbol{x} + \boldsymbol{n}^i t : 0 \leq t \leq |\ell(\boldsymbol{x})|\,,\ \boldsymbol{x} \in e\}.$$

We denote by $h_e^\perp$ (resp. δ_e) the largest distance of a point inside K_e^1 (resp. K_e^{ext}) to the plane determined by the face e. In other words,

$$h_e^\perp = \max_{\boldsymbol{x} \in K_e} |\text{dist}(\boldsymbol{x}, e)|\,, \qquad \delta_e := \max_{\boldsymbol{x} \in e} |\ell(\boldsymbol{x})|\,,$$

where $\text{dist}(\boldsymbol{x}, e)$ denotes the distance from $\boldsymbol{x}$ to the face e. We note that δ_e is a measure to the local size of the gap and $\delta := \max_e \delta_e$ is an upper bound of the gap. We define the ratio $r_e := \delta_e / h_e^\perp$ and its maximum $R_i := \max\limits_{e \in \mathcal{I}_h^i} r_e$. An illustration of this notation can be seen in Figure 3 for the leftmost element of the upper mesh.

2.2.1 Spaces and norms

We follow the usual notation and denote the space of polynomials of degree at most k on K as $\mathbb{P}_k(K)$. Similarly, for any face e, $\mathbb{P}_k(e)$ denotes the space of polynomials of degree at most k on e. Given a region $D \subset \mathrm{R}^d$, we denote by $(\cdot,\cdot)_D$ and $\langle \cdot,\cdot \rangle_{\partial D}$ the $L^2(D)$ and $L^2(\partial D)$ inner products, respectively, with induced norms $\|\cdot\|_D$ and $\|\cdot\|_{\partial D}$. We use the standard notation for Sobolev spaces and their associated norms and seminorms, where vector-valued functions and their corresponding spaces are denoted in bold face, and blackboard bold for the tensor-valued case.

For a given polynomial of degree k and $i \in \{1,2\}$, we introduce the finite dimensional spaces

$$\begin{aligned}
\mathbb{V}_h^i &:= \{\mathrm{G} \in \mathrm{L}^2(\Omega_h^i) : \quad \mathrm{G}\big|_K \in [\mathbb{P}_k(K)]^{d \times d}, \quad \forall K \in \Omega_h^i\},\\
\boldsymbol{V}_h^i &:= \{\boldsymbol{v} \in \boldsymbol{L}^2(\Omega_h^i) : \quad \boldsymbol{v}\big|_K \in [\mathbb{P}_k(K)]^d, \quad \forall K \in \Omega_h^i\},\\
V_h^i &:= \{q \in L^2(\Omega_h^i) : \quad q\big|_K \in \mathbb{P}_k(K), \quad \forall K \in \Omega_h^i\},\\
\boldsymbol{M}_h^i &:= \{\boldsymbol{\mu} \in \boldsymbol{L}^2(\mathcal{E}_h^i) : \quad \boldsymbol{\mu}\big|_e \in [\mathbb{P}_k(e)]^d, \quad \forall e \in \mathcal{E}_h^i\},\\
\boldsymbol{M}_h(\mathcal{I}_h^i) &:= \{\boldsymbol{\mu} \in \boldsymbol{L}^2(\mathcal{I}_h^i) : \quad \boldsymbol{\mu}\big|_e \in [\mathbb{P}_k(e)]^d, \quad \forall e \in \mathcal{I}_h^i\}.
\end{aligned}$$

The inner products for the triangulation Ω_h^i, $(i = 1,2)$ are given by

$$(\cdot,\cdot)_{\Omega_h^i} := \sum_{K \in \Omega_h^i} (\cdot,\cdot)_K, \qquad \langle \cdot,\cdot \rangle_{\partial\Omega_h^i} := \sum_{K \in \Omega_h^i} \langle \cdot,\cdot \rangle_{\partial K}, \quad \text{and} \quad \langle \cdot,\cdot \rangle_{\mathcal{I}_h^i} := \sum_{e \in \mathcal{I}_h^i} \langle \cdot,\cdot \rangle_e,$$

and their corresponding norms will be denoted, respectively, by

$$\|\cdot\|_{\Omega_h^i} := \left(\sum_{K \in \Omega_h^i} \|\cdot\|_K^2\right)^{1/2}, \ \|\cdot\|_{\partial\Omega_h^i} := \left(\sum_{K \in \Omega_h^i} \|\cdot\|_{\partial K}^2\right)^{1/2}, \text{ and } \|\cdot\|_{\mathcal{I}_h^i} := \left(\sum_{e \in \mathcal{I}_h^i} \|\cdot\|_e^2\right)^{1/2}.$$

To avoid proliferation of unimportant constants, we will use the terminology $a \lesssim b$ whenever $a \le Cb$ and C is a positive constant independent of h.

2.3 Extrapolation operator

The region enclosed by Ω_h^1 and Ω_h^2 will be denoted by Ω_h^{ext}. We notice that Ω_h^{ext} is not meshed. As a consequence, we don't have an HDG approximation in there. That is why the HDG approximation of the velocity gradient L and the pressure field $\tilde{p}$ will be locally extrapolated from the computational domain $\Omega_h^1 \cup \Omega_h^2$ to Ω_h^{ext}. More precisely, let $\mathrm{G}|_K : [\mathbb{P}_k(K)]^{d\times d} \to \mathrm{R}$ be a tensor-valued polynomial function which is defined on an element K in $\Omega_h^1 \cup \Omega_h^2$ such that $\overline{K} \cap \overline{\Omega_h^{\text{ext}}} \neq \emptyset$. We will define its extension to Ω_h^{ext} as

$$\boldsymbol{E}_{\mathrm{G}|_K}(\boldsymbol{y}) := \mathrm{G}|_K(\boldsymbol{y}) \qquad \forall \boldsymbol{y} \in \Omega_h^{\text{ext}}. \tag{2}$$

Note that the extended function $\boldsymbol{E}_{\boldsymbol{p}|_K}$ is a tensor-valued function whose support includes Ω_h^{ext}. Each element K will have its own extended function.

2.3.1 The HDG projection

In the analysis, we will employ the HDG projection defined in [17]. Let $i \in \{1,2\}$ and $(\mathrm{L}, \boldsymbol{u}, \tilde{p}) \in \mathbb{H}^1(\Omega_h^i) \times \boldsymbol{H}^1(\Omega_h^i) \times H^1(\Omega_h^i)$, we take its projection $\Pi_h^i(\mathrm{L}, \boldsymbol{u}, \tilde{p}) := (\Pi_{\mathbb{V}^i}\mathrm{L}, \Pi_{\boldsymbol{V}^i}\boldsymbol{u}, \Pi_{V^i}\tilde{p})$ as the element of $\mathbb{V}_h^i \times \boldsymbol{V}_h^i \times V_h^i$ defines as follows. On an arbitrary element K of Ω_h^i, the values of the projected function on K are determined by requiring that

$$\begin{aligned}
(\Pi_{\mathbb{V}^i}\mathrm{L}, \mathrm{G})_K &= (\mathrm{L}, \mathrm{G})_K && \forall \mathrm{G} \in [\mathbb{P}_{k-1}(K)]^{d\times d} && \text{(3a)}\\
(\Pi_{\boldsymbol{V}^i}\boldsymbol{u}, \boldsymbol{v})_K &= (\boldsymbol{u}, \boldsymbol{v})_K && \forall \boldsymbol{v} \in [\mathbb{P}_{k-1}(K)]^{d} && \text{(3b)}\\
(\Pi_{V^i}\tilde{p}, q)_K &= (\tilde{p}, q)_K && \forall q \in \mathbb{P}_{k-1}(K) && \text{(3c)}\\
(\operatorname{tr}\Pi_{\mathbb{V}^i}\mathrm{L}, q)_K &= (\operatorname{tr}\mathrm{L}, q)_K && \forall \mathrm{G} \in \mathbb{P}_{k}(K) && \text{(3d)}\\
\langle \nu\Pi_{\mathbb{V}^i}\mathrm{L}\boldsymbol{n} - \Pi_{V^i}\tilde{p}\boldsymbol{n} - \tau\nu\Pi_{\boldsymbol{V}^i}\boldsymbol{u}, \boldsymbol{\mu}\rangle_e &= \langle \nu\mathrm{L}\boldsymbol{n} - \tilde{p}\boldsymbol{n} - \tau\nu\boldsymbol{u}, \boldsymbol{\mu}\rangle_e && \forall \boldsymbol{\mu} \in [\mathbb{P}_{k}(e)]^{d} && \text{(3e)}
\end{aligned}$$

for all faces e of the simplex K, where $\tau > 0$ is the stabilization parameter of the HDG method. Furthermore, if $(\mathrm{L}, \boldsymbol{u}, \tilde{p}) \in \mathbb{H}^{l_\sigma+1}(\Omega_h^i) \times \boldsymbol{H}^{l_{\boldsymbol{u}}+1}(\Omega_h^i) \times H^{l_\sigma+1}(\Omega_h^i)$, for $l_\sigma, l_{\boldsymbol{u}} \in [0,k]$, we have that the above defined projection satisfies (cf. [17, Theorem 2.1]) the following properties:

$$\|\boldsymbol{u} - \Pi_{\boldsymbol{V}^i}\boldsymbol{u}\|_K \lesssim h_K^{l_{\boldsymbol{u}}+1} |\boldsymbol{u}|_{\boldsymbol{H}^{k+1}(K)} + h_K^{l_\sigma+1}(\tau\nu)^{-1} |\nabla\cdot(\nu\mathrm{L} - \tilde{p}\mathbb{I})|_{\mathbb{H}^k(K)}, \tag{4a}$$

$$\begin{aligned}
\|\nu(\mathrm{L} - \Pi_{\mathbb{V}^i}\mathrm{L})\|_K + \|\tilde{p} - \Pi_{V^i}\tilde{p}\|_K \lesssim{}& h_K^{l_\sigma+1} |\nu\mathrm{L} - \tilde{p}\mathbb{I}|_{\mathbb{H}^{k+1}(K)} + h_K^{l_{\boldsymbol{u}}+1}\tau\nu |\boldsymbol{u}|_{\boldsymbol{H}^{k+1}(K)}\\
&+ \tau\nu \|\boldsymbol{u} - \Pi_{\boldsymbol{V}^i}\boldsymbol{u}\|_K,
\end{aligned} \tag{4b}$$

where $\mathbb{I}$ is the identity tensor.

3 The numerical method.

3.1 The treatment of the pressure.

Since the computational domain $\Omega_h^1 \cup \Omega_h^2$ does not necessarily coincide with the physical domain Ω, we introduce the following decomposition to impose the zero-mean of the pressure

$$p = \overline{p}^{\Omega_h} + \tilde{p},$$

where $\overline{p}^{\Omega_h} := \dfrac{1}{|\Omega_h^1 \cup \Omega_h^2|}\displaystyle\int_{\Omega_h^1 \cup \Omega_h^2} p$ is the mean of p on the computational domain and $\widetilde{p}$ is a function that belongs to $L_0^2(\Omega_h^1 \cup \Omega_h^2) := \{q \in L^2(\Omega_h^1 \cup \Omega_h^2) : (q,1)_{\Omega_h^1 \cup \Omega_h^2} = 0\}$; we write $\tilde{p}^i := \tilde{p}|_{\Omega_h^i}$.

3.2 The HDG scheme

For $i \in \{1,2\}$, we look for the approximation $(\mathrm{L}_h^i, \boldsymbol{u}_h^i, \tilde{p}_h^i, \widehat{\boldsymbol{u}}_h^i) \in \mathbb{V}_h^i \times \boldsymbol{V}_h^i \times V_h^i \times \boldsymbol{M}_h^i$ of $(\mathrm{L}|_{\Omega_h^i}, \boldsymbol{u}|_{\Omega_h^i}, \tilde{p}_{\Omega_h^i}, \boldsymbol{u}|_{\mathcal{E}_h^i})$ that satisfies

$$(\mathrm{L}_h^i, \mathrm{G})_{\Omega_h^i} + (\boldsymbol{u}_h^i, \nabla \cdot \mathrm{G})_{\Omega_h^i} - \langle \widehat{\boldsymbol{u}}_h^i, \mathrm{G}\boldsymbol{n}\rangle_{\partial\Omega_h^i} = 0, \tag{5a}$$

$$(\nu \mathrm{L}_h^i, \nabla \boldsymbol{v})_{\Omega_h^i} - (\tilde{p}_h^i, \nabla \cdot \boldsymbol{v})_{\Omega_h^i} - \langle \widehat{\sigma}_h^i \boldsymbol{n}^i, \boldsymbol{v}\rangle_{\partial\Omega_h^i} = (\boldsymbol{f}, \boldsymbol{v})_{\Omega_h^i}, \tag{5b}$$

$$-(\boldsymbol{u}_h^i, \nabla q)_{\Omega_h^i} + \langle \widehat{\boldsymbol{u}}_h^i \cdot \boldsymbol{n}, q\rangle_{\partial\Omega_h^i} = 0, \tag{5c}$$

$$\langle \widehat{\boldsymbol{u}}_h^i, \boldsymbol{\mu}\rangle_{\Gamma_h^i \backslash \mathcal{I}_h^i} = \langle \boldsymbol{g}, \boldsymbol{\mu}\rangle_{\Gamma_h^i \backslash \mathcal{I}_h^i}, \tag{5d}$$

$$\langle \widehat{\sigma}_h^i \boldsymbol{n}^i, \boldsymbol{\mu}\rangle_{\partial\Omega_h^i \backslash \Gamma_h^i} = 0, \tag{5e}$$

for all $(\mathrm{G}, \boldsymbol{v}, q, \boldsymbol{\mu}) \in \mathbb{V}_h^i \times \boldsymbol{V}_h^i \times V_h^i \times \boldsymbol{M}_h^i$, where

$$\widehat{\sigma}_h^i \boldsymbol{n}^i := \nu \mathrm{L}_h^i \boldsymbol{n}^i - \tilde{p}_h^i \boldsymbol{n}^i - \tau\nu(\boldsymbol{u}_h^i - \widehat{\boldsymbol{u}}_h^i) \qquad \text{on } \partial\Omega_h^i. \tag{5f}$$

and τ is a positive stabilization function defined in $\partial\Omega_h^1 \cup \partial\Omega_h^2$, assumed to be uniformly bounded. The previous system is coupled via a global *uniqueness condition* of the pressure across both subdomains

$$(\tilde{p}_h^1, 1)_{\Omega_h^1} + (\tilde{p}_h^2, 1)_{\Omega_h^2} = 0, \tag{5g}$$

and the imposition of suitable *transmission conditions*,

$$\langle \widehat{\boldsymbol{u}}_h^1 - \tilde{\boldsymbol{u}}_h^2, \boldsymbol{\mu}\rangle_{\mathcal{I}_h^1} = 0, \qquad \forall \boldsymbol{\mu} \in \boldsymbol{M}_h(\mathcal{I}_h^1), \tag{5h}$$

$$\langle \widehat{\sigma}_h^2 \boldsymbol{n}^2 + \tilde{\boldsymbol{\sigma}}_h^1, \boldsymbol{\mu}\rangle_{\mathcal{I}_h^2} = 0, \qquad \forall \boldsymbol{\mu} \in \boldsymbol{M}_h(\mathcal{I}_h^2), \tag{5i}$$

where $\tilde{\boldsymbol{u}}_h^2$ and $\tilde{\boldsymbol{\sigma}}_h^1$ are approximations of $\boldsymbol{u}|_{\mathcal{I}_h^1}$ and $-(\nu\mathrm{L} - p\mathbb{I})\boldsymbol{n}^2|_{\mathcal{I}_h^2}$ on the opposite interface, respectively, defined as

$$\tilde{u}_h^2(\boldsymbol{x}^1) = \widehat{\boldsymbol{u}}_h^2(\boldsymbol{x}^2) + \left|\ell(\boldsymbol{x}^2)\right| \int_0^1 \boldsymbol{E}_{\mathrm{L}_h^2}(\boldsymbol{x}(s))\boldsymbol{m}(\boldsymbol{x}(s))\mathrm{d}s \tag{5j}$$

and

$$\tilde{\boldsymbol{\sigma}}_h^1(\boldsymbol{x}^2) = -\nu \boldsymbol{E}_{\mathrm{L}_h^1}(\boldsymbol{x}^2)\boldsymbol{n}^2 + \boldsymbol{E}_{\tilde{p}_h^1}(\boldsymbol{x}^2)\boldsymbol{n}^2 - \tau\nu(\boldsymbol{u}_h^1(\boldsymbol{x}^1) - \widehat{\boldsymbol{u}}_h^1(\boldsymbol{x}^1)), \tag{5k}$$

where $\boldsymbol{x}^1 \in \mathcal{I}_h^1$ is the corresponding point to $\boldsymbol{x}^2 \in \mathcal{I}_h^2$ under the mapping $\boldsymbol{\varphi}$ and $\boldsymbol{x}(s) := \boldsymbol{x}^1 + (\boldsymbol{x}^1 - \boldsymbol{x}^2)s$ for $s \in [0,1]$. Here $\boldsymbol{E}$ denotes the local extrapolation defined in subsection 2.3.

Remark 1. *Instead of the transmission conditions* (5h) *and* (5i)*, it is also possible to alternatively choose*

$$\langle \widehat{\boldsymbol{u}}_h^2 - \tilde{\boldsymbol{u}}_h^1, \boldsymbol{\mu}\rangle_{\mathcal{I}_h^2} = 0, \qquad \forall \boldsymbol{\mu} \in \boldsymbol{M}_h(\mathcal{I}_h^2), \tag{6a}$$

$$\langle \widehat{\sigma}_h^1 \boldsymbol{n}^1 + \tilde{\boldsymbol{\sigma}}_h^2, \boldsymbol{\mu}\rangle_{\mathcal{I}_h^1} = 0, \qquad \forall \boldsymbol{\mu} \in \boldsymbol{M}_h(\mathcal{I}_h^1) \tag{6b}$$

where, for $\boldsymbol{x}^1 \in \mathcal{I}_h^1$, its corresponding point $\boldsymbol{x}^2 \in \mathcal{I}_h^2$ and $\widetilde{\boldsymbol{x}}(s) = \boldsymbol{x}^2 + (\boldsymbol{x}^1 - \boldsymbol{x}^2)s$, for $s \in [0,1]$, we define

$$\tilde{u}_h^1(\boldsymbol{x}^2) = \widehat{\boldsymbol{u}}_h^1(\boldsymbol{x}^1) + \left|\ell(\boldsymbol{x}^2)\right| \int_0^1 \boldsymbol{E}_{\mathrm{L}_h^1}(\widetilde{\boldsymbol{x}}(s))\boldsymbol{m}(\widetilde{\boldsymbol{x}}(s))\mathrm{d}s \tag{6c}$$

and

$$\tilde{\boldsymbol{\sigma}}_h^1(\boldsymbol{x}^1) = -\nu \boldsymbol{E}_{\mathrm{L}_h^2}(\boldsymbol{x}^1)\boldsymbol{n}^1 + \boldsymbol{E}_{\tilde{p}_h^2}(\boldsymbol{x}^1)\boldsymbol{n}^1 - \tau\nu(\boldsymbol{u}_h^2(\boldsymbol{x}^2) - \widehat{\boldsymbol{u}}_h^2(\boldsymbol{x}^2)). \tag{6d}$$

4 Analysis of the method

This section is devoted to the analysis of the method. We first introduce auxiliary results and assumptions necessary for the proof of our main results. We then state the main results and present their proof.

4.1 Auxiliary results

For $e \in \mathcal{I}_h^1 \cup \mathcal{I}_h^2$, we define $\mathbb{V}^k := \left\{ \mathrm{G} \in [\mathbb{P}_k(K_e^{\mathrm{ext}})]^{d\times d} : \mathrm{G}\boldsymbol{n}_e \neq 0 \text{ on each } e \subset \partial K_e^{\mathrm{ext}} \right\}$, where $\boldsymbol{n}_e$ is the interior normal vector to K_e^{ext} along the face e, i.e. the exterior normal vector to K_e pointing in the direction of K_e^{ext}. We can then introduce the constants

$$C_e^{\mathrm{ext}} := \frac{1}{\sqrt{r_e}} \sup_{\mathrm{G}\in\mathbb{V}^k} \frac{\|\mathrm{G}\boldsymbol{n}_e\|_{K_e^{\mathrm{ext}}}}{\|\mathrm{G}\boldsymbol{n}_e\|_{K_e}}, \qquad C_e^{\mathrm{inv}} := h_e^{\perp} \sup_{\mathrm{G}\in\mathbb{V}^k} \frac{\|\partial_{\boldsymbol{n}_e}\mathrm{G}\|_{K_e}}{\|\mathrm{G}\boldsymbol{n}_e\|_{K_e}} \tag{7}$$

Adapting the result in Lemma A.2 of [20] to the tensor-valued case, we have that these constants are independent of the meshsize, but depend on the polynomial degree k.

On the other hand, following the ideas in [20] adapted to our case, it will be useful to introduce the following auxiliary functions. Let $e \in \mathcal{I}_h^2$ that belongs to K_e and K_e^{ext}. For a polynomial function G on K_e, we define

$$\Lambda^i_{\mathrm{G}|_{K_e}}(\boldsymbol{x}^2) := \frac{1}{|\ell(\boldsymbol{x}^2)|}\int_0^{|\ell(\boldsymbol{x}^2)|} \left(\boldsymbol{E}_{\mathrm{G}|_{K_e}}(\boldsymbol{x}^2 + \boldsymbol{n}^2 s) - \boldsymbol{E}_{\mathrm{G}|_{K_e}}(\boldsymbol{x}^i) \right) \boldsymbol{n}^2 \mathrm{d}s, \tag{8}$$

for $i \in \{1, 2\}$, where we recall that $\boldsymbol{x}^2 \in e$ and $\boldsymbol{x}^1 \in \mathcal{I}_h^1$ are connected by the segment $\ell(\boldsymbol{x}^2)$. Adapting Lemma 5.2 in [20], we have that

$$\left\| |\ell|^{1/2}\, \Lambda^i_{\mathrm{G}|_{K_e}} \right\|_e \leq \frac{1}{\sqrt{3}} r_e^{3/2} C_e^{\mathrm{ext}} C_e^{\mathrm{inv}} \|\mathrm{G}\|_{K_e} \qquad \forall \mathrm{G} \in \mathbb{V}(K_e) \tag{9a}$$

$$\left\| |\ell|^{1/2}\, \Lambda^i_{\mathrm{G}|_{K_e}} \right\|_e \leq \frac{1}{\sqrt{3}} r_e \left\| h_e^{\perp} \partial_{\boldsymbol{n}} \mathrm{G}\boldsymbol{n} \right\|_{K_e^{\mathrm{ext}}} \qquad \forall \mathrm{G} \in \mathrm{H}^1(K_e^{\mathrm{ext}}) \tag{9b}$$

The following lemma, adapted from [43] to the tensor-valued case, will be useful in the error analysis of the method and, specifically, in the development of a duality argument later on.

Lemma 2. *Suppose that $\boldsymbol{\varphi} : \mathcal{I}_h^2 \to \mathcal{I}_h^1$ is a bijection. The following assertions hold true: If $\boldsymbol{\phi} \in \boldsymbol{H}^2(\Omega)$ and $\boldsymbol{\Phi} := \nabla\boldsymbol{\phi}$, then*

$$\left\| |\ell|^{-1/2} (\boldsymbol{\phi} - \boldsymbol{\phi}\circ\boldsymbol{\varphi}) - |\ell|^{1/2} (\boldsymbol{\Phi}\circ\boldsymbol{\varphi})\boldsymbol{n}^2 \right\|_{\mathcal{I}_h^2} \lesssim \delta \|\boldsymbol{\phi}\|_{\boldsymbol{H}^2(\Omega)} \tag{10a}$$

$$\left\| |\ell|^{-1/2} (\boldsymbol{\phi} - \boldsymbol{\phi}\circ\boldsymbol{\varphi}) \right\|_{\mathcal{I}_h^2} \lesssim \delta^{1/2} \|\boldsymbol{\phi}\|_{\boldsymbol{H}^2(\Omega)} \tag{10b}$$

If $\boldsymbol{\Phi} \in \mathrm{H}^1(\Omega)$, then

$$\left\| |\ell|^{-1/2} (\boldsymbol{\Phi} - \boldsymbol{\Phi} \circ\boldsymbol{\varphi})\boldsymbol{n}^2 \right\|_{\mathcal{I}_h^2} \lesssim \|\boldsymbol{\Phi}\|_{\mathrm{H}^1(\Omega)} \tag{10c}$$

Let $F \in \mathcal{F}_h$, $e = \boldsymbol{\varphi}(F)$ and K_e the element e belongs to. If $p \in \mathbb{P}_k(K_e)$, then

$$\|p - p\circ\boldsymbol{\varphi}\|_F \lesssim C_e^{\mathrm{ext}} \delta_e h_e^{-3/2} \|p\|_{K_e} \tag{10d}$$

Finally, we recall the discrete trace inequality ([39, Lemma 1.21]): if ϕ is a scalar, vector or tensor-valued polynomial in K_e, then

$$\|\phi\|_e \leq C_e^{\mathrm{tr}} h_e^{-1/2} \|\phi\|_{K_e}, \tag{11}$$

where C_e^{tr} is independent of the meshsize but depends on the polynomial degree.

4.2 Assumptions.

In this section we state the assumptions under which the stability and error analysis hold. Some of them are technical assumptions that allow us to simplify the analysis and present the proofs in a more readable manner, whereas the others establishes the relation between the gap- and mesh- sizes that are required in order to ensure the convergence and optimality of the method.

First of all, we consider the following conditions related to the connection between both computational interfaces:

(A.1) $\Omega_h^1 \cap \Omega_h^2 = \emptyset$, i.e. there is no overlap between the subdomains,

(A.2) the mapping $\boldsymbol{\varphi} : \mathcal{I}_h^2 \to \mathcal{I}_h^2$ is a bijection,

(A.3) for each $e \in \mathcal{I}_h^1$, $\boldsymbol{m} = \boldsymbol{n}^2$ and $\boldsymbol{m} = -\boldsymbol{n}^1$,

(A.4) there are no hanging nodes, i.e. $\mathcal{F} = \mathcal{I}_h^2$.

The purpose of (A.1) is to simplify the analysis, but our method still works, without any modification, when there are overlaps, as long as the other assumptions are satisfied. An example of this is given in Section 5.3. As discussed in [43], assumption (A.2) is not too strong when $\mathcal{I}_h^1$ and $\mathcal{I}_h^2$ share the same topological properties, which is expected when both meshes are built from the same geometry. Assumption (A.3) means that the direction of the connecting segments must be parallel to the normal vectors computed at its ends. This condition can be relaxed by assuming of $1 + \boldsymbol{m} \cdot \boldsymbol{n}^1$ and $1 - \boldsymbol{m} \cdot \boldsymbol{n}^2$ are small enough, i.e., the direction of the connecting segments does not deviate too much from the normal vectors. Assumption (A.4) is related to the fact that, under the presence of hanging nodes, the map $\boldsymbol{\varphi}$ fails to preserve polynomials on $e \in \mathcal{I}_h^2$ to polynomials on the corresponding faces $\{F\} \subset \mathcal{I}_h^2$. This would force us to use the $\boldsymbol{L}^2$ projection onto $\boldsymbol{M}_h^2$ in our arguments, which will ultimately lead us to prove that the method is still optimal in all the variables, except for L where the order of convergence loses half a power of h as will be detailed in Section 5.4.

In addition, we need the following restrictions that relate the closeness δ between $\mathcal{I}_h^1$ and $\mathcal{I}_h^2$ relative to the meshsize h:

(A.5) $$\left(4 \max_{e\in\mathcal{I}_h^1} (C_e^1 C_e^{\text{ext}})^2 \delta_e^{12/7} h_e^{-3} \tau^{-1} + \frac{8}{3} \max_{e\in\mathcal{I}_h^2} \delta_F^3 (h_F^{\perp})^{-3} (C_e^{\text{ext}} C_e^{\text{inv}})^2 + \frac{1}{4} \max_{e\in\mathcal{I}_h^2} \delta_e (C_e^{\text{tr}})^2\right) \leq \frac{1}{64},$$

(A.6) $$\frac{1}{2} \max_{e\in\mathcal{I}_h^2} \delta^{2/7} + 8 \max_{e\in\mathcal{I}_h^2} \delta\tau \leq \frac{1}{64},$$

(A.7) $C_2 \delta \max_{e\in\mathcal{I}_h^2} h_e^{-1} (C_e^{\text{tr}})^2 \leq \frac{1}{4}$, where C_2 is a positive constant, independent of the meshsize, that will appear in (25).

(A.8) Let $h := \max\{h_1, h_2\}$. We require

$$C_2 \left\{ \delta^2 \left(\tau + \nu^2 + \max_{e\in\mathcal{I}_h^2} h_e^{-3} (C_e^{\text{ext}})^2 \right) + \delta \left(\tau^{-1} + 1 + \delta \max_{e\in\mathcal{I}_h^2} \delta_e^3 (h_e^{\perp})^{-3} (C_e^{\text{ext}} C_e^{\text{inv}})^2 \right) + 2\nu^2 h^2 \right\} \leq \frac{1}{16}.$$

(A.9) $C_{\boldsymbol{u}}^{\mathcal{S}} C_{\mathcal{S}}^{\boldsymbol{u}} + \left(C_{\boldsymbol{u}}^{\mathcal{S}} C_{\tilde{p}}^{\boldsymbol{u}} + C_{\tilde{p}}^{\mathcal{S}}\right) 8\nu^2 C_3 \leq \frac{2}{64}$, where C_3 is a positive constant, independent of the meshsize, that will appear in Lemma 10,

$$C_{\tilde{p}}^{\mathcal{S}} := 4\nu^{-2} \max_{e\in\mathcal{I}_h^1} (C_e^1 C_e^{\text{ext}})^2 \delta_e^{12/7} h_e^{-3} \tau^{-1} + \frac{1}{4} \max_{e\in\mathcal{I}_h^2} \delta_e (C_e^{\text{tr}})^2 + 2\nu^{-2} \max_{e\in\mathcal{I}_h^2} \delta_e h_e^{-1} C_e^{\text{tr}} + \frac{\nu^{-2}}{8},$$
$$C_{\boldsymbol{u}}^{\mathcal{S}} := \frac{1}{4} + \max_{e\in\mathcal{I}_h^1} (C_e^{\text{tr}})^2 \delta_e^{2/7} h_e^{-1} \tau$$

are constants that will appear in Lemma 7, and

$$C_{\mathcal{S}}^{\boldsymbol{u}} := 2C_2 \Big(\delta^2 \tau + \delta \tau^{-1} + \delta \max_{e\in\mathcal{I}_h^2} r_e^3 (C_e^{\text{ext}} C_e^{\text{inv}})^2 + \nu^2 \delta^2 + \delta + \max_{e\in\mathcal{I}_h^2} \delta_e^2 h_e^{-3} (C_e^{\text{ext}})^2 + \nu^2 h_1^{2\min\{1,k\}} + \nu^2 h_2^{2\min\{1,k\}} \Big),$$
$$C_{\tilde{p}}^{\boldsymbol{u}} := 2C_2 \max_{e\in\mathcal{I}_h^2} \left\{ \delta_e h_e^{-1} (C_e^{\text{tr}})^2 + (\delta_e^2 h_e^{-3} (C_e^{\text{ext}})^2) \right\}$$

are constants that will appear in Lemma 9.

(A.10) $\beta\widehat{C}^1_{\text{tr}}\max_{e\in\mathcal{I}^1_h} C^1_e C^{\text{ext}}_e \delta_e h_e^{-3/2} + \beta\widehat{C}^2_{\text{ext}}\max_{e\in\mathcal{I}^2_h}\delta_e h_e^{-1/2} \leq 1-2^{-1/2}$, where β is the constant associated to an inf-sup condition that will appear in the proof of Lemma 10.

We note that these assumptions are satisfied considering τ of order one, h small enough and δ is proportional, at least, to h^2, which is the case when $\mathcal{I}^1_h$ and $\mathcal{I}^2_h$ correspond to piecewise linear interpolations of the interface $\mathcal{I}$. We end this section by mentioning that, while most constants present in assumptions (A.5)-(A.10) vanish when there is no gap, this is not the case for (A.9). This is coherent with [44], where a similar inf-sup argument is used in order to prove an estimate of the pressure when there is no such gap in the mesh. We also observe that the left-hand sides in all the assumptions are bounded even for small viscosity.

4.3 Main results

We introduce a modified version of (5) with artificial source terms that will help us to be more explicit with our estimates in order to reuse these results both for the well-posedness of the scheme and the error bounds. Therefore, we consider the same problem (5), but (5a) is replaced by

$$(\mathrm{L}^i_h, \mathrm{G})_{\Omega^i_h} + (\boldsymbol{u}^i_h, \nabla\cdot\mathrm{G})_{\Omega^i_h} - \langle\widehat{\boldsymbol{u}}^i_h, \mathrm{G}\boldsymbol{n}\rangle_{\partial\Omega^i_h} = (\mathrm{H}^i, \mathrm{G})_{\Omega^i_h}, \tag{12a}$$

where $\mathrm{H}^i \in \mathrm{L}^2(\Omega^i_h)$ is a given function such that it is orthogonal to polynomials of degree $k-1$, and (5h) and (5i) are replaced by

$$\langle\widehat{\boldsymbol{u}}^1_h - \tilde{\boldsymbol{u}}^2_h, \boldsymbol{\mu}\rangle_{\mathcal{I}^1_h} = \langle\boldsymbol{T}_1, \boldsymbol{\mu}\rangle_{\mathcal{I}^1_h}, \qquad \forall\boldsymbol{\mu}\in\boldsymbol{M}_h(\mathcal{I}^1_h) \tag{12b}$$

$$\langle\widehat{\sigma}^2_h\boldsymbol{n}^2 + \tilde{\boldsymbol{\sigma}}^1_h, \boldsymbol{\mu}\rangle_{\mathcal{I}^2_h} = \langle\boldsymbol{T}_2, \boldsymbol{\mu}\rangle_{\mathcal{I}^2_h}, \qquad \forall\boldsymbol{\mu}\in\boldsymbol{M}_h(\mathcal{I}^2_h), \tag{12c}$$

where $\boldsymbol{T}_1$ and $\boldsymbol{T}_2$ are given functions belonging to $\boldsymbol{L}^2(\mathcal{I}^1_h)$ and $\boldsymbol{L}^2(\mathcal{I}^2_h)$, respectively. In particular, to show well-posedness, H^i and $\boldsymbol{T}_i$ will be zero, whereas H^i and $\boldsymbol{T}_i$ will be related to projection errors when proving the error bounds.

For our convenience, let us define

$$\begin{aligned}\mathcal{S}(\mathrm{L}_h, \boldsymbol{u}_h, \widehat{\boldsymbol{u}}_h, \tilde{\boldsymbol{u}}_h) := \Bigg(&\sum_{i=1}^2 \left\|\mathrm{L}^i_h\right\|^2_{\Omega^i_h} + \sum_{i=1}^2\left\|\tau^{1/2}(\boldsymbol{u}^i_h - \widehat{\boldsymbol{u}}^i_h)\right\|^2_{\partial\Omega^i_h} \\ &+ \left\||\ell|^{-1/2}\left(\tilde{\boldsymbol{u}}^2_h\circ\boldsymbol{\varphi} - \widehat{\boldsymbol{u}}^2_h\right)\right\|^2_{\mathcal{I}^2_h} + \|\delta_e^{1/7}\tau^{1/2}\widehat{\boldsymbol{u}}^1_h\|^2_{\mathcal{I}^1_h}\Bigg)^{1/2}.\end{aligned} \tag{13}$$

We are now ready to state the main results of this section.

Theorem 3. *Suppose Assumptions A hold true. If τ is of order one, $k\geq 1$ and $h<1$, then there exists $h_0\in(0,1)$ such that, for all $h<h_0$, it holds*

$$\mathcal{S}(\mathrm{L}_h, \boldsymbol{u}_h, \widehat{\boldsymbol{u}}_h, \tilde{\boldsymbol{u}}_h)^2 \lesssim \sum_{i=1}^2\left\|\mathrm{H}^i\right\|^2_{\Omega^i_h} + \frac{1}{\nu^2}\|\boldsymbol{f}\|^2_\Omega + \|\boldsymbol{g}\|^2_\Gamma + \left\|h_e^{-1/2}\boldsymbol{T}_1\right\|^2_{\mathcal{I}^1_h} + \left\|h_e^{-1/2}\boldsymbol{T}_2\right\|^2_{\mathcal{I}^2_h} \tag{14}$$

Morover, if elliptic regularity of the dual problem (21) holds true, it holds

$$\begin{aligned}\sum_{i=1}^2\left\|\boldsymbol{u}^i_h\right\|^2_{\Omega^i_h} \lesssim &\left(\delta + \nu\delta^2 + \max_{e\in\mathcal{I}^2_h}\delta_e^2 h_e^{-3} + h_1^2 + h_2^2\right)\mathcal{S}(\mathrm{L}_h, \boldsymbol{u}_h, \widehat{\boldsymbol{u}}_h, \tilde{\boldsymbol{u}}_h)^2 \\ &+ \sum_{i=1}^2\left\|\mathrm{H}^i\right\|^2_{\Omega^i_h} + \|\boldsymbol{f}\|^2_\Omega + \|\boldsymbol{g}\|^2_\Gamma + \|\boldsymbol{T}_1\|^2_{\mathcal{I}^1_h} + \|\boldsymbol{T}_2\|^2_{\mathcal{I}^2_h}\end{aligned} \tag{15}$$

and

$$\sum_{i=1}^2\left\|\tilde{p}^i_h\right\|^2_{\Omega^i_h} \lesssim \nu^2\mathcal{S}(\mathrm{L}_h, \boldsymbol{u}_h, \widehat{\boldsymbol{u}}_h, \tilde{\boldsymbol{u}}_h)^2 + \|\boldsymbol{f}\|^2_\Omega\,. \tag{16}$$

The fact that the right hand sides in the inequalities above depend solely on the sources, will provide an easy proof of the well-posedness of the scheme and, later on, of the error estimates of the scheme.

Corollary 3.1. *The HDG scheme* (5) *has a unique solution.*

Proof. Let all sources to be equal to zero, i.e., $\mathrm{H}^1 \equiv 0$, $\mathrm{H}^2 \equiv 0$, $\boldsymbol{f} \equiv 0$, $\boldsymbol{g} \equiv 0$, $\boldsymbol{T}_1 \equiv 0$ and $\boldsymbol{T}_2 \equiv 0$. Theorem 3 implies that, for $i \in \{1, 2\}$, $\mathrm{L}_h^i \equiv 0$, $\boldsymbol{u}_h^i \equiv 0$, $\tilde{p}_h^i \equiv 0$ and $\widehat{\boldsymbol{u}}_h^i \equiv 0$. $\square$

Theorem 4. *Suppose Assumptions A and elliptic regularity hold true. If τ is of order one, $k \geq 1$ and $(\mathrm{L}, \boldsymbol{u}, \tilde{p}) \in \mathrm{H}^{l_\sigma+1}(\Omega) \times \boldsymbol{H}^{l_{\boldsymbol{u}}+1}(\Omega) \times H^{l_\sigma+1}(\Omega)$ for $l_\sigma, l_{\boldsymbol{u}} \in [0, k]$, then there exists $h_0 \in (0, 1)$ such that for all $h < h_0$, it holds*

$$\left(\sum_{i=1}^{2} \left\|\mathrm{L} - \mathrm{L}_h^i\right\|_{\Omega_h^i}^2\right)^{1/2} + \left(\sum_{i=1}^{2} \left\|\boldsymbol{u} - \boldsymbol{u}_h^i\right\|_{\Omega_h^i}^2\right)^{1/2} + \left(\sum_{i=1}^{2} \left\|\tilde{p} - \tilde{p}_h^i\right\|_{\Omega_h^i}^2\right)^{1/2}$$
$$\lesssim (1 + \nu^{-1})^{1/2} h^{l_\sigma+1} \left|\nu \mathrm{L} - \tilde{p}\mathbb{I}\right|_{\mathrm{H}^{l_\sigma+1}(\Omega)} + (1 + \nu)^{1/2} h^{l_{\boldsymbol{u}}+1} \left|\boldsymbol{u}\right|_{\boldsymbol{H}^{l_{\boldsymbol{u}}+1}(\Omega)}. \tag{17}$$

The results of the error estimates show that all the approximate variables converge optimally when Assumptions A and elliptic regularity hold.

4.4 Proof of the stability estimates.

This section is devoted to the proof of the stability estimates presented in Theorem 3.

4.4.1 An energy argument

First, in order to showcase an important technique that will be used constantly throughout the analysis of the terms associated to the mismatch between $\mathcal{I}_h^1$ and $\mathcal{I}_h^2$, we prove the following lemma.

Lemma 5. *Let $i \in \{1, 2\}$. We define $\mathbb{T}^i := \langle \widehat{\sigma}_h^i \boldsymbol{n}^i, \widehat{\boldsymbol{u}}_h^i \rangle_{\mathcal{I}_h^i}$ and denote $\sigma_h^i := \nu \mathrm{L}_h^i - \tilde{p}_h^i \mathbb{I}$. It holds that*

$$\begin{aligned}
\mathbb{T}^1 + \mathbb{T}^2 = {}& \langle \sigma_h^1 \boldsymbol{n}^1 + \boldsymbol{E}_{\sigma_h^1 \boldsymbol{n}^2} \circ \boldsymbol{\varphi}^{-1}, \widehat{\boldsymbol{u}}_h^1 \rangle_{\mathcal{I}_h^1} - \nu \left\| |\ell|^{-1/2} \left(\tilde{\boldsymbol{u}}_h^2 \circ \boldsymbol{\varphi} - \widehat{\boldsymbol{u}}_h^2\right) \right\|_{\mathcal{I}_h^2} + \nu \langle \Lambda^2_{\mathrm{L}_h^2}(\boldsymbol{x}^2), \tilde{\boldsymbol{u}}_h^2 \circ \boldsymbol{\varphi} - \widehat{\boldsymbol{u}}_h^2 \rangle_{\mathcal{I}_h^2} \\
& + \langle \tilde{p}_h^2 \boldsymbol{n}^2, \tilde{\boldsymbol{u}}_h^2 \circ \boldsymbol{\varphi} - \widehat{\boldsymbol{u}}_h^2 \rangle_{\mathcal{I}_h^2} + \nu \langle \tau(\boldsymbol{u}_h^2 - \widehat{\boldsymbol{u}}_h^2), \tilde{\boldsymbol{u}}_h^2 \circ \boldsymbol{\varphi} - \widehat{\boldsymbol{u}}_h^2 \rangle_{\mathcal{I}_h^2} \\
& - \nu \|\delta_e^{1/7} \tau^{1/2} \widehat{\boldsymbol{u}}_h^1\|^2_{\mathcal{I}_h^1} - \nu \langle \delta_e^{2/7} \tau(\boldsymbol{u}_h^1 - \widehat{\boldsymbol{u}}_h^1), \widehat{\boldsymbol{u}}_h^1 \rangle_{\mathcal{I}_h^1} + \nu \langle \delta_e^{2/7} \tau \boldsymbol{u}_h^1, \widehat{\boldsymbol{u}}_h^1 \rangle_{\mathcal{I}_h^1} \\
& - \langle (\widehat{\sigma}_h^2 \boldsymbol{n}^2) \circ \boldsymbol{\varphi}^{-1}, \boldsymbol{T}_1 \rangle_{\mathcal{I}_h^1} + \langle \boldsymbol{T}_2, \widehat{\boldsymbol{u}}_h^1 \circ \boldsymbol{\varphi} \rangle_{\mathcal{I}_h^2}.
\end{aligned}$$

Before proving this result, we point out that in the case where there is no gap, $\mathbb{T}^1 + \mathbb{T}^2 = 0$ in virtue of the fact that $\mathcal{I}_h^1 = \mathcal{I}_h^2$, $\tilde{\boldsymbol{u}}_h^2 = \widehat{\boldsymbol{u}}_h^2$ and (5j).

Proof. We decompose $\mathbb{T}^1 + \mathbb{T}^2 = \langle \widehat{\sigma}_h^1 \boldsymbol{n}^1 - \tilde{\boldsymbol{\sigma}}_h^1 \circ \boldsymbol{\varphi}^{-1}, \widehat{\boldsymbol{u}}_h^1 \rangle_{\mathcal{I}_h^1} + \langle \widehat{\sigma}_h^2 \boldsymbol{n}^2, \widehat{\boldsymbol{u}}_h^2 - \tilde{\boldsymbol{u}}_h^2 \circ \boldsymbol{\varphi} \rangle_{\mathcal{I}_h^2} + T$, where

$$T = \langle \tilde{\boldsymbol{\sigma}}_h^1 \circ \boldsymbol{\varphi}^{-1}, \widehat{\boldsymbol{u}}_h^1 \rangle_{\mathcal{I}_h^1} + \langle \widehat{\sigma}_h^2 \boldsymbol{n}^2, \tilde{\boldsymbol{u}}_h^2 \circ \boldsymbol{\varphi} \rangle_{\mathcal{I}_h^2}.$$

Moreover, we know that $\widehat{\sigma}_h^1 \boldsymbol{n}^1 - \tilde{\boldsymbol{\sigma}}_h^1 \circ \boldsymbol{\varphi}^{-1} = \sigma_h^1 \boldsymbol{n}^1 + \boldsymbol{E}_{\sigma_h^1 \boldsymbol{n}^2} \circ \boldsymbol{\varphi}^{-1}$ from the definition of the flux (5f) and definition (5k). Then we can rewrite the first term to obtain that

$$\mathbb{T}^1 + \mathbb{T}^2 = \langle \sigma_h^1 \boldsymbol{n}^1 + \boldsymbol{E}_{\sigma_h^1 \boldsymbol{n}^2} \circ \boldsymbol{\varphi}^{-1}, \widehat{\boldsymbol{u}}_h^1 \rangle_{\mathcal{I}_h^1} + \langle \widehat{\sigma}_h^2 \boldsymbol{n}^2, \widehat{\boldsymbol{u}}_h^2 - \tilde{\boldsymbol{u}}_h^2 \circ \boldsymbol{\varphi} \rangle_{\mathcal{I}_h^2} + T,$$

On the other hand, since $\boldsymbol{\varphi} : \mathcal{I}_h^2 \to \mathcal{I}_h^1$ is a bijection such that $\boldsymbol{x}^2 - \boldsymbol{\varphi}(\boldsymbol{x}^2) = \left|\ell(\boldsymbol{x}^2)\right| \boldsymbol{m}(\boldsymbol{x}^2)$ and we are under the assumption that $\boldsymbol{m} = \boldsymbol{n}^2 = -\boldsymbol{n}^1$, which implies that both interfaces are parallel, then $\boldsymbol{\varphi}$ must be affine (a translation, even) on each $F \in \mathcal{I}_h^2$. Furthermore, if we assume that there are no hanging nodes, then $\boldsymbol{\varphi}^{-1}$ is also affine for each $e \in \mathcal{I}_h^1$. Thus, both $\widehat{\boldsymbol{u}}_h^1 \circ \boldsymbol{\varphi}$ and $(\widehat{\sigma}_h^2 \boldsymbol{n}^2) \circ \boldsymbol{\varphi}^{-1}$ are polynomial when restricted to $F \in \mathcal{I}_h^2$ and $e \in \mathcal{I}_h^1$, respectively. In other words, $\widehat{\boldsymbol{u}}_h^1 \circ \boldsymbol{\varphi} \in \boldsymbol{M}_h(\mathcal{I}_h^2)$ and $(\widehat{\sigma}_h^2 \boldsymbol{n}^2) \circ \boldsymbol{\varphi}^{-1} \in \boldsymbol{M}_h(\mathcal{I}_h^1)$. Thus, using the transmission conditions (12c) and (12b), we have that

$$T = \langle \boldsymbol{T}_2 - \widehat{\sigma}_h \boldsymbol{n}^2, \widehat{\boldsymbol{u}}_h^1 \circ \boldsymbol{\varphi} \rangle_{\mathcal{I}_h^2} + \langle (\widehat{\sigma}_h^2 \boldsymbol{n}^2) \circ \boldsymbol{\varphi}^{-1}, \widehat{\boldsymbol{u}}_h^1 - \boldsymbol{T}_1 \rangle_{\mathcal{I}_h^1}$$

and therefore

$$\begin{aligned} \mathbb{T}^1 + \mathbb{T}^2 = &\langle \sigma_h^1 \boldsymbol{n}^1 + \boldsymbol{E}_{\sigma_h^1 \boldsymbol{n}^2} \circ \boldsymbol{\varphi}^{-1}, \widehat{\boldsymbol{u}}_h^1 \rangle_{\mathcal{I}_h^1} + \langle \widehat{\sigma}_h^2 \boldsymbol{n}^2, \widehat{\boldsymbol{u}}_h^2 - \tilde{\boldsymbol{u}}_h^2 \circ \boldsymbol{\varphi} \rangle_{\mathcal{I}_h^2} - \langle \widehat{\sigma}_h \boldsymbol{n}^2, \widehat{\boldsymbol{u}}_h^1 \circ \boldsymbol{\varphi} \rangle_{\mathcal{I}_h^2} \\ &+ \langle (\widehat{\sigma}_h^2 \boldsymbol{n}^2) \circ \boldsymbol{\varphi}^{-1}, \widehat{\boldsymbol{u}}_h^1 \rangle_{\mathcal{I}_h^1} - \langle (\widehat{\sigma}_h^2 \boldsymbol{n}^2) \circ \boldsymbol{\varphi}^{-1}, \boldsymbol{T}_1 \rangle_{\mathcal{I}_h^1} + \langle \boldsymbol{T}_2, \widehat{\boldsymbol{u}}_h^1 \circ \boldsymbol{\varphi} \rangle_{\mathcal{I}_h^2} \end{aligned}$$

Now, from (5j), assumption $\boldsymbol{m} = \boldsymbol{n}^2$, definition (8) and the fact that $\sigma_h^2 = \nu \mathrm{L}_h^2(\boldsymbol{x}^2) - \tilde{p}_h^2(\boldsymbol{x}^2)\mathbb{I}$, we have

$$\begin{aligned} \tilde{\boldsymbol{u}}_h^2 \circ \boldsymbol{\varphi}(\boldsymbol{x}^2) &= \widehat{\boldsymbol{u}}_h^2(\boldsymbol{x}^2) + \left|\ell(\boldsymbol{x}^2)\right| \int_0^1 \boldsymbol{E}_{\mathrm{L}_h^2}(\boldsymbol{x}^2 + \boldsymbol{n}^2 \left|\ell(\boldsymbol{x}^2)\right| s)\boldsymbol{n}^2 \mathrm{d}s \\ &= \widehat{\boldsymbol{u}}_h^2(\boldsymbol{x}^2) + \left|\ell(\boldsymbol{x}^2)\right| \Lambda^2_{\mathrm{L}_h^2}(\boldsymbol{x}^2) + \frac{\left|\ell(\boldsymbol{x}^2)\right|}{\nu} \sigma_h^2 \boldsymbol{n}^2(\boldsymbol{x}^2) + \frac{\left|\ell(\boldsymbol{x}^2)\right|}{\nu} \tilde{p}_h^2(\boldsymbol{x}^2)\boldsymbol{n}^2 \end{aligned}$$

and so

$$\sigma_h^2 \boldsymbol{n}^2(\boldsymbol{x}^2) = -\frac{\nu}{|\ell(\boldsymbol{x}^2)|} \left(\widehat{\boldsymbol{u}}_h^2(\boldsymbol{x}^2) - \tilde{\boldsymbol{u}}_h^2 \circ \boldsymbol{\varphi}(\boldsymbol{x}^2)\right) - \nu \Lambda^2_{\mathrm{L}_h^2}(\boldsymbol{x}^2) - \tilde{p}_h^2(\boldsymbol{x}^2)\boldsymbol{n}^2. \tag{18}$$

Replacing this in $\mathbb{T}^1 + \mathbb{T}^2$ and using also (5f), we have

$$\begin{aligned} \mathbb{T}^1 + \mathbb{T}^2 = &\langle \sigma_h^1 \boldsymbol{n}^1 + \boldsymbol{E}_{\sigma_h^1 \boldsymbol{n}^2} \circ \boldsymbol{\varphi}^{-1}, \widehat{\boldsymbol{u}}_h^1 \rangle_{\mathcal{I}_h^1} - \left\langle \frac{\nu}{|\ell(\boldsymbol{x}^2)|} \left(\widehat{\boldsymbol{u}}_h^2(\boldsymbol{x}^2) - \tilde{\boldsymbol{u}}_h^2 \circ \boldsymbol{\varphi}(\boldsymbol{x}^2)\right), \widehat{\boldsymbol{u}}_h^2 - \tilde{\boldsymbol{u}}_h^2 \circ \boldsymbol{\varphi} \right\rangle_{\mathcal{I}_h^2} \\ &- \langle \nu \Lambda^2_{\mathrm{L}_h^2}(\boldsymbol{x}^2), \widehat{\boldsymbol{u}}_h^2 - \tilde{\boldsymbol{u}}_h^2 \circ \boldsymbol{\varphi} \rangle_{\mathcal{I}_h^2} - \langle \tilde{p}_h^2 \boldsymbol{n}^2, \widehat{\boldsymbol{u}}_h^2 - \tilde{\boldsymbol{u}}_h^2 \circ \boldsymbol{\varphi} \rangle_{\mathcal{I}_h^2} - \langle \tau\nu(\boldsymbol{u}_h^2 - \widehat{\boldsymbol{u}}_h^2), \widehat{\boldsymbol{u}}_h^2 - \tilde{\boldsymbol{u}}_h^2 \circ \boldsymbol{\varphi} \rangle_{\mathcal{I}_h^2} \\ &- \langle (\widehat{\sigma}_h^2 \boldsymbol{n}^2) \circ \boldsymbol{\varphi}^{-1}, \boldsymbol{T}_1 \rangle_{\mathcal{I}_h^1} + \langle \boldsymbol{T}_2, \widehat{\boldsymbol{u}}_h^1 \circ \boldsymbol{\varphi} \rangle_{\mathcal{I}_h^2}. \end{aligned}$$

Finally, we add $0 = -\nu \langle \delta_e^{2/7} \tau \widehat{\boldsymbol{u}}_h^1, \widehat{\boldsymbol{u}}_h^1 \rangle_{\mathcal{I}_h^1} - \nu \langle \delta_e^{2/7} \tau (\boldsymbol{u}_h^1 - \widehat{\boldsymbol{u}}_h^1), \widehat{\boldsymbol{u}}_h^1 \rangle_{\mathcal{I}_h^1} + \nu \langle \delta_e^{2/7} \tau \boldsymbol{u}_h^1, \widehat{\boldsymbol{u}}_h^1 \rangle_{\mathcal{I}_h^1}$ in the right hand side and obtain the desired result. □

Now we continue with the proof of Theorem 3. To that end, we provide the following lemma.

Lemma 6. *It holds that*

$$\nu \mathcal{S}(\mathrm{L}_h, \boldsymbol{u}_h, \widehat{\boldsymbol{u}}_h, \tilde{\boldsymbol{u}}_h)^2 = \sum_{i=1}^{8} I^i + \sum_{i=1}^{2} \left(\nu(\mathrm{H}, \mathrm{L}_h^i)_{\Omega_h^i} + (\boldsymbol{f}, \boldsymbol{u}_h^i)_{\Omega_h^i} + \langle \boldsymbol{g}, \widehat{\sigma} \boldsymbol{n}_h^i \rangle_{\Gamma_h^i \setminus \mathcal{I}_h^i} \right) \tag{19}$$

where

$$\begin{aligned} I^1 &:= \langle \sigma_h^1 \boldsymbol{n}^1 + \boldsymbol{E}_{\sigma_h^1 \boldsymbol{n}^2} \circ \boldsymbol{\varphi}^{-1}, \widehat{\boldsymbol{u}}_h^1 \rangle_{\mathcal{I}_h^1}, & I^5 &:= \nu \langle \delta^{2/7} \tau \boldsymbol{u}_h^1, \widehat{\boldsymbol{u}}_h^1 \rangle_{\mathcal{I}_h^1} \\ I^2 &:= \nu \langle \Lambda_{\mathrm{L}_h^2}, \tilde{\boldsymbol{u}}_h^2 \circ \boldsymbol{\varphi} - \widehat{\boldsymbol{u}}_h^2 \rangle_{\mathcal{I}_h^2}, & I^6 &:= \langle \boldsymbol{T}_2, \widehat{\boldsymbol{u}}_{\boldsymbol{h}}^{\boldsymbol{1}} \circ \boldsymbol{\varphi} \rangle_{\mathcal{I}_h^2} \\ I^3 &:= \nu \langle \tau(\boldsymbol{u}_h^2 - \widehat{\boldsymbol{u}}_h^2), \tilde{\boldsymbol{u}}_h^2 \circ \boldsymbol{\varphi} - \widehat{\boldsymbol{u}}_h^2 \rangle_{\mathcal{I}_h^2}, & I^7 &:= -\langle (\widehat{\sigma}_h^2 \boldsymbol{n}^2) \circ \boldsymbol{\varphi}^{-1}, \boldsymbol{T}_1 \rangle_{\mathcal{I}_h^1} \\ I^4 &:= -\nu \langle \delta^{2/7} \tau (\boldsymbol{u}_h^1 - \widehat{\boldsymbol{u}}_h^1), \widehat{\boldsymbol{u}}_h^1 \rangle_{\mathcal{I}_h^1} & I^8 &:= \langle \tilde{p}^2 \boldsymbol{n}^2, \tilde{\boldsymbol{u}}_h^2 \circ \boldsymbol{\varphi} - \widehat{\boldsymbol{u}}_h^2 \rangle_{\mathcal{I}_h^2}. \end{aligned}$$

Proof. In (5), for $i \in \{1, 2\}$, we test with $\mathrm{G}|_{\Omega_h^i} = \nu \mathrm{L}_h^i$, $\boldsymbol{v}|_{\Omega_h^i} = \boldsymbol{u}_h^i$, $q|_{\Omega_h^i} = \tilde{p}_h^i$ and $\boldsymbol{\mu} = \begin{cases} \widehat{\sigma}_h^i \boldsymbol{n}_h^i & \text{on } \Gamma_h^i \setminus \mathcal{I}_h^i, \\ \widehat{\boldsymbol{u}}_h^i & \text{on } \partial\Omega_h^i \setminus \Gamma_h^i. \end{cases}$ Adding both equations, after integrating by parts the second one, we obtain

$$\begin{aligned} \nu(\mathrm{L}_h^i, \mathrm{L}_h^i)_{\Omega_h^i} &+ \langle \nu \mathrm{L}_h^i - \tilde{p}_h^i \mathbb{I}, \boldsymbol{u}_h^i \rangle_{\partial\Omega_h^i} - \langle \widehat{\sigma}_h^i \boldsymbol{n}, \boldsymbol{u}_h^i \rangle_{\partial\Omega_h^i} + \langle \widehat{\boldsymbol{u}}_h^i \cdot \boldsymbol{n}, (\tilde{p}_h^i \mathbb{I} - \nu \mathrm{L}_h^i)\boldsymbol{n} \rangle_{\partial\Omega_h^i} \\ &+ \langle \widehat{\boldsymbol{u}}_h^i, \widehat{\sigma}_h^i \boldsymbol{n}_h^i \rangle_{\Gamma_h^i \setminus \mathcal{I}_h^i} + \langle \widehat{\sigma}_h^i \boldsymbol{n}, \widehat{\boldsymbol{u}}_h^i \rangle_{\partial\Omega_h^i \setminus \Gamma_h^i} = \nu(\mathrm{H}, \mathrm{L}_h^i)_{\Omega_h^i} + (\boldsymbol{f}, \boldsymbol{u}_h^i)_{\Omega_h^i} + \langle \boldsymbol{g}, \widehat{\sigma}_h^i \boldsymbol{n}_h^i \rangle_{\Gamma_h^i \setminus \mathcal{I}_h^i}. \end{aligned} \tag{20}$$

On the other hand, the fourth term can be rewritten as

$$\langle \widehat{\boldsymbol{u}}_h^i, (\tilde{p}_h^i \mathbb{I} - \nu \mathrm{L}_h^i)\boldsymbol{n} \rangle_{\partial\Omega_h^i} = -\langle \widehat{\boldsymbol{u}}_h^i, \widehat{\sigma}_h^i \boldsymbol{n}^i \rangle_{\partial\Omega_h^i} - \langle \tau\nu(\boldsymbol{u}_h^i - \widehat{\boldsymbol{u}}_h^i), \widehat{\boldsymbol{u}}_h^i \rangle_{\partial\Omega_h^i}.$$

Noting that the first term of this expression is the same as the last two terms of the left-hand side of (20), albeit integrated on different regions, we write

$$-\langle \widehat{\boldsymbol{u}}_h^i, \widehat{\sigma}_h^i \boldsymbol{n}^i \rangle_{\partial\Omega_h^i} + \langle \widehat{\boldsymbol{u}}_h^i, \widehat{\sigma}_h^i \boldsymbol{n}^i \rangle_{\Gamma_h^i \setminus \mathcal{I}_h^i} + \langle \widehat{\sigma} \boldsymbol{n}_h^i, \widehat{\boldsymbol{u}}_h^i \rangle_{\partial\Omega_h^i \setminus \Gamma_h^i} = -\langle \widehat{\boldsymbol{u}}_h^i, \widehat{\sigma}_h^i \boldsymbol{n}^i \rangle_{\mathcal{I}_h^i}.$$

Thus, (20) is simplified to,

$$\nu(\mathrm{L}_h^i, \mathrm{L}_h^i)_{\Omega_h^i} + \langle \tau\nu(\boldsymbol{u}_h^i - \widehat{\boldsymbol{u}}_h^i), \boldsymbol{u}_h^i - \widehat{\boldsymbol{u}}_h^i \rangle_{\partial\Omega_h^i} - \langle \widehat{\boldsymbol{u}}_h^i, \widehat{\sigma}_h^i \boldsymbol{n}^i \rangle_{\mathcal{I}_h^i} = \nu(\mathrm{H}, \mathrm{L}_h^i)_{\Omega_h^i} + (\boldsymbol{f}, \boldsymbol{u}_h^i)_{\Omega_h^i} + \langle \boldsymbol{g}, \widehat{\sigma}_h^i \boldsymbol{n}^i \rangle_{\Gamma_h^i \setminus \mathcal{I}_h^i},$$

The result follows after summing over $i \in \{1, 2\}$ and Lemma 5. □

Based on the above results, the next lemma provides an upper bound of the energy term $\mathcal{S}(\mathrm{L}_h, \boldsymbol{u}_h, \widehat{\boldsymbol{u}}_h, \tilde{\boldsymbol{u}}_h)$. This bound depends on the norms of the approximations of the velocity and pressure, in addition to the dependence on the sources. Its proof is postponed to the appendix.

Lemma 7. *Let us suppose that Assumptions A, hold. There exists a positive constant $C_{\mathcal{S}}$ independent of h, δ and ν such that*

$$\frac{3}{64}\mathcal{S}(\mathrm{L}_h, \boldsymbol{u}_h, \widehat{\boldsymbol{u}}_h, \tilde{\boldsymbol{u}}_h)^2 \leq C_{\boldsymbol{u}}^{\mathcal{S}} \sum_{i=1}^{2} \left\| \boldsymbol{u}_h^i \right\|_{\Omega_h^i}^2 + C_{\tilde{p}}^{\mathcal{S}} \sum_{i=1}^{2} \left\| \tilde{p}_h^i \right\|_{\Omega_h^i}^2 + C_{\mathcal{S}} \Bigg(\max_{e \in \Gamma_h^1 \setminus \mathcal{I}_h^1 \cup \Gamma_h^2 \setminus \mathcal{I}_h^2} \left(h_e^{-1} + \tau \right) \|\boldsymbol{g}\|_\Gamma^2 + \sum_{i=1}^{2} \|\mathrm{H}\|_{\Omega_h^i}^2 + \nu^{-2} \|\boldsymbol{f}\|_\Omega^2 + \left\| \nu^{-1/2} \delta_e^{-1/7} \tau^{-1/2} \boldsymbol{T}_2 \right\|_{\mathcal{I}_h^2}^2 + \left\| (1 + \nu^{-1} h_e^{-1}) \delta_e^{-1/2} \boldsymbol{T}_1 \right\|_{\mathcal{I}_h^1}^2 \Bigg).$$

where we recall that $C_{\boldsymbol{u}}^{\mathcal{S}}$ and $C_{\tilde{p}}^{\mathcal{S}}$ are defined in (A.9).

We observe that the right-hand side of (7) depends on $\sum_{i=1}^{2} \left\| \boldsymbol{u}_h^i \right\|_{\Omega_h^i}$ and $\sum_{i=1}^{2} \left\| \tilde{p}_h^i \right\|_{\Omega^i}$. To bound $\sum_{i=1}^{2} \left\| \boldsymbol{u}_h^i \right\|_{\Omega_h^i}$ we will employ a duality argument (section 4.4.2), and to bound $\sum_{i=1}^{2} \left\| \tilde{p}_h^i \right\|_{\Omega_h^i}$, we will use an inf-sup condition (section 4.4.3).

4.4.2 A duality argument

We now provide a bound for $\sum_{i=1}^{2} \left\| \boldsymbol{u}_h^i \right\|_{\Omega_h^i}$ via a duality argument.

For $\boldsymbol{\theta} \in \boldsymbol{L}^2(\Omega)$, let $(\boldsymbol{\Phi}, \boldsymbol{\phi}, \phi)$ be the solution of

$$\boldsymbol{\Phi} + \nabla \boldsymbol{\phi} = 0 \quad \text{on } \Omega, \tag{21a}$$

$$\nabla \cdot (\nu \boldsymbol{\Phi} - \phi \mathbb{I}) = \boldsymbol{\theta} \quad \text{on } \Omega, \tag{21b}$$

$$-\nabla \cdot \boldsymbol{\phi} = 0 \quad \text{on } \Omega, \tag{21c}$$

$$\boldsymbol{\phi} = \boldsymbol{0} \quad \text{on } \Gamma. \tag{21d}$$

Suppose that elliptic regularity holds, that is,

$$\nu \|\boldsymbol{\Phi}\|_{\mathrm{H}^1(\Omega)} + \nu \|\boldsymbol{\phi}\|_{\boldsymbol{H}^2(\Omega)} + \|\phi\|_{H^1(\Omega)} \lesssim \|\boldsymbol{\theta}\|_{\boldsymbol{H}^1(\Omega)}, \tag{22}$$

which is the case if Ω convex in two dimensions [35] or a convex polyhedron in the three-dimensional case [25].

The following result provides an identity that relates the approximation of the velocity and the solution of the dual problem (21). Since $\boldsymbol{\theta}$ is an arbitrary function in L^2, it will be properly chosen in order to have control on the L^2-norm of the velocity.

Lemma 8. *It holds that*

$$\sum_{i=1}^{2}(\boldsymbol{u}_h^i,\boldsymbol{\theta})_{\Omega_h^i} = -\nu\sum_{i=1}^{2}\Big\{(\mathrm{H}^i,\boldsymbol{\Phi}-\Pi_{\mathbb{V}^i}\boldsymbol{\Phi})_{\Omega_h^i}+(\mathrm{H}^i,\nabla(\boldsymbol{\phi}-\Pi_{\boldsymbol{V}^i}\boldsymbol{\phi}))_{\Omega_h^i}\Big\}+\sum_{i=1}^{2}(\nu\mathrm{L}_h^i,\boldsymbol{\Phi}-\Pi_{\mathbb{V}^i}\boldsymbol{\Phi})_{\Omega_h^i} \tag{23}$$
$$+\sum_{i=1}^{2}(\boldsymbol{f},\Pi_{\boldsymbol{V}^i}\boldsymbol{\phi})_{\Omega_h^i}+\sum_{i=1}^{2}\langle\boldsymbol{g},\mathrm{P}_{\boldsymbol{M}^i}(\nu\boldsymbol{\Phi}\boldsymbol{n}-\phi\boldsymbol{n})\rangle_{\Gamma_h^i\setminus\mathcal{I}_h^i}+\sum_{i=1}^{2}\mathbb{T}_{\boldsymbol{u}}^i.$$

where $\mathbb{T}_{\boldsymbol{u}}^i := \langle\widehat{\sigma}_h^i\boldsymbol{n}^i,\boldsymbol{\phi}\rangle_{\mathcal{I}_h^i}+\langle\widehat{\boldsymbol{u}}_h^i,\nu\boldsymbol{\Phi}\boldsymbol{n}^i-\phi\boldsymbol{n}^i\rangle_{\mathcal{I}_h^i}$.

We observe here that the right hand side not only depends on the sources and the projection errors of the solution of (21), but also on the terms $\mathbb{T}_{\boldsymbol{u}}^i$ that arise from gap between the discrete interfaces. Therefore, similarly to Lemma 5, we emphasize that $\mathbb{T}_{\boldsymbol{u}}^1+\mathbb{T}_{\boldsymbol{u}}^2$ vanishes if there is no gap.

Proof. For $i\in\{1,2\}$, testing (21) with $(\mathrm{G},\boldsymbol{v},q)\in\mathbb{V}_h^i\times\boldsymbol{V}_h^i\times V_h^i$, employing the identities (31) in [44], using the properties of the HDG projectors and and performing algebraic manipulations, it is possible to deduce that

$$\begin{aligned}(\boldsymbol{v},\boldsymbol{\theta})_{\Omega_h^i} =&(\mathrm{G},\boldsymbol{\Phi}-\Pi_{\mathbb{V}^i}\boldsymbol{\Phi})_{\Omega_h^i}+\langle\mathrm{G}\boldsymbol{n},\boldsymbol{\phi}\rangle_{\partial\Omega_h^i}+\langle\boldsymbol{v},\nu(\boldsymbol{\Phi}-\Pi_{\mathbb{V}^i}\boldsymbol{\Phi})-(\phi-\Pi_{V^i}\phi)\boldsymbol{n}\rangle_{\partial\Omega_h^i}-\langle q,\boldsymbol{n},\boldsymbol{\phi}\rangle_{\partial\Omega_h^i}\\&-(\boldsymbol{v},\nabla\Pi_{V^i}\phi)_{\Omega_h^i}+\Big\{(\mathrm{G},\Pi_{\mathbb{V}^i}\boldsymbol{\Phi})_{\Omega_h^i}+(\boldsymbol{v},\nu\nabla\cdot\Pi_{\mathbb{V}^i}\boldsymbol{\Phi})_{\Omega_h^i}\Big\}-\Big\{(\nabla\cdot(\mathrm{G}-q\mathbb{I}),\Pi_{\boldsymbol{V}^i}\boldsymbol{\phi})_{\Omega_h^i}\Big\}.\end{aligned}$$

Now, taking $\mathrm{G}=\nu\mathrm{L}_h^i$, $\boldsymbol{v}=\boldsymbol{u}_h^i$, $q=\tilde{p}_h^i$, using (5), and adding and substracting convenient terms, we obtain

$$\begin{aligned}(\boldsymbol{u}_h^i,\boldsymbol{\theta})_{\Omega_h^i} =& (\nu\mathrm{L}_h^i,\boldsymbol{\Phi}-\Pi_{\mathbb{V}^i}\boldsymbol{\Phi})_{\Omega_h^i}+\langle\widehat{\sigma}_h^i\boldsymbol{n}^i,\boldsymbol{\phi}\rangle_{\partial\Omega_h^i}+\langle\widehat{\boldsymbol{u}}_h^i,\nu\boldsymbol{\Phi}\boldsymbol{n}-\phi\boldsymbol{n}\rangle_{\partial\Omega_h^i}+\nu(\mathrm{H}^i,\Pi_{\mathbb{V}^i}\boldsymbol{\Phi})_{\Omega_h^i}\\&+(\boldsymbol{f},\Pi_{\boldsymbol{V}^i}\boldsymbol{\phi})_{\Omega_h^i}+\langle\boldsymbol{u}_h^i-\widehat{\boldsymbol{u}}_h^i,\nu(\boldsymbol{\Phi}-\Pi_{\mathbb{V}^i}\boldsymbol{\Phi})\boldsymbol{n}-(\phi-\Pi_{V^i}\phi)\boldsymbol{n}+\tau\nu(\boldsymbol{\phi}-\Pi_{\boldsymbol{V}^i}\boldsymbol{\phi})\rangle_{\partial\Omega_h^i}.\end{aligned}$$

We can rewrite the second term as $\langle\widehat{\sigma}_h^i\boldsymbol{n}^i,\boldsymbol{\phi}\rangle_{\partial\Omega_h^i}=\langle\widehat{\sigma}_h^i\boldsymbol{n}^i,\mathrm{P}_{\boldsymbol{M}^i}\boldsymbol{\phi}\rangle_{\mathcal{I}_h^i}$, where we used (5e) with $\boldsymbol{\mu}=\mathrm{P}_{\boldsymbol{M}^i}\boldsymbol{\phi}$ and the fact that $\boldsymbol{\phi}|_\Gamma=\boldsymbol{0}$. Moreover, the last term vanishes by (3e) with $\boldsymbol{\mu}=\boldsymbol{u}_h^i-\widehat{\boldsymbol{u}}_h^i$.

On the other hand, using (5d) with $\boldsymbol{\mu}=\mathrm{P}_{\boldsymbol{M}^i}(\nu\boldsymbol{\Phi}\boldsymbol{n}-\phi\boldsymbol{n})$ and the fact that $\widehat{\boldsymbol{u}}_h^i$ is single valued on internal faces, it follows that

$$\langle\widehat{\boldsymbol{u}}_h^i,\nu\boldsymbol{\Phi}\boldsymbol{n}-\phi\boldsymbol{n}\rangle_{\partial\Omega_h^i}=\langle\boldsymbol{g},\mathrm{P}_{\boldsymbol{M}^i}(\nu\boldsymbol{\Phi}\boldsymbol{n}-\phi\boldsymbol{n})\rangle_{\Gamma_h^i\setminus\mathcal{I}_h^i}+\langle\widehat{\boldsymbol{u}}_h^i,\nu\boldsymbol{\Phi}\boldsymbol{n}-\phi\boldsymbol{n}\rangle_{\mathcal{I}_h^i}.$$

Furthermore, since H^i is assumed orthogonal to $[\mathbb{P}_{k-1}(\Omega)]^{d\times d}$, we have

$$(\mathrm{H}^i,\Pi_{\mathbb{V}^i}\boldsymbol{\Phi})_{\Omega_h^i}=(\mathrm{H}^i,\Pi_{\mathbb{V}^i}\boldsymbol{\Phi}-\boldsymbol{\Phi})_{\Omega_h^i}+(\mathrm{H}^i,\boldsymbol{\Phi})_{\Omega_h^i}=-(\mathrm{H}^i,\boldsymbol{\Phi}-\Pi_{\mathbb{V}^i}\boldsymbol{\Phi})_{\Omega_h^i}+(\mathrm{H}^i,\nabla(\boldsymbol{\phi}-\Pi_{\boldsymbol{V}^i}\boldsymbol{\phi}))_{\Omega_h^i}$$

and so

$$\begin{aligned}(\boldsymbol{u}_h^i,\boldsymbol{\theta})_{\Omega_h^i} =& (\nu\mathrm{L}_h^i,\boldsymbol{\Phi}-\Pi_{\mathbb{V}^i}\boldsymbol{\Phi})_{\Omega_h^i}+\langle\widehat{\sigma}_h^i\boldsymbol{n}^i,\boldsymbol{\phi}\rangle_{\mathcal{I}_h^i}+\langle\widehat{\boldsymbol{u}}_h^i,\nu\boldsymbol{\Phi}\boldsymbol{n}^i-\phi\boldsymbol{n}^i\rangle_{\mathcal{I}_h^i}-\nu(\mathrm{H}^i,\boldsymbol{\Phi}-\Pi_{\mathbb{V}^i}\boldsymbol{\Phi})_{\Omega_h^i}\\&+\nu(\mathrm{H}^i,\nabla(\boldsymbol{\phi}-\Pi_{\boldsymbol{V}^i}\boldsymbol{\phi}))_{\Omega_h^i}+(\boldsymbol{f},\Pi_{\boldsymbol{V}^i}\boldsymbol{\phi})_{\Omega_h^i}+\langle\boldsymbol{g},\mathrm{P}_{\boldsymbol{M}^i}(\nu\boldsymbol{\Phi}\boldsymbol{n}-\phi\boldsymbol{n})\rangle_{\Gamma_h^i\setminus\mathcal{I}_h^i}.\end{aligned}$$

The result follows after summing over $i\in\{1,2\}$. □

As we commented before, the presence of a gap between the discrete interfaces implies that $\mathbb{T}_{\boldsymbol{u}}^1+\mathbb{T}_{\boldsymbol{u}}^2$ does not vanish. However, it is possible to bound this quantity as stated in the following lemma. The proof can be found in the appendix.

Lemma 9. *It holds that*

$$\begin{aligned}\mathbb{T}_{\boldsymbol{u}}^1+\mathbb{T}_{\boldsymbol{u}}^2 \lesssim \|\boldsymbol{\theta}\|_\Omega\Bigg(&(\delta\tau^{1/2}+\delta^{1/2}\tau^{-1/2})\left\|\tau^{1/2}(\boldsymbol{u}_h^2-\widehat{\boldsymbol{u}}_h^2)\right\|_{\mathcal{I}_h^2}+\delta^{1/2}h_2^{-1/2}\left\|\boldsymbol{u}_h^2\right\|_{\Omega_h^2}\\&+\delta^{1/2}\max_{e\in\mathcal{I}_h^2}r_e^{3/2}C_e^{\mathrm{ext}}C_e^{\mathrm{inv}}\left\|\mathrm{L}_h^2\right\|_{\Omega_h^2}+(\nu\delta+\delta^{1/2})\left\||\ell|^{-1/2}(\tilde{\boldsymbol{u}}_h^2\circ\boldsymbol{\varphi}-\widehat{\boldsymbol{u}}_h^2)\right\|_{\mathcal{I}_h^2}\\&+\delta^{1/2}\max_{e\in\mathcal{I}_h^2}h_e^{-1/2}C_e^{\mathrm{tr}}\left\|\tilde{p}_h^2\right\|_{\Omega_h^2}+\max_{e\in\mathcal{I}_h^2}(\delta_e h_e^{-3/2}C_e^{\mathrm{ext}})\left\|\mathrm{L}_h^1\right\|+\max_{e\in\mathcal{I}_h^2}(\delta_e h_e^{-3/2}C_e^{\mathrm{ext}})\left\|\tilde{p}_h^1\right\|_{\Omega_h^1}\Bigg)\\&+\|\boldsymbol{T}_1\|_{\mathcal{I}_h^1}\|\boldsymbol{\theta}\|_\Omega+\|\boldsymbol{T}_2\|_{\mathcal{I}_h^2}\|\boldsymbol{\theta}\|_\Omega\end{aligned} \tag{24}$$

Finally, by taking $\boldsymbol{\theta} = \begin{cases} \boldsymbol{u}_h^1 & \text{in } \Omega_h^1, \\ \boldsymbol{u}_h^2 & \text{in } \Omega_h^2. \end{cases}$ in the identity (23), together with the estimate in (9), we conclude that

$$\sum_{i=1}^{2} \left\|\boldsymbol{u}_h^i\right\|_{\Omega_h^i}^2 \leq C_{\mathcal{S}}^{\boldsymbol{u}} \mathcal{S}(\mathrm{L}_h, \boldsymbol{u}_h, \widehat{\boldsymbol{u}}_h, \tilde{\boldsymbol{u}}_h)^2 + C_{\tilde{p}}^{\boldsymbol{u}} \sum_{i=1}^{2} \left\|\tilde{p}_h^i\right\|_{\Omega_h^i}^2$$
$$+ 2C_2 \left(\nu^2 \sum_{i=1}^{2} h_i^{2\min\{1,k\}} \left\|\mathrm{H}^i\right\|_{\Omega_h^i}^2 + \sum_{i=1}^{2} \|\boldsymbol{f}\|_{\Omega_h^i}^2 + \sum_{i=1}^{2} \|\boldsymbol{g}\|_{\Gamma_h^i \setminus \mathcal{I}_h^i}^2 + \|\boldsymbol{T}_1\|_{\mathcal{I}_h^1}^2 + \|\boldsymbol{T}_2\|_{\mathcal{I}_h^2}^2 \right), \tag{25}$$

where $C_{\mathcal{S}}^{\boldsymbol{u}}$ and $C_{\tilde{p}}^{\boldsymbol{u}}$ are as defined in (A.9) and C_2 is a positive constant independent of the meshsize.

Under assumption (A.8), we can replace (25) in (7) to obtain the following corollary.

Corollary 9.1. *It holds that*

$$\frac{1}{8}\mathcal{S}(\mathrm{L}_h, \boldsymbol{u}_h, \widehat{\boldsymbol{u}}_h, \tilde{\boldsymbol{u}}_h)^2 \leq \left(1 + 2C_2\nu^2 \left(h_1^{2\min\{1,k\}} + h_2^{2\min\{1,k\}}\right)\right) \sum_{i=1}^{2} \|\mathrm{H}\|_{\Omega_h^i}^2 + \left(\frac{2}{\nu^2} + 4C_2\right) \|\boldsymbol{f}\|_{\Omega}^2$$
$$+ \left(\frac{4}{\nu^2} \max_{e\in\mathcal{I}_h^2} \delta_e^{-1} h_e^{-1} + 4\tau + 4C_2\right) \|\boldsymbol{g}\|_{\Gamma} + \left(C_{\tilde{p}}^{\boldsymbol{u}} + C_{\tilde{p}}^{\mathrm{L}}\right) \sum_{i=1}^{2} \left\|\tilde{p}_h^i\right\|_{\Omega_h^i}^2 \tag{26}$$
$$+ \left\|(2C_2^{1/2} + 2^{-1}\nu^{-1}(\nu\tau^{1/2} + \delta^{-1}8\nu(C_e^{\mathrm{tr}})^2 h_e^{-1}))^{1/2}\boldsymbol{T}_1\right\|_{\mathcal{I}_h^1}^2$$
$$+ \left\|(2C_2^{1/2} + 2^{-1}\nu^{-1}(4\delta_e + 4\tau^{-1} + 2(C_e^{\mathrm{tr}})^2 h_e^{-1}))^{1/2}\boldsymbol{T}_2\right\|_{\mathcal{I}_h^2}^2,$$

where we recall that $C_{\tilde{p}}^{\boldsymbol{u}}$ has been defined in (A.8).

It only remains to bound the L^2-norm of the pressure and this is the purpose of next section.

4.4.3 Estimate of the pressure

Adjusting the proof of Lemma 2 in [44] to our context, we provide a bound for $\sum_{i=1}^{2} \left\|\tilde{p}_h^i\right\|_{\Omega_h^i}$ as follows.

Lemma 10. *It h olds that*

$$\sum_{i=1}^{2} \left\|\tilde{p}_h^i\right\|_{\Omega_h^i}^2 \leq 8\nu^2 C_3 \mathcal{S}(\mathrm{L}_h, \boldsymbol{u}_h, \widehat{\boldsymbol{u}}_h, \tilde{\boldsymbol{u}}_h)^2 + 8C_3 \|\boldsymbol{f}\|_{\Omega}^2, \tag{27}$$

where C_3 is a positive constant independent of the meshsize.

Proof. Let $\tilde{\tilde{p}}_h := \begin{cases} \tilde{p}_h, & \text{on } \Omega_h^1 \cup \Omega_h^2 \\ 0, & \text{on } \Omega \setminus (\Omega_h^1 \cup \Omega_h^2) \end{cases}$. It is clear that $\tilde{\tilde{p}}_h \in L^2(\Omega)$ and $\int_\Omega \tilde{\tilde{p}}_h = \int_{\Omega_h^1 \cup \Omega_h^2} \tilde{p}_h = 0$. Therefore, there exists $\beta > 0$ such that

$$\left\|\tilde{\tilde{p}}_h\right\|_{\Omega} \leq \beta \sup_{\substack{\boldsymbol{w}\in \boldsymbol{H}_0^1(\Omega) \\ \boldsymbol{w}\neq \boldsymbol{0}}} \frac{(\tilde{\tilde{p}}_h, \nabla\cdot\boldsymbol{w})_\Omega}{\|\boldsymbol{w}\|_{\boldsymbol{H}^1(\Omega)}}. \tag{28}$$

Note that, since $\tilde{\tilde{p}}_h$ is an extension by zero of $\tilde{p}$, then $\left\|\tilde{\tilde{p}}_h\right\|_\Omega = \|\tilde{p}\|_{\Omega_h^1\cup\Omega_h^2}$ and, for $\boldsymbol{v} \in \boldsymbol{L}^2(\Omega)$, $(\tilde{\tilde{p}}_h, \boldsymbol{v})_\Omega = (\tilde{p}_h^1, \boldsymbol{v})_{\Omega_h^1} + (\tilde{p}_h^2, \boldsymbol{v})_{\Omega_h^2}$. Replacing this in (28), we get

$$\|\tilde{p}\|_{\Omega_h^1\cup\Omega_h^2} \leq \beta \sup_{\substack{\boldsymbol{w}\in \boldsymbol{H}_0^1(\Omega) \\ \boldsymbol{w}\neq \boldsymbol{0}}} \frac{(\tilde{p}_h^1, \nabla\cdot\boldsymbol{w})_{\Omega_h^1} + (\tilde{p}_h^2, \nabla\cdot\boldsymbol{w})_{\Omega_h^2}}{\|\boldsymbol{w}\|_{\boldsymbol{H}^1(\Omega)}} \tag{29}$$

For $i \in \{1,2\}$, let $\boldsymbol{P}^i : \boldsymbol{H}^1(\Omega) \to \boldsymbol{V}_h^i$ be any projection such that $(\boldsymbol{P}^i \boldsymbol{w} - \boldsymbol{w}, \boldsymbol{v})_K = 0$, $\forall \boldsymbol{v} \in [\mathbb{P}_{k-1}(K)]^d$ for all $K \in \Omega_h^i$. Following the same steps as in the proof of Lemma 2 in [44] applied to our context, it is possible to deduce that

$$(\tilde{p}_h^i, \nabla \cdot \boldsymbol{w})_{\Omega_h^i} = (\nu \mathrm{L}_h^i, \nabla \boldsymbol{w})_{\Omega_h^i} - \langle \widehat{\sigma}_h^i \boldsymbol{n}^i, \mathrm{P}_{\boldsymbol{M}^i} \boldsymbol{w} \rangle_{\mathcal{I}_h^i} + \langle \tau \nu (\boldsymbol{u}_h^i - \widehat{\boldsymbol{u}}_h^i), \boldsymbol{P}^i \boldsymbol{w} - \mathrm{P}_{\boldsymbol{M}^i} \boldsymbol{w} \rangle_{\partial \Omega_h^i} - (\boldsymbol{f}, \boldsymbol{P}^i \boldsymbol{w})_{\Omega_h^i}.$$

Using the Cauchy-Schwartz inequality, we obtain

$$\begin{aligned}
(\nu \mathrm{L}_h^i, \nabla \boldsymbol{w})_{\Omega_h^i} &\leq \nu \left\| \mathrm{L}_h^i \right\|_{\Omega_h^i} \|\nabla \boldsymbol{w}\|_{\Omega_h^i} \leq \nu \left\| \mathrm{L}_h^i \right\|_{\Omega_h^i} \|\boldsymbol{w}\|_{\boldsymbol{H}^1(\Omega)} \\
\langle \tau \nu (\boldsymbol{u}_h^i - \widehat{\boldsymbol{u}}_h^i), \boldsymbol{P}^i \boldsymbol{w} - \mathrm{P}_{\boldsymbol{M}^i} \boldsymbol{w} \rangle_{\partial \Omega_h^i} &\leq \nu \left\| \tau^{1/2} (\boldsymbol{u}_h^i - \widehat{\boldsymbol{u}}_h^i) \right\|_{\partial \Omega_h^i} \left\| \tau^{1/2} \left(\boldsymbol{P}^i \boldsymbol{w} - \mathrm{P}_{\boldsymbol{M}^i} \boldsymbol{w} \right) \right\|_{\partial \Omega_h^i} \\
-(\boldsymbol{f}, \boldsymbol{P}^i \boldsymbol{w})_{\Omega_h^i} &\leq \|\boldsymbol{f}\|_{\Omega_h^i} \left\| \boldsymbol{P}^i \boldsymbol{w} \right\|_{\Omega_h^i} \leq \|\boldsymbol{f}\|_{\Omega_h^i} \|\boldsymbol{w}\|_{\Omega_h^i} \leq \|\boldsymbol{f}\|_{\Omega_h^i} \|\boldsymbol{w}\|_{\boldsymbol{H}^1(\Omega)}
\end{aligned}$$

and so, since,

$$\sup_{\substack{\boldsymbol{w} \in \boldsymbol{H}_0^1(\Omega) \\ \boldsymbol{w} \neq \boldsymbol{0}}} \frac{\left\| \tau^{1/2} \left(\boldsymbol{P}^i \boldsymbol{w} - \mathrm{P}_{\boldsymbol{M}^i} \boldsymbol{w} \right) \right\|_{\partial \Omega_h^i}}{\|\boldsymbol{w}\|_{\boldsymbol{H}^1(\Omega)}} \leq \max \left\{ 1, \max_{K \in \Omega_h^1 \cup \Omega_h^2} (\tau h_K)^{1/2} \right\},$$

we can control all the terms on the right-hand side of (29) save for the ones with numerator $\langle \widehat{\sigma}_h^i \boldsymbol{n}^i, \mathrm{P}_{\boldsymbol{M}^i} \boldsymbol{w} \rangle_{\mathcal{I}_h^i}$.

We deal with those terms as follows: first, since the first arguments of both terms are polynomials, we can drop the $\boldsymbol{L}^2$ projections and then add and substract convenient terms as we did when expanding $\mathbb{T}^1 + \mathbb{T}^2$, leading to

$$\begin{aligned}
\langle \widehat{\sigma}_h^1 \boldsymbol{n}^1, \mathrm{P}_{\boldsymbol{M}_h^1} \boldsymbol{w} \rangle_{\mathcal{I}_h^1} + \langle \widehat{\sigma}_h^2 \boldsymbol{n}^2, \mathrm{P}_{\boldsymbol{M}_h^2} \boldsymbol{w} \rangle_{\mathcal{I}_h^2} =& \langle \widehat{\sigma}_h^1 \boldsymbol{n}^1, \boldsymbol{w} \rangle_{\mathcal{I}_h^1} + \langle \widehat{\sigma}_h^2 \boldsymbol{n}^2, \boldsymbol{w} \rangle_{\mathcal{I}_h^2} \\
=& \langle \widehat{\sigma}_h^1 \boldsymbol{n}^1 - \tilde{\sigma}_h^1 \circ \boldsymbol{\varphi}^{-1}, \boldsymbol{w} \rangle_{\mathcal{I}_h^1} + \langle \widehat{\sigma}_h^2 \boldsymbol{n}^2, \boldsymbol{w} - \boldsymbol{w} \circ \boldsymbol{\varphi} \rangle_{\mathcal{I}_h^2} \\
&+ \langle \tilde{\sigma}_h^1 \circ \boldsymbol{\varphi}^{-1}, \boldsymbol{w} \rangle_{\mathcal{I}_h^1} + \langle \widehat{\sigma}_h^2 \boldsymbol{n}^2, \boldsymbol{w} \circ \boldsymbol{\varphi} \rangle_{\mathcal{I}_h^2},
\end{aligned} \tag{30}$$

and the last two terms cancel out as

$$\langle \tilde{\sigma}_h^1 \circ \boldsymbol{\varphi}^{-1}, \boldsymbol{w} \rangle_{\mathcal{I}_h^1} + \langle \widehat{\sigma}_h^2 \boldsymbol{n}^2, \boldsymbol{w} \circ \boldsymbol{\varphi} \rangle_{\mathcal{I}_h^2} = \langle \tilde{\sigma}_h^1, \boldsymbol{w} \circ \boldsymbol{\varphi} \rangle_{\mathcal{I}_h^2} + \langle \widehat{\sigma}_h^2 \boldsymbol{n}^2, \boldsymbol{w} \circ \boldsymbol{\varphi} \rangle_{\mathcal{I}_h^2} = \langle \tilde{\sigma}_h^1 + \widehat{\sigma}_h^2 \boldsymbol{n}^2, \mathrm{P}_{\boldsymbol{M}_h^2} (\boldsymbol{w} \circ \boldsymbol{\varphi}) \rangle_{\mathcal{I}_h^2} = 0,$$

with the last equality coming from (5i).

Since $\widehat{\sigma}_h^1 \boldsymbol{n}^1 - \tilde{\sigma}_h^1 \circ \boldsymbol{\varphi}^1 = \sigma_h^1 \boldsymbol{n}^1 + \boldsymbol{E}_{\sigma_h^1 \boldsymbol{n}^2} \circ \boldsymbol{\varphi}^{-1}$ and $\widehat{\sigma}_h^2 \boldsymbol{n}^2 = \nu \mathrm{L}_h^2 \boldsymbol{n}^2 - \tilde{p}_h^2 \boldsymbol{n}^2 - \tau \nu (\boldsymbol{u}_h^2 - \widehat{\boldsymbol{u}}_h^2)$, we replace this in (30) and use the Cauchy-Schwartz inequality to obtain

$$\begin{aligned}
\langle \widehat{\sigma}_h^1 \boldsymbol{n}^1, \boldsymbol{w} \rangle_{\mathcal{I}_h^1} + \langle \widehat{\sigma}_h^2 \boldsymbol{n}^2, \boldsymbol{w} \rangle_{\mathcal{I}_h^2} =& \langle \sigma_h^1 \boldsymbol{n}^1 + \boldsymbol{E}_{\sigma_h^1 \boldsymbol{n}^2} \circ \boldsymbol{\varphi}^{-1}, \boldsymbol{w} \rangle_{\mathcal{I}_h^1} + \langle \nu \mathrm{L}_h^2 \boldsymbol{n}^2, \boldsymbol{w} - \boldsymbol{w} \circ \boldsymbol{\varphi} \rangle_{\mathcal{I}_h^2} \\
&- \langle \tilde{p}_h^2 \boldsymbol{n}^2, \boldsymbol{w} - \boldsymbol{w} \circ \boldsymbol{\varphi} \rangle_{\mathcal{I}_h^2} - \langle \tau \nu (\boldsymbol{u}_h^2 - \widehat{\boldsymbol{u}}_h^2), \boldsymbol{w} - \boldsymbol{w} \circ \boldsymbol{\varphi} \rangle_{\mathcal{I}_h^2} \\
\leq& \left\| \sigma_h^1 \boldsymbol{n}^1 + \boldsymbol{E}_{\sigma_h^1 \boldsymbol{n}^2} \circ \boldsymbol{\varphi}^{-1} \right\|_{\mathcal{I}_h^1} \|\boldsymbol{w}\|_{\mathcal{I}_h^1} + \nu \left\| h_e^{1/2} \mathrm{L}_h^2 \right\|_{\mathcal{I}_h^2} \left\| h_e^{-1/2} (\boldsymbol{w} - \boldsymbol{w} \circ \boldsymbol{\varphi}) \right\|_{\mathcal{I}_h^2} \\
&+ \left\| \tilde{p}_h^2 \right\|_{\mathcal{I}_h^2} \|\boldsymbol{w} - \boldsymbol{w} \circ \boldsymbol{\varphi}\|_{\mathcal{I}_h^2} + \nu \left\| \tau^{1/2} (\boldsymbol{u}_h^2 - \widehat{\boldsymbol{u}}_h^2) \right\|_{\mathcal{I}_h^2} \left\| \tau^{1/2} (\boldsymbol{w} - \boldsymbol{w} \circ \boldsymbol{\varphi}) \right\|_{\mathcal{I}_h^2}.
\end{aligned}$$

Since $\boldsymbol{w} \in \boldsymbol{H}^1(\Omega) \subset \boldsymbol{H}^1(\Omega_h^i)$, for $i \in \{1,2\}$, we have that

$$\begin{aligned}
\|\boldsymbol{w}\|_{\mathcal{I}_h^1} &\leq \widehat{C}_{\mathrm{tr}}^1 \|\boldsymbol{w}\|_{\boldsymbol{H}^1(\Omega)}, \\
\|\boldsymbol{w} - \boldsymbol{w} \circ \boldsymbol{\varphi}\|_{\mathcal{I}_h^2} &\leq \widehat{C}_{\mathrm{ext}}^2 \max_{e \in \mathcal{I}_h^2} \delta_e \|\boldsymbol{w}\|_{\boldsymbol{H}^1(\Omega)}, \\
\left\| h_e^{-1/2} (\boldsymbol{w} - \boldsymbol{w} \circ \boldsymbol{\varphi}) \right\|_{\mathcal{I}_h^2} &\leq \widehat{C}_{\mathrm{ext}}^2 \max_{e \in \mathcal{I}_h^2} \delta_e h_e^{-1/2} \|\boldsymbol{w}\|_{\boldsymbol{H}^1(\Omega)}, \\
\left\| \tau^{1/2} (\boldsymbol{w} - \boldsymbol{w} \circ \boldsymbol{\varphi}) \right\|_{\mathcal{I}_h^2} &\leq \widehat{C}_{\mathrm{ext}}^2 \max_{e \in \mathcal{I}_h^2} \delta_e \tau^{1/2} \|\boldsymbol{w}\|_{\boldsymbol{H}^1(\Omega)},
\end{aligned}$$

where $\widehat{C}_{\rm tr}^1 > 0$ is a constant related to the trace inequality on Ω_h^1 and $\widehat{C}_{\rm ext}^2 > 0$ is a constant related to the extrapolation error.

Putting everything together and using previously established bounds, we obtain

$$\frac{1}{\nu}\left(1-\tilde{\tilde{C}}^3\right)\|\tilde{p}_h\|_{\Omega_h^1\cup\Omega_h^2} \leq \tilde{\tilde{C}}^1\sum_{i=1}^2\left\|{\rm L}_h^i\right\|_{\Omega_h^i} + \tilde{\tilde{C}}^2\sum_{i=1}^2\left\|\tau^{1/2}(\boldsymbol{u}_h^i-\widehat{\boldsymbol{u}}_h^i)\right\|_{\partial\Omega_h^i} + \frac{2}{\nu}\|\boldsymbol{f}\|_\Omega$$

where

$$\begin{aligned}
\tilde{\tilde{C}}^1 &:= \beta\left(1+\widehat{C}_{\rm tr}^1\max_{e\in\mathcal{I}_h^1}C_e^1C_e^{\rm ext}\delta_e h_e^{-3/2}+\max_{e\in\mathcal{I}_h^2}h_e^{-1/2}\delta_e\right)\\
\tilde{\tilde{C}}^2 &= \beta\max\left\{1,\max_{K\in\Omega_h^1\cup\Omega_h^2}(\tau h_K)^{1/2}\right\}+\beta\widehat{C}_{\rm ext}^2\max_{e\in\mathcal{I}_h^2}\delta_e\tau^{1/2}\\
\tilde{\tilde{C}}^3 &= \beta\widehat{C}_{\rm tr}^1\max_{e\in\mathcal{I}_h^1}C_e^1C_e^{\rm ext}\delta_e h_e^{-3/2}+\beta\widehat{C}_{\rm ext}^2\max_{e\in\mathcal{I}_h^2}\delta_e h_e^{-1/2}.
\end{aligned}$$

If we assume that $\tilde{\tilde{C}}^1, \tilde{\tilde{C}}^2 \leq 2$, then we can conclude that there exists $C_3 > 0$, independent of the meshsize, such that

$$\begin{aligned}
\frac{1}{4\nu^2}\left(1-\tilde{\tilde{C}}^3\right)^2\sum_{i=1}^2\left\|\tilde{p}_h^i\right\|_{\Omega_h^i}^2 &\leq C_3\left(\sum_{i=1}^2\left\|{\rm L}_h^i\right\|_{\Omega_h^i}^2+\sum_{i=1}^2\left\|\tau^{1/2}(\boldsymbol{u}_h^i-\widehat{\boldsymbol{u}}_h^i)\right\|_{\partial\Omega_h^i}^2\right)+\frac{C_3}{\nu^2}\|\boldsymbol{f}\|_\Omega^2\\
&\leq C_3\mathcal{S}({\rm L}_h,\boldsymbol{u}_h,\widehat{\boldsymbol{u}}_h,\tilde{\boldsymbol{u}}_h)^2+\frac{C_3}{\nu^2}\|\boldsymbol{f}\|_\Omega^2
\end{aligned}$$

and so

$$\sum_{i=1}^2\left\|\tilde{p}_h^i\right\|_{\Omega_h^i}^2 \leq \left[\frac{4\nu^2C_3}{\left(1-\tilde{\tilde{C}}^3\right)^2}\right]\mathcal{S}({\rm L}_h,\boldsymbol{u}_h,\widehat{\boldsymbol{u}}_h,\tilde{\boldsymbol{u}}_h)^2+\left[\frac{4C_3}{\left(1-\tilde{\tilde{C}}^3\right)^2}\right]\|\boldsymbol{f}\|_\Omega^2.$$

By assumption (A.10), we have $\dfrac{1}{(1-\tilde{\tilde{C}}^3)^2} \leq 2$ and so the result follows. □

Finally, the statement of Theorem 3 follows from (25), Lemma 10 and Assumption (A.9).

4.5 Error analysis

In this section we employ the stability estimate obtained Theorem 3 in order to deduce the error estimates presented in Theorem 4. To that end, let $i \in \{1,2\}$. We define $E^{{\rm L}^i} := \Pi_{\mathbb{V}^i}{\rm L}-{\rm L}_h^i$, $\boldsymbol{\varepsilon}^{\boldsymbol{u}^i} := \Pi_{\boldsymbol{V}^i}\boldsymbol{u}-\boldsymbol{u}_h^i$, $\varepsilon^{p^i} := \Pi_{V^i}\tilde{p}-\tilde{p}_h^i$, $\boldsymbol{\varepsilon}^{\widehat{\boldsymbol{u}}^i} := {\rm P}_{\boldsymbol{M}^i}\boldsymbol{u}-\widehat{\boldsymbol{u}}_h^i$, $\boldsymbol{\varepsilon}^{\widehat{\sigma}^i}\boldsymbol{n}^i := {\rm P}_{\boldsymbol{M}^i}\left(\nu{\rm L}\boldsymbol{n}^i-\tilde{p}\boldsymbol{n}^i\right)-\widehat{\sigma}_h^i\boldsymbol{n}^i$, where ${\rm P}_{\boldsymbol{M}^i}$ is the $\boldsymbol{L}^2$ projection onto $\boldsymbol{M}_h^i$. Moreover, for $\boldsymbol{x}^1 \in \mathcal{I}_h^1$, let

$$\varepsilon^{\tilde{\boldsymbol{u}}^2}(\boldsymbol{x}^1) = \boldsymbol{\varepsilon}^{\widehat{\boldsymbol{u}}^2}(\boldsymbol{x}^2)+\left|\ell(\boldsymbol{x}^2)\right|\int_0^1\boldsymbol{E}_{E^{{\rm L}^2}}(\boldsymbol{x}(s))\boldsymbol{n}^2{\rm d}s$$

and for $\boldsymbol{x}^2 \in \mathcal{I}_h^2$, let $\varepsilon^{\tilde{\sigma}^1}(\boldsymbol{x}^2) = -\nu\boldsymbol{E}_{E^{{\rm L}^1}}(\boldsymbol{x}^2)\boldsymbol{n}^2+\boldsymbol{E}_{\varepsilon^{p^1}}(\boldsymbol{x}^2)\boldsymbol{n}^2-\tau\nu(\boldsymbol{\varepsilon}^{\boldsymbol{u}^1}-\boldsymbol{\varepsilon}^{\widehat{\boldsymbol{u}}^1})(\boldsymbol{\varphi}(\boldsymbol{x}^2))$.

By Lemma 3.1 in [17], it follows that, for $i \in \{1,2\}$, these projection of the errors satisfy

$$(E_h^{{\rm L}^i},{\rm G})_{\Omega_h^i}+(\boldsymbol{\varepsilon}^{\boldsymbol{u}^i},\nabla\cdot{\rm G})_{\Omega_h^i}-\langle\boldsymbol{\varepsilon}^{\widehat{\boldsymbol{u}}^i},{\rm G}\boldsymbol{n}\rangle_{\partial\Omega_h^i} = -({\rm L}-\Pi_{\mathbb{V}^i}{\rm L},{\rm G})_{\Omega_h^i}, \tag{31a}$$

$$(\nu E_h^{{\rm L}^i},\nabla\boldsymbol{v})_{\Omega_h^i}-(\varepsilon^{p^i},\nabla\cdot\boldsymbol{v})_{\Omega_h^i}-\langle\widehat{\sigma}_h^i\boldsymbol{n}^i,\boldsymbol{v}\rangle_{\partial\Omega_h^i} = 0, \tag{31b}$$

$$-(\boldsymbol{\varepsilon}^{\boldsymbol{u}^i},\nabla q)_{\Omega_h^i}+\langle\boldsymbol{\varepsilon}^{\widehat{\boldsymbol{u}}^i}\cdot\boldsymbol{n},q\rangle_{\partial\Omega_h^i} = 0, \tag{31c}$$

$$\langle\boldsymbol{\varepsilon}^{\widehat{\boldsymbol{u}}^i},\boldsymbol{\mu}\rangle_{\Gamma_h^i\setminus\mathcal{I}_h^i} = 0, \tag{31d}$$

$$\langle\boldsymbol{\varepsilon}^{\widehat{\sigma}^i},\boldsymbol{\mu}\rangle_{\partial\Omega_h^i\setminus\Gamma_h^i} = 0, \tag{31e}$$

where

$$\boldsymbol{\varepsilon}^{\widehat{\sigma}^i}\boldsymbol{n}^i = \nu E^{\mathrm{L}^i}\boldsymbol{n}^i - \varepsilon^{p^i}\boldsymbol{n}^i - \tau\nu(\boldsymbol{\varepsilon}^{\boldsymbol{u}^i} - \boldsymbol{\varepsilon}^{\widehat{\boldsymbol{u}}^i}) \qquad \text{on } \partial\Omega_h^i. \tag{31f}$$

Furthermore, the uniqueness conditions reads

$$(\varepsilon^{p^1}, 1)_{\Omega_h^1} + (\varepsilon^{p^2}, 1)_{\Omega_h^2} = (\Pi_{V^1}\tilde{p} - \tilde{p})_{\Omega_h^1} + (\Pi_{V^2}\tilde{p} - \tilde{p})_{\Omega_h^2}, \tag{31g}$$

which, for $k > 0$, is simply

$$(\varepsilon^{p^1}, 1)_{\Omega_h^1} + (\varepsilon^{p^2}, 1)_{\Omega_h^2} = 0.$$

For the analogue of the transmission conditions, we have that, for $\boldsymbol{x}^1 = \boldsymbol{\varphi}(\boldsymbol{x}^2)$,

$$\begin{aligned}
\varepsilon^{\tilde{\boldsymbol{u}}^2}(\boldsymbol{x}^1) &= \boldsymbol{\varepsilon}^{\widehat{\boldsymbol{u}}^2}(\boldsymbol{x}^2) + \left|\ell(\boldsymbol{x}^2)\right| \int_0^1 \boldsymbol{E}_{E^{\mathrm{L}^2}}(\boldsymbol{x}(s))\boldsymbol{n}^2 \mathrm{d}s \\
&= (\mathrm{P}_{\boldsymbol{M}^2}\boldsymbol{u} - \widehat{\boldsymbol{u}}_h^2)(\boldsymbol{x}^2) + \left|\ell(\boldsymbol{x}^2)\right| \int_0^1 \boldsymbol{E}_{\Pi_{\mathbb{V}^2}\mathrm{L}^2}(\boldsymbol{x}(s))\boldsymbol{n}^2 \mathrm{d}s - \left|\ell(\boldsymbol{x}^2)\right| \int_0^1 \boldsymbol{E}_{\mathrm{L}_h^2}(\boldsymbol{x}(s))\boldsymbol{n}^2 \mathrm{d}s \\
&= \mathrm{P}_{\boldsymbol{M}^2}\boldsymbol{u}(\boldsymbol{x}^2) + \left|\ell(\boldsymbol{x}^2)\right| \int_0^1 \boldsymbol{E}_{\Pi_{\mathbb{V}^2}\mathrm{L}^2}(\boldsymbol{x}(s))\boldsymbol{n}^2 \mathrm{d}s - \tilde{\boldsymbol{u}}_h^2(\boldsymbol{x}^1) \\
&= \mathrm{P}_{\boldsymbol{M}^2}\boldsymbol{u}(\boldsymbol{x}^2) + \left|\ell(\boldsymbol{x}^2)\right| \int_0^1 \Pi_{\mathbb{V}^2}\mathrm{L}^2(\boldsymbol{x}(s))\boldsymbol{n}^2 \mathrm{d}s - \tilde{\boldsymbol{u}}_h^2(\boldsymbol{x}^1)
\end{aligned}$$

where we used (5j) and the definition of the extension operator. Furthermore, since

$$\boldsymbol{u}(\boldsymbol{x}^1) = \boldsymbol{u}(\boldsymbol{x}^2) + \left|\ell(\boldsymbol{x}^2)\right| \int_0^1 \mathrm{L}(\boldsymbol{x}(s))\boldsymbol{n}^2 \mathrm{d}s,$$

we have that

$$\begin{aligned}
\boldsymbol{u}(\boldsymbol{x}^1) - \varepsilon^{\tilde{\boldsymbol{u}}^2}(\boldsymbol{x}^1) &= (\boldsymbol{u} - \mathrm{P}_{\boldsymbol{M}^2}\boldsymbol{u})(\boldsymbol{x}^2) + \left|\ell(\boldsymbol{x}^2)\right| \int_0^1 (\mathrm{L} - \Pi_{\mathbb{V}^2}\mathrm{L})(\boldsymbol{x}(s))\boldsymbol{n}^2 + \tilde{\boldsymbol{u}}_h^2(\boldsymbol{x}^1) \\
&= (\boldsymbol{u} - \mathrm{P}_{\boldsymbol{M}^2}\boldsymbol{u})(\boldsymbol{x}^2) + \left|\ell(\boldsymbol{x}^2)\right| \Lambda_{(\mathrm{L}-\Pi_{\mathbb{V}^2}\mathrm{L})}(\boldsymbol{x}^2) + \left|\ell(\boldsymbol{x}^2)\right| (\mathrm{L} - \Pi_{\mathbb{V}^2}\mathrm{L})(\boldsymbol{x}^1) + \tilde{\boldsymbol{u}}_h^2(\boldsymbol{x}^1)
\end{aligned}$$

Thus, if we take $\boldsymbol{\mu} \in \boldsymbol{M}_h^1$, we have

$$\begin{aligned}
\langle \mathrm{P}_{\boldsymbol{M}_h^1}\boldsymbol{u} - \varepsilon^{\tilde{\boldsymbol{u}}^2}, \boldsymbol{\mu}\rangle_{\mathcal{I}_h^1} &= \langle (\boldsymbol{u} - \mathrm{P}_{\boldsymbol{M}^2}\boldsymbol{u})\circ\boldsymbol{\varphi}^{-1} + |\ell|\,\Lambda_{(\mathrm{L}-\Pi_{\mathbb{V}^2}\mathrm{L})} + |\ell|\,(\mathrm{L} - \Pi_{\mathbb{V}^2}\mathrm{L}), \boldsymbol{\mu}\rangle_{\mathcal{I}_h^1} + \langle \tilde{\boldsymbol{u}}_h^2, \boldsymbol{\mu}\rangle_{\mathcal{I}_h^1} \\
&= \langle (\boldsymbol{u} - \mathrm{P}_{\boldsymbol{M}^2}\boldsymbol{u})\circ\boldsymbol{\varphi}^{-1} + |\ell|\,\Lambda_{(\mathrm{L}-\Pi_{\mathbb{V}^2}\mathrm{L})} + |\ell|\,(\mathrm{L} - \Pi_{\mathbb{V}^2}\mathrm{L}), \boldsymbol{\mu}\rangle_{\mathcal{I}_h^1} + \langle \hat{\boldsymbol{u}}_h^1, \boldsymbol{\mu}\rangle_{\mathcal{I}_h^1}
\end{aligned}$$

Note that, since our analysis is free of hanging nodes, $\boldsymbol{\mu}\circ\boldsymbol{\varphi} \in \boldsymbol{M}_h^2$ and so

$$\langle (\boldsymbol{u} - \mathrm{P}_{\boldsymbol{M}^2}\boldsymbol{u})\circ\boldsymbol{\varphi}^{-1}, \boldsymbol{\mu}\rangle_{\mathcal{I}_h^1} = \langle \boldsymbol{u} - \mathrm{P}_{\boldsymbol{M}^2}\boldsymbol{u}, \boldsymbol{\mu}\circ\boldsymbol{\varphi}\rangle_{\mathcal{I}_h^2} = 0.$$

Substracting the last term of the right-hand side, we obtain

$$\langle \boldsymbol{\varepsilon}^{\widehat{\boldsymbol{u}}^1} - \varepsilon^{\tilde{\boldsymbol{u}}^2}, \boldsymbol{\mu}\rangle_{\mathcal{I}_h^1} = \langle |\ell|\,\Lambda_{(\mathrm{L}-\Pi_{\mathbb{V}^2}\mathrm{L})} + |\ell|\,(\mathrm{L} - \Pi_{\mathbb{V}^2}\mathrm{L}), \boldsymbol{\mu}\rangle_{\mathcal{I}_h^1},$$

which is the analogue to (5h).

On the other hand, following the proof of [43] with $\sigma := \nu\mathrm{L} - \tilde{p}\boldsymbol{I}$ taking the role of $\boldsymbol{q}$, we arrive at

$$\begin{aligned}
\langle \boldsymbol{\varepsilon}^{\widehat{\sigma}^2}\boldsymbol{n}^2 + \varepsilon^{\tilde{\sigma}^1}, \boldsymbol{\mu}\rangle_{\mathcal{I}_h^2} &= \langle \nu\left[(\mathrm{L} - \Pi_{\mathbb{V}^1}\mathrm{L}) - (\mathrm{L} - \Pi_{\mathbb{V}^1}\mathrm{L})\circ\boldsymbol{\varphi}\right]\boldsymbol{n}^1\rangle_{\mathcal{I}_h^2} \\
&\quad - \langle [(\tilde{p} - \Pi_{V^1}\tilde{p}) - (\tilde{p} - \Pi_{V^1}\tilde{p})\circ\boldsymbol{\varphi}]\,\boldsymbol{n}^1\rangle_{\mathcal{I}_h^2}
\end{aligned} \tag{31h}$$

which is the analogue to (5i).

The equations that the projection of the errors satisfy are similar to those of the HDG scheme, where $(\mathrm{L} - \Pi_{\mathbb{V}^i})$ plays the role of H^i and $\boldsymbol{0}$ plays the role of $\boldsymbol{f}$ and $\boldsymbol{g}$. For the transmission conditions, we see that

$$\boldsymbol{T}_1 = |\ell|\,\Lambda_{\boldsymbol{I}^{\mathrm{L}^2}} + |\ell|\,\boldsymbol{I}^{\mathrm{L}^2}$$

and

$$\boldsymbol{T}_2 = \left\{ (\nu \boldsymbol{I}^{\mathrm{L}^1} - \boldsymbol{I}^{p^1}) - (\nu \boldsymbol{I}^{\mathrm{L}^1} - \boldsymbol{I}^{p^1}) \circ \boldsymbol{\varphi} \right\} \boldsymbol{n}^1,$$

in this context, where $\boldsymbol{I}^{\mathrm{L}^1} := \mathrm{L} - \Pi_{\mathbb{V}^1}\mathrm{L}$, $\boldsymbol{I}^{\mathrm{L}^2} := \mathrm{L} - \Pi_{\mathbb{V}^2}\mathrm{L}$ and $\boldsymbol{I}^{p^1} := \tilde{p} - \Pi_{V^1}\tilde{p}$.

To apply our previous estimates, we notice that

$$\left\| h_e^{-1/2} \left(|\ell| \, \Lambda_{\boldsymbol{I}^{\mathrm{L}^2}} + |\ell| \, \boldsymbol{I}^{\mathrm{L}^2} \right) \right\|^2_{\mathcal{I}_h^1} = \left\| h_e^{-1/2} \, |\ell| \, \Lambda_{\boldsymbol{I}^{\mathrm{L}^2}} \right\|^2_{\mathcal{I}_h^1} + \left\| h_e^{-1/2} \, |\ell| \, \boldsymbol{I}^{\mathrm{L}^2} \right\|^2_{\mathcal{I}_h^1} \lesssim \delta^4 h_1^{-4} \left\| \boldsymbol{I}^{\mathrm{L}^2} \right\|^2_{\Omega_h^1} + \delta h_1^{-1} \left\| \boldsymbol{I}^{\mathrm{L}^2} \right\|^2_{\Omega_h^1}$$

and

$$\left\| h_e^{-1/2} \left\{ (\nu \boldsymbol{I}^{\mathrm{L}^1} - \boldsymbol{I}^{p^1}) - (\nu \boldsymbol{I}^{\mathrm{L}^1} - \boldsymbol{I}^{p^1}) \circ \boldsymbol{\varphi} \right\} \boldsymbol{n}^1 \right\|^2_{\mathcal{I}_h^2} \lesssim \delta h_2^{-1} \left\| (\nu \boldsymbol{I}^{\mathrm{L}^1} - \boldsymbol{I}^{p^1}) \right\|^2_{\Omega_h^2} \lesssim \delta h_2^{-1} \left(\left\| \nu \boldsymbol{I}^{\mathrm{L}^1} \right\|^2_{\Omega_h^2} + \left\| \boldsymbol{I}^{p^1} \right\|^2_{\Omega_h^2} \right).$$

By our assumptions, the terms of the form δh_i^{-1} are bounded for $i \in \{1, 2\}$. Therefore, by applying Theorem 3 to the context of the projection of the errors, we have the estimate

$$\mathcal{E}(E^L, \boldsymbol{\varepsilon}^{\boldsymbol{u}}, \varepsilon^p, \boldsymbol{\varepsilon}^{\widehat{\boldsymbol{u}}})^2 \lesssim \left\| \boldsymbol{I}^{\mathrm{L}^2} \right\|^2_{\Omega_h^1} + \left\| \nu \boldsymbol{I}^{\mathrm{L}^1} \right\|^2_{\Omega_h^2} + \left\| \boldsymbol{I}^{p^1} \right\|^2_{\Omega_h^2}, \tag{32}$$

where $\mathcal{E}(E^L, \boldsymbol{\varepsilon}^{\boldsymbol{u}}, \varepsilon^p, \boldsymbol{\varepsilon}^{\widehat{\boldsymbol{u}}})$ is the analogue to $\mathcal{S}(\mathrm{L}_h, \boldsymbol{u}_h, \widehat{\boldsymbol{u}}_h, \tilde{\boldsymbol{u}}_h)$ in the context of the projection of the errors. Thus, Theorem 4 follows by (4) and the estimates from Theorem 3 applied to our context. More precisely, if $(\mathrm{L}, \boldsymbol{u}, \tilde{p}) \in \mathrm{H}^{l_\sigma+1}(\Omega_h^i) \times \boldsymbol{H}^{l_{\boldsymbol{u}}+1}(\Omega_h^i) \times H^{l_\sigma+1}(\Omega_h^i)$, for $l_\sigma, l_{\boldsymbol{u}} \in [0, k]$, we have that

$$\left\| \boldsymbol{I}^{\mathrm{L}^2} \right\|^2_{\Omega_h^1} \lesssim \nu^{-1} h_2^{2(l_\sigma+1)} \left| \nu \mathrm{L} - \tilde{p}\mathbb{I} \right|^2_{\mathrm{H}^{l_\sigma+1}(\Omega)} + h_2^{2(l_{\boldsymbol{u}}+1)} \left| \boldsymbol{u} \right|^2_{\boldsymbol{H}^{l_{\boldsymbol{u}}+1}(\Omega)},$$

and

$$\left\| \nu \boldsymbol{I}^{\mathrm{L}^1} \right\|^2_{\Omega_h^2} + \left\| \boldsymbol{I}^{p^1} \right\|^2_{\Omega_h^2} \lesssim h_1^{2(l_\sigma+1)} \left| \nu \mathrm{L} - \tilde{p}\mathbb{I} \right|^2_{\mathrm{H}^{l_\sigma+1}(\Omega)} + h_1^{2(l_{\boldsymbol{u}}+1)} \nu \left| \boldsymbol{u} \right|^2_{\boldsymbol{H}^{l_{\boldsymbol{u}}+1}(\Omega)},$$

and so, recalling that we set $h = \max\{h_1, h_2\}$, it follows that

$$\mathcal{E}(E^L, \boldsymbol{\varepsilon}^{\boldsymbol{u}}, \varepsilon^p, \boldsymbol{\varepsilon}^{\widehat{\boldsymbol{u}}})^2 \lesssim (1 + \nu^{-1}) h^{2(l_\sigma+1)} \left| \nu \mathrm{L} - \tilde{p}\mathbb{I} \right|^2_{\mathrm{H}^{l_\sigma+1}(\Omega)} + (1 + \nu) h^{2(l_{\boldsymbol{u}}+1)} \left| \boldsymbol{u} \right|^2_{\boldsymbol{H}^{l_{\boldsymbol{u}}+1}(\Omega)}. \tag{33}$$

Adapting the proof of Theorem 3 to our context and using (33), we obtain the upper bounds found in (17). □

5 Numerical experiments

In this section we present the numerical results for the HDG scheme presented in (5) for the two dimensional case in order to validate the theoretical results. In addition we compute the divergence-free postprocessing $(\boldsymbol{u}^*)_h^i$ of $\boldsymbol{u}_h^i$, for $i \in \{1, 2\}$, proposed in [17]. To that end, we define

$$e_{\mathrm{L}} := \left(\sum_{i=1}^{2} \|\mathrm{L} - \mathrm{L}_h^i\|^2_{\Omega_h^i} \right)^{1/2}, \quad e_{\boldsymbol{u}} := \left(\sum_{i=1}^{2} \|\boldsymbol{u} - \boldsymbol{u}_h^i\|^2_{\Omega_h^i} \right)^{1/2}, \quad e_p := \left(\sum_{i=1}^{2} \|p - p_h^i\|^2_{\Omega_h^i} \right)^{1/2}$$

$$e_{\widehat{\boldsymbol{u}}} := \left(\sum_{i=1}^{2} \|\mathrm{P}_{\boldsymbol{M}^i}\boldsymbol{u} - \widehat{\boldsymbol{u}}\|^2_{h, \partial\Omega_h^i} \right)^{1/2}, \quad e_{\boldsymbol{u}^\star} := \left(\sum_{i=1}^{2} \|\boldsymbol{u} - (\boldsymbol{u}_h^\star)^i\|^2_{\Omega_h^i} \right)^{1/2}.$$

Denoting by q_1 and q_2 any of the previous quantities for two consecutive meshes with N_1 and N_2 elements, respectively, we define its estimated order of convergence as

$$\text{e.o.c.} := -2 \frac{\log(q_2/q_1)}{\log(N_2/N_1)}.$$

In all of the following experiments, we will consider the stabilization parameter $\tau \equiv 1$, the exact solution $\boldsymbol{u} = \begin{bmatrix} \sin(\pi x)\sin(\pi y) \\ \cos(\pi x)\cos(\pi y) \end{bmatrix}$, $p = \sin(2\pi x)\sin(2\pi y)$. In our experiments we have observed that the viscosity does not affect the behavior of the errors and hence, in all the experiments except the last one, we will show the convergence tables only for $\nu = 10^{-6}$. For the last experiment we will also report the results for $\nu = 1$.

5.1 Flat interface

We consider the physical domain $\Omega := (0,1)^2$ divided by the flat interface $y = 0.5$ and approximated via two subdomains $\Omega_h^1 := (0,1) \times (0.5 + \delta/2, 1)$ and $\Omega_h^2 := (0,1) \times (0.5 - \delta/2, 1)$, i.e. two rectangular subdomains that are a distance δ apart in the vertical sense. We note that, while our method is proposed to deal with curved interfaces, the actual shape of the physical interface is irrelevant as the estimates depend of the gap between the discretizations of the subdomains.

5.1.1 No gap

We take $\delta = 0$ and, as expected, this is the best-behaved case. In Table 1 we observe the expected $k+1$ convergence for the first quantities and the $k+2$ convergence of the last two, as predicted by Theorem 4.

Table 1: History of convergence of the HDG scheme for $\nu = 10^{-6}$ and $\delta = 0$.

k	N	e_{L}	e.o.c.	$e_{\boldsymbol{u}}$	e.o.c.	e_p	e.o.c.	$e_{\hat{\boldsymbol{u}}}$	e.o.c.	$e_{\boldsymbol{u}^\star}$	e.o.c.
1	32	5.74e+04	—	4.20e+04	—	7.38e-02	—	5.83e+03	—	2.08e+03	—
	120	2.00e+04	1.59	1.28e+04	1.80	2.21e-02	1.83	1.07e+03	2.57	3.72e+02	2.60
	466	5.30e+03	1.96	3.17e+03	2.05	5.43e-03	2.07	1.39e+02	3.01	5.44e+01	2.84
	1812	1.36e+03	2.00	8.15e+02	2.00	1.37e-03	2.02	1.81e+01	3.00	6.83e+00	3.06
	7186	3.56e+02	1.95	2.06e+02	2.00	3.54e-04	1.97	2.40e+00	2.93	9.38e-01	2.88
	28794	8.90e+01	2.00	5.10e+01	2.01	8.80e-05	2.01	3.00e-01	3.00	1.17e-01	2.99
2	32	1.41e+04	—	9.04e+03	—	1.87e-02	—	1.12e+03	—	3.47e+02	—
	120	1.78e+03	3.13	1.15e+03	3.12	2.04e-03	3.36	7.04e+01	4.18	2.03e+01	4.30
	466	2.77e+02	2.74	1.71e+02	2.82	3.07e-04	2.79	5.50e+00	3.76	1.76e+00	3.60
	1812	3.55e+01	3.03	2.17e+01	3.04	3.90e-05	3.04	3.56e-01	4.03	1.17e-01	4.00
	7186	4.61e+00	2.96	2.73e+00	3.01	5.01e-06	2.98	2.37e-02	3.93	7.82e-03	3.92
	28794	5.83e-01	2.98	3.41e-01	3.00	6.31e-07	2.98	1.49e-03	3.98	4.95e-04	3.98
3	32	1.91e+03	—	1.35e+03	—	2.53e-03	—	1.21e+02	—	2.93e+01	—
	120	1.68e+02	3.67	1.09e+02	3.81	2.04e-04	3.81	5.65e+00	4.64	1.24e+00	4.79
	466	1.19e+01	3.90	6.96e+00	4.05	1.36e-05	3.99	2.03e-01	4.90	5.41e-02	4.62
	1812	7.45e-01	4.08	4.49e-01	4.04	8.49e-07	4.09	6.55e-03	5.06	1.68e-03	5.12
	7186	5.27e-02	3.85	2.98e-02	3.94	5.87e-08	3.88	2.37e-04	4.82	6.37e-05	4.75
	28794	3.28e-03	4.00	1.84e-03	4.01	3.66e-09	4.00	7.43e-06	4.99	1.99e-06	4.99

5.1.2 Positive gap of order h

This case is not covered in the theory previously discussed, since (A.5), (A.9) and (A.10) do not hold. However, in Table 2 we see that we have $k+1$ convergence for the first variables in all three cases, but the convergence of $e_{\hat{\boldsymbol{u}}}$ and $e_{\boldsymbol{u}^\star}$ turns sub-optimal. For $k = 1$, we observe that it is strictly greater than $k+1$ but not quite $k+2$, while for $k = 2$ and $k = 3$, it completely goes down to $k+1$ as the rest of the variables.

5.2 Positive gap of order h^2

In Table 3 we observe that the theoretical results are validated as the gap being of order h^2 recovers all the superconvergent quantities of the method, much like in the no gap case.

5.3 Negative gap

While assumption (A.1) ruled out the case with overlaps between the meshes, as we mentioned before, the method works exactly the same as we can observe in Tables 4, 5 and 6. We note that, in this case, in order to carry out the pressure postprocess, we consider all overlaps as regions with “negative area”.

Table 2: History of convergence of the HDG scheme for $\nu = 10^{-6}$ and $\delta = \mathcal{O}(h)$.

k	N	e_{L}	e.o.c.	$e_{\boldsymbol{u}}$	e.o.c.	e_p	e.o.c.	$e_{\hat{\boldsymbol{u}}}$	e.o.c.	$e_{\boldsymbol{u}^\star}$	e.o.c.
1	32	5.35e+04	—	3.86e+04	—	6.52e-02	—	5.92e+03	—	2.50e+03	—
	120	1.99e+04	1.50	1.25e+04	1.71	2.15e-02	1.68	1.12e+03	2.52	4.12e+02	2.73
	468	5.32e+03	1.94	3.16e+03	2.02	5.43e-03	2.02	1.49e+02	2.97	6.13e+01	2.80
	1824	1.36e+03	2.01	8.09e+02	2.00	1.37e-03	2.03	2.01e+01	2.94	8.05e+00	2.99
	7204	3.58e+02	1.94	2.05e+02	2.00	3.55e-04	1.97	3.12e+00	2.71	1.35e+00	2.59
	28888	8.92e+01	2.00	5.10e+01	2.01	8.82e-05	2.00	5.16e-01	2.59	2.42e-01	2.48
2	32	1.61e+04	—	9.02e+03	—	2.08e-02	—	1.67e+03	—	6.41e+02	—
	120	1.99e+03	3.16	1.15e+03	3.12	2.42e-03	3.25	1.79e+02	3.37	8.26e+01	3.10
	468	2.87e+02	2.84	1.67e+02	2.83	3.31e-04	2.92	1.97e+01	3.24	9.66e+00	3.15
	1824	3.73e+01	3.00	2.15e+01	3.02	4.27e-05	3.01	2.49e+00	3.04	1.25e+00	3.00
	7204	4.78e+00	2.99	2.72e+00	3.01	5.55e-06	2.97	3.58e-01	2.83	1.81e-01	2.81
	28888	5.92e-01	3.01	3.38e-01	3.00	6.75e-07	3.03	3.80e-02	3.23	1.93e-02	3.23
3	32	2.25e+03	—	1.12e+03	—	2.84e-03	—	4.12e+02	—	1.74e+02	—
	120	1.76e+02	3.86	1.04e+02	3.60	2.10e-04	3.94	1.20e+01	5.34	5.05e+00	5.35
	468	1.25e+01	3.88	7.01e+00	3.96	1.44e-05	3.94	5.09e-01	4.65	2.29e-01	4.55
	1824	7.83e-01	4.08	4.47e-01	4.05	8.93e-07	4.09	2.41e-02	4.49	1.15e-02	4.40
	7204	5.32e-02	3.92	2.96e-02	3.95	6.00e-08	3.93	1.27e-03	4.28	6.28e-04	4.23
	28888	3.36e-03	3.98	1.85e-03	3.99	3.77e-09	3.98	7.04e-05	4.17	3.53e-05	4.14

Table 3: History of convergence o the HDG scheme for $\nu = 10^{-6}$ and $\delta = \mathcal{O}(h^2)$.

k	N	e_{L}	e.o.c.	$e_{\boldsymbol{u}}$	e.o.c.	e_p	e.o.c.	$e_{\hat{\boldsymbol{u}}}$	e.o.c.	$e_{\boldsymbol{u}^\star}$	e.o.c.
1	32	5.25e+04	—	3.96e+04	—	6.45e-02	—	5.21e+03	—	2.00e+03	—
	120	1.96e+04	1.49	1.27e+04	1.72	2.15e-02	1.66	1.04e+03	2.44	3.58e+02	2.60
	462	5.37e+03	1.92	3.20e+03	2.04	5.51e-03	2.02	1.43e+02	2.94	5.53e+01	2.77
	1816	1.36e+03	2.00	8.15e+02	2.00	1.38e-03	2.03	1.80e+01	3.03	6.85e+00	3.05
	7170	3.58e+02	1.95	2.07e+02	2.00	3.56e-04	1.97	2.42e+00	2.92	9.38e-01	2.90
	28832	8.91e+01	2.00	5.11e+01	2.01	8.81e-05	2.01	3.01e-01	3.00	1.18e-01	2.98
2	32	1.53e+04	—	9.51e+03	—	2.03e-02	—	1.29e+03	—	4.12e+02	—
	120	1.85e+03	3.20	1.19e+03	3.15	2.16e-03	3.39	7.59e+01	4.28	2.39e+01	4.31
	462	2.80e+02	2.80	1.73e+02	2.86	3.11e-04	2.87	5.71e+00	3.84	1.89e+00	3.77
	1816	3.49e+01	3.04	2.15e+01	3.05	3.84e-05	3.06	3.55e-01	4.06	1.20e-01	4.03
	7170	4.60e+00	2.95	2.74e+00	3.00	5.01e-06	2.97	2.42e-02	3.91	8.24e-03	3.90
	28832	5.83e-01	2.97	3.41e-01	2.99	6.31e-07	2.98	1.52e-03	3.98	5.12e-04	3.99
3	32	1.63e+03	—	1.19e+03	—	2.08e-03	—	1.43e+02	—	5.00e+01	—
	120	1.61e+02	3.50	1.06e+02	3.66	1.96e-04	3.57	5.52e+00	4.92	1.29e+00	5.53
	462	1.22e+01	3.82	7.14e+00	4.01	1.40e-05	3.91	2.13e-01	4.83	5.57e-02	4.66
	1816	7.44e-01	4.09	4.49e-01	4.04	8.48e-07	4.10	6.55e-03	5.08	1.70e-03	5.10
	7170	5.27e-02	3.86	3.00e-02	3.94	5.90e-08	3.88	2.39e-04	4.82	6.38e-05	4.78
	28832	3.30e-03	3.98	1.85e-03	4.00	3.68e-09	3.99	7.50e-06	4.98	2.03e-06	4.96

5.4 Hanging nodes

Following our assumption that $h_2 > h_1$, we added the hanging nodes on the top mesh. For the case $\nu = 1$, shown in Table 7, we observe the loss of half a power of h for the approximation of the velocity gradient, the velocity trace and the postprocessed velocity, while the rest of the variables achieve optimal convergence as before. This behavior, as explained in Remark 9 in, [43] is due to the fact that a polynomial of degree k in a face of $\mathcal{I}_h^1$ is not a polynomial on the corresponding face of $\mathcal{I}_h^2$, therefore L^2-projection error appears producing a loss of half a power of h. This is not the case in Table 8, where small enough ν allows us to

Table 4: History of convergence of the HDG scheme for $\nu = 1$ and negative gap of order h^2.

k	N	e_{L}	e.o.c.	$e_{\boldsymbol{u}}$	e.o.c.	e_p	e.o.c.	$e_{\hat{\boldsymbol{u}}}$	e.o.c.	$e_{u^\star}$	e.o.c.
1	32	1.58e-01	—	8.74e-02	—	1.10e-01	—	1.11e-02	—	9.66e-03	—
	124	4.04e-02	2.02	2.32e-02	1.96	2.45e-02	2.22	1.29e-03	3.18	7.79e-04	3.72
	464	1.13e-02	1.93	6.29e-03	1.98	6.14e-03	2.10	1.89e-04	2.91	1.17e-04	2.87
	1812	2.84e-03	2.03	1.59e-03	2.02	1.53e-03	2.04	2.41e-05	3.03	1.49e-05	3.04
	7234	7.27e-04	1.97	4.02e-04	1.99	3.93e-04	1.96	3.20e-06	2.92	1.96e-06	2.93
	28870	1.82e-04	2.00	9.97e-05	2.01	9.76e-05	2.02	3.97e-07	3.02	2.48e-07	2.99
2	32	1.79e-02	—	1.02e-02	—	1.30e-02	—	9.64e-04	—	2.52e-03	—
	124	2.61e-03	2.85	1.44e-03	2.88	2.07e-03	2.72	7.65e-05	3.74	3.57e-05	6.29
	464	3.85e-04	2.90	2.24e-04	2.83	3.18e-04	2.84	6.09e-06	3.84	2.78e-06	3.87
	1812	4.95e-05	3.01	2.83e-05	3.03	4.01e-05	3.04	3.93e-07	4.02	1.82e-07	4.00
	7234	6.41e-06	2.95	3.57e-06	2.99	5.13e-06	2.97	2.57e-08	3.94	1.23e-08	3.89
	28870	8.05e-07	3.00	4.46e-07	3.01	6.44e-07	3.00	1.63e-09	3.99	7.68e-10	4.01
3	32	3.02e-03	—	1.81e-03	—	3.82e-03	—	2.34e-04	—	1.25e-03	—
	124	1.81e-04	4.15	1.09e-04	4.15	1.98e-04	4.37	5.75e-06	5.47	1.83e-06	9.64
	464	1.35e-05	3.94	7.67e-06	4.02	1.38e-05	4.04	2.11e-07	5.01	6.66e-08	5.02
	1812	8.38e-07	4.08	4.89e-07	4.04	8.55e-07	4.08	6.67e-09	5.07	2.07e-09	5.10
	7234	5.91e-08	3.83	3.26e-08	3.92	5.99e-08	3.84	2.47e-10	4.76	7.67e-11	4.76
	28870	3.68e-09	4.01	2.01e-09	4.02	3.70e-09	4.02	7.61e-12	5.03	2.42e-12	5.00

Table 5: History of convergence of the HDG scheme for $\nu = 10^{-3}$ and negative gap of order h^2.

k	N	e_{L}	e.o.c.	$e_{\boldsymbol{u}}$	e.o.c.	e_p	e.o.c.	$e_{\hat{\boldsymbol{u}}}$	e.o.c.	$e_{u^\star}$	e.o.c.
1	32	7.01e+01	—	4.79e+01	—	9.64e-02	—	7.63e+00	—	2.53e+00	—
	124	1.97e+01	1.88	1.22e+01	2.02	2.14e-02	2.22	1.02e+00	2.98	3.81e-01	2.80
	464	5.31e+00	1.98	3.18e+00	2.04	5.45e-03	2.08	1.40e-01	3.00	5.44e-02	2.95
	1812	1.36e+00	2.00	8.15e-01	2.00	1.38e-03	2.02	1.81e-02	3.01	6.83e-03	3.05
	7234	3.58e-01	1.93	2.05e-01	1.99	3.55e-04	1.96	2.45e-03	2.89	9.44e-04	2.86
	28870	8.92e-02	2.01	5.11e-02	2.01	8.81e-05	2.01	3.01e-04	3.03	1.18e-04	3.00
2	32	9.49e+00	—	6.58e+00	—	1.18e-02	—	7.14e-01	—	2.53e-01	—
	124	1.79e+00	2.47	1.06e+00	2.70	2.00e-03	2.62	7.07e-02	3.41	2.23e-02	3.59
	464	2.79e-01	2.82	1.72e-01	2.76	3.09e-04	2.83	5.66e-03	3.83	1.86e-03	3.76
	1812	3.56e-02	3.02	2.17e-02	3.04	3.91e-05	3.04	3.64e-04	4.03	1.23e-04	3.99
	7234	4.58e-03	2.96	2.72e-03	3.00	4.98e-06	2.97	2.38e-05	3.94	8.11e-06	3.93
	28870	5.79e-04	2.99	3.39e-04	3.01	6.27e-07	3.00	1.51e-06	3.98	5.13e-07	3.99
3	32	2.73e+00	—	1.70e+00	—	3.80e-03	—	2.37e-01	—	8.02e-02	—
	124	1.64e-01	4.15	1.01e-01	4.17	1.97e-04	4.37	5.84e-03	5.47	1.70e-03	5.69
	464	1.20e-02	3.96	7.02e-03	4.04	1.37e-05	4.04	2.09e-04	5.05	5.65e-05	5.16
	1812	7.46e-04	4.08	4.49e-04	4.03	8.50e-07	4.08	6.60e-06	5.07	1.71e-06	5.13
	7234	5.33e-05	3.81	2.99e-05	3.91	5.95e-08	3.84	2.44e-07	4.76	6.49e-08	4.73
	28870	3.31e-06	4.02	1.85e-06	4.02	3.68e-09	4.02	7.50e-09	5.03	2.03e-09	5.01

recover the optimality of the method. This suggests that the ratio between ν and the meshsize may dominate the error estimate for the previously sub-optimal quantities. However, following Example 5.3 in [43], the use of the transmission conditions (6) might lead to a recovery of the optimal convergence by assigning the transfer of numerical fluxes on the finer mesh as opposed to the coarser one as shown in this work.

Table 6: History of convergence of the HDG scheme for $\nu = 10^{-6}$ and negative gap of order h^2.

k	N	e_{L}	e.o.c.	$e_{\boldsymbol{u}}$	e.o.c.	e_p	e.o.c.	$e_{\hat{\boldsymbol{u}}}$	e.o.c.	$e_{u^\star}$	e.o.c.
2	32	9.49e+03	—	6.58e+03	—	1.18e-02	—	7.13e+02	—	2.53e+02	—
	124	1.79e+03	2.47	1.06e+03	2.70	2.00e-03	2.62	7.07e+01	3.41	2.23e+01	3.59
	464	2.79e+02	2.82	1.72e+02	2.76	3.09e-04	2.83	5.66e+00	3.83	1.86e+00	3.76
	1812	3.56e+01	3.02	2.17e+01	3.04	3.91e-05	3.04	3.64e-01	4.03	1.23e-01	3.99
	7234	4.58e+00	2.96	2.72e+00	3.00	4.98e-06	2.97	2.38e-02	3.94	8.11e-03	3.93
	28870	5.79e-01	2.99	3.39e-01	3.01	6.27e-07	3.00	1.51e-03	3.98	5.13e-04	3.99
3	32	2.73e+03	—	1.70e+03	—	3.80e-03	—	2.37e+02	—	8.02e+01	—
	124	1.64e+02	4.15	1.01e+02	4.17	1.97e-04	4.37	5.84e+00	5.47	1.70e+00	5.69
	464	1.20e+01	3.96	7.02e+00	4.04	1.37e-05	4.04	2.09e-01	5.05	5.65e-02	5.16
	1812	7.46e-01	4.08	4.49e-01	4.03	8.50e-07	4.08	6.60e-03	5.07	1.71e-03	5.13
	7234	5.33e-02	3.81	2.99e-02	3.91	5.95e-08	3.84	2.44e-04	4.76	6.49e-05	4.73
	28870	3.31e-03	4.02	1.85e-03	4.02	3.68e-09	4.02	7.50e-06	5.03	2.03e-06	5.01

Table 7: History of convergence of the HDG scheme for $\nu = 1$, $\delta = \mathcal{O}(h^2)$ and hanging nodes present on the discrete interfaces.

k	N	e_{L}	e.o.c.	$e_{\boldsymbol{u}}$	e.o.c.	e_p	e.o.c.	$e_{\hat{\boldsymbol{u}}}$	e.o.c.	$e_{u^\star}$	e.o.c.
1	76	1.85e-01	—	5.40e-02	—	1.54e-01	—	1.98e-02	—	7.70e-03	—
	290	5.71e-02	1.76	1.66e-02	1.77	3.88e-02	2.06	2.71e-03	2.97	9.42e-04	3.14
	1150	1.93e-02	1.58	4.52e-03	1.88	1.33e-02	1.55	4.53e-04	2.60	1.39e-04	2.78
	4492	6.56e-03	1.58	1.17e-03	1.98	4.49e-03	1.60	8.07e-05	2.53	2.43e-05	2.56
	17986	2.29e-03	1.52	2.97e-04	1.98	1.59e-03	1.50	1.46e-05	2.47	4.45e-06	2.45
	70030	7.90e-04	1.56	7.24e-05	2.08	5.43e-04	1.58	2.62e-06	2.52	8.23e-07	2.49
2	76	4.03e-02	—	7.94e-03	—	4.58e-02	—	8.52e-03	—	4.01e-03	—
	290	4.18e-03	3.38	1.10e-03	2.95	4.39e-03	3.50	3.75e-04	4.66	1.77e-04	4.66
	1150	6.21e-04	2.77	1.53e-04	2.87	5.07e-04	3.13	2.29e-05	4.06	1.05e-05	4.11
	4492	1.00e-04	2.68	2.01e-05	2.98	7.47e-05	2.81	1.11e-06	4.44	4.47e-07	4.63
	17986	1.73e-05	2.53	2.57e-06	2.97	1.30e-05	2.52	1.08e-07	3.37	4.52e-08	3.30
	70030	2.98e-06	2.59	3.16e-07	3.08	2.20e-06	2.62	8.96e-09	3.66	3.66e-09	3.70
3	76	3.34e-02	—	3.12e-03	—	7.20e-02	—	6.89e-03	—	3.03e-03	—
	290	6.20e-04	5.95	9.01e-05	5.29	1.25e-03	6.05	1.04e-04	6.26	4.75e-05	6.21
	1150	2.80e-05	4.50	5.67e-06	4.02	5.05e-05	4.66	4.12e-06	4.69	1.96e-06	4.63
	4492	1.50e-06	4.29	3.72e-07	4.00	2.25e-06	4.57	1.67e-07	4.70	8.26e-08	4.65
	17986	1.05e-07	3.84	2.37e-08	3.97	1.29e-07	4.12	8.38e-09	4.31	4.21e-09	4.29
	70030	8.05e-09	3.77	1.43e-09	4.14	8.29e-09	4.04	4.44e-10	4.32	2.24e-10	4.31

6 Conclusions and discussion

In this work we developed an HDG method for the Stokes equations of an incompressible fluid whose domain is discretized by two independent polygonal subdomains with different meshes. In order to obtain a stability estimate, we employed an energy argument, a duality argument to bound the norm of the discrete velocity and an inf-sup condition for the norm of the discrete pressure. In particular, the proposed scheme is stable under certain hypothesis related to the size of the gap δ in comparison to the meshsize h. To obtain the previous estimates, a transferring technique, originally designed for non- polygonal domains, was successfully adapted to our context. On the other hand, to deduce the error estimates we used the stability bounds and the properties of the HDG projection. This allows to conclude that our method is optimal under the assumptions that relate the size of the gap and the meshsize. Moreover, the numerical experiments presented validate these results, showing $k+1$ convergence for all the variables and $k+2$

Table 8: History of convergence of the HDG scheme for $\nu = 10^{-6}$, $\delta = \mathcal{O}(h^2)$ and hanging nodes present on the discrete interfaces.

k	N	$e_{\rm L}$	e.o.c.	$e_{\boldsymbol{u}}$	e.o.c.	e_p	e.o.c.	$e_{\hat{\boldsymbol{u}}}$	e.o.c.	$e_{u^\star}$	e.o.c.
1	76	3.91e+04	—	2.67e+04	—	4.64e-02	—	5.78e+03	—	2.48e+03	—
	290	1.43e+04	1.50	8.97e+03	1.63	1.54e-02	1.64	7.92e+02	2.97	2.92e+02	3.19
	1150	3.88e+03	1.90	2.29e+03	1.98	3.95e-03	1.98	1.00e+02	3.00	4.00e+01	2.88
	4492	1.02e+03	1.96	6.02e+02	1.96	1.03e-03	1.97	1.38e+01	2.91	5.11e+00	3.02
	17986	2.62e+02	1.97	1.51e+02	1.99	2.60e-04	1.99	1.76e+00	2.98	6.70e-01	2.93
	70030	6.48e+01	2.05	3.70e+01	2.07	6.40e-05	2.06	2.14e-01	3.10	8.46e-02	3.04
2	76	1.32e+04	—	5.42e+03	—	2.11e-02	—	2.86e+03	—	1.37e+03	—
	290	1.36e+03	3.40	8.02e+02	2.85	1.69e-03	3.77	1.29e+02	4.63	6.11e+01	4.64
	1150	1.94e+02	2.83	1.16e+02	2.81	2.13e-04	3.00	6.03e+00	4.45	2.67e+00	4.54
	4492	2.46e+01	3.03	1.53e+01	2.97	2.73e-05	3.02	3.64e-01	4.12	1.59e-01	4.14
	17986	3.26e+00	2.92	1.96e+00	2.97	3.55e-06	2.94	2.17e-02	4.07	9.03e-03	4.14
	70030	4.10e-01	3.05	2.40e-01	3.09	4.45e-07	3.06	1.34e-03	4.10	5.52e-04	4.11
3	76	4.61e+03	—	8.07e+02	—	7.13e-03	—	1.10e+03	—	4.87e+02	—
	290	1.24e+02	5.39	7.17e+01	3.62	1.50e-04	5.77	9.71e+00	7.06	4.28e+00	7.07
	1150	8.39e+00	3.91	4.87e+00	3.90	9.64e-06	3.99	2.06e-01	5.59	8.12e-02	5.76
	4492	5.73e-01	3.94	3.34e-01	3.93	6.50e-07	3.96	5.75e-03	5.25	1.77e-03	5.61
	17986	3.78e-02	3.92	2.14e-02	3.96	4.22e-08	3.94	1.79e-04	5.00	5.13e-05	5.11
	70030	2.32e-03	4.10	1.30e-03	4.13	2.59e-09	4.11	5.43e-06	5.15	1.58e-06	5.12

convergence for the divergence-free postprocess of the discrete velocity. Furthermore, experiments that do not exactly fit under our assumptions were presented with positive results, suggesting the robustness of the method in broader contexts.

The extension of the method proposed here to the case of Oseen equations is straight forward. In that case, the flux (5f) must be defined as

$$\widehat{\sigma}_h^i \boldsymbol{n}^i := \nu \mathrm{L}_h^i \boldsymbol{n}^i - \tilde{p}_h^i \boldsymbol{n}^i - (\widehat{\boldsymbol{u}}_h^i \otimes \boldsymbol{\beta}) \boldsymbol{n}^i - \tau\nu(\boldsymbol{u}_h^i - \widehat{\boldsymbol{u}}_h^i) \qquad \text{on } \partial\Omega_h^i,$$

where $\boldsymbol{\beta}$ is the given convective velocity and the stabilization parameter must satisfy that $\tau\nu - \frac{1}{2}(\boldsymbol{\beta}\cdot\boldsymbol{n}) > 0$. Similarly, the transferred interface condition (5k) becomes

$$\tilde{\boldsymbol{\sigma}}_h^1(\boldsymbol{x}^2) = -\nu \boldsymbol{E}_{\mathrm{L}_h^1}(\boldsymbol{x}^2)\boldsymbol{n}^2 + \boldsymbol{E}_{\tilde{p}_h^1}(\boldsymbol{x}^2)\boldsymbol{n}^2 - (\widehat{\boldsymbol{u}}_h^i(\boldsymbol{x}^1) \otimes \boldsymbol{\beta}(\boldsymbol{x}^2))\boldsymbol{n}^i - \tau\nu(\boldsymbol{u}_h^1(\boldsymbol{x}^1) - \widehat{\boldsymbol{u}}_h^1(\boldsymbol{x}^1)).$$

The stability and error analysis of the method follows by the techniques presented in this work, together with the results shown in [45]. Extending the method to the incompressible Navier-Stokes equations is an ongoing work.

Acknowledgement

Ngoc-Cuong Nguyen gratefully acknowledge the NASA for supporting this work under grant number NNX16AP15A. Manuel Solano was supported by ANID–Chile through Fondecyt 1200569 and by Centro de Modelamiento Matemático (CMM), ACE210010 and FB210005, BASAL funds for center of excellence from ANID-Chile

A Appendix

A.1 Proof of Lemma 7

Proof. Since $\boldsymbol{\varphi}$ is an isometric bijection, we have that $\boldsymbol{n}^1 \circ \boldsymbol{\varphi} = -\boldsymbol{n}^2$ and write $F = \boldsymbol{\varphi}(e)$. We bound each term in the right-hand side of (19) as follows:

For I^1, we have

$$I^1 \leq \sum_{e\in\mathcal{I}_h^1} \frac{2}{\nu}\delta_e^{-2/7}\tau^{-1}\left\|\sigma_h^1\boldsymbol{n}^1 + \boldsymbol{E}_{\sigma_h^1\boldsymbol{n}^2}\circ\boldsymbol{\varphi}^{-1}\right\|_e^2 + \frac{\nu}{8}\left\|\delta_e^{1/7}\tau^{1/2}\hat{\boldsymbol{u}}_h^1\right\|_e^2$$

Furthermore,

$$\begin{aligned}\left\|\sigma_h^1\boldsymbol{n}^1 + \boldsymbol{E}_{\sigma_h^1\boldsymbol{n}^2}\circ\boldsymbol{\varphi}^{-1}\right\|_e^2 &= \left\|\left(\sigma_h^1\boldsymbol{n}^1\circ\boldsymbol{\varphi} + \boldsymbol{E}_{\sigma_h^1\boldsymbol{n}^2}\right)\right\|_F^2 = \left\|\left(\nu(\boldsymbol{E}_{\mathrm{L}_h^1} - \mathrm{L}_h^1\circ\boldsymbol{\varphi})\boldsymbol{n}^2 + (\boldsymbol{E}_{\tilde{p}_h^1} - \tilde{p}_h^1\circ\boldsymbol{\varphi})\boldsymbol{n}^2\right)\right\|_F^2 \\ &\leq 2\left\{\left\|\left(\nu(\boldsymbol{E}_{\mathrm{L}_h^1} - \mathrm{L}_h^1\circ\boldsymbol{\varphi})\right)\right\|_F^2 + \left\|\left(\boldsymbol{E}_{\tilde{p}_h^1} - \tilde{p}_h^1\circ\boldsymbol{\varphi}\right)\right\|_F^2\right\}.\end{aligned}$$

According to Lemma 2, there exists $C_e^1 > 0$ such that

$$\left\|\nu(\boldsymbol{E}_{\mathrm{L}_h^1} - \mathrm{L}_h^1\circ\boldsymbol{\varphi})\right\|_F \leq \nu C_e^1 C_e^{\mathrm{ext}}\delta_e h_e^{-3/2}\left\|\mathrm{L}_h^1\right\|_{K_e},$$

and

$$\left\|\boldsymbol{E}_{\tilde{p}_h^1} - \tilde{p}_h^1\circ\boldsymbol{\varphi}\right\|_F \leq C_e^1 C_e^{\mathrm{ext}}\delta_e h_e^{-3/2}\left\|\tilde{p}_h^1\right\|_{K_e},$$

thus obtaining the bound

$$I^1 \leq 4\nu^{-1}\max_{e\in\mathcal{I}_h^1}\left(C_e^1 C_e^{\mathrm{ext}}\right)^2\delta_e^{12/7}h_e^{-3}\tau^{-1}\left(\nu^2\left\|\mathrm{L}_h^1\right\|_{\Omega_h^1}^2 + \left\|\tilde{p}_h^1\right\|_{\Omega_h^1}\right) + \frac{\nu}{8}\left\|\delta_e^{1/7}\tau^{1/2}\hat{\boldsymbol{u}}_h^1\right\|_{\mathcal{I}_h^1}.$$

For I^2 we use the estimates in (9) to obtain

$$\begin{aligned}I^2 &\leq \nu\sum_{e\in\mathcal{I}_h^2}\left\{8\left\||\ell|^{1/2}\,\Lambda_{\mathrm{L}_h^2}\right\|_e^2 + \frac{1}{32}\left\||\ell|^{-1/2}\left(\tilde{\boldsymbol{u}}_h^2\circ\boldsymbol{\varphi} - \hat{\boldsymbol{u}}_h^2\right)\right\|_F^2\right\} \\ &\leq \nu\left[\max_{e\in\mathcal{I}_h^2} 8r_F^3\left(C_F^{\mathrm{ext}}C_F^{\mathrm{inv}}\right)^2\right]\left\|\mathrm{L}_h^2\right\|_{\Omega_h^2}^2 + \nu\frac{1}{32}\left\||\ell|^{-1/2}\left(\tilde{\boldsymbol{u}}_h^2\circ\boldsymbol{\varphi} - \hat{\boldsymbol{u}}_h^2\right)\right\|_{\mathcal{I}_h^2}^2.\end{aligned}$$

and for I^3, by Young's inequality and the fact that $l(\boldsymbol{x}) \leq \delta_F$, we have that

$$I^3 \leq 8\nu\left[\max_{F\in\mathcal{I}_h^2}\delta_F\tau\right]\left\|\tau^{1/2}(\boldsymbol{u}_h^2 - \hat{\boldsymbol{u}}_h^2)\right\|_{\mathcal{I}_h^2}^2 + \nu\frac{1}{32}\left\||\ell|^{-1/2}\left(\tilde{\boldsymbol{u}}_h^2\circ\boldsymbol{\varphi} - \hat{\boldsymbol{u}}_h^2\right)\right\|_{\mathcal{I}_h^2}^2.$$

Similarly, for I^4, I^5 and I^6, we have the straightforward bounds

$$\begin{aligned}I^4 &\leq \nu\max_{e\in\mathcal{I}_h^1}\delta_e^{2/7}\left\|\tau^{1/2}(\boldsymbol{u}_h^1 - \hat{\boldsymbol{u}}_h^1)\right\|_{\mathcal{I}_h^1}^2 + \frac{\nu}{4}\left\|\delta_e^{1/7}\tau^{1/2}\hat{\boldsymbol{u}}_h^1\right\|_{\mathcal{I}_h^1}^2, \\ I^5 &\leq \nu\max_{e\in\mathcal{I}_h^1}\left(C_e^{\mathrm{tr}}\right)^2\delta_e^{2/7}h_e^{-1}\tau\left\|\boldsymbol{u}_h^1\right\|_{\Omega_h^1}^2 + \frac{\nu}{4}\left\|\delta_e^{1/7}\tau^{1/2}\hat{\boldsymbol{u}}_h^1\right\|_{\mathcal{I}_h^1}^2, \\ I^6 &\leq 2\nu^{-1}\left\|\delta_e^{-1/7}\tau^{-1/2}\boldsymbol{T}_2\right\|_{\mathcal{I}_h^2}^2 + \frac{\nu}{8}\left\|\delta_e^{1/7}\tau^{1/2}\hat{\boldsymbol{u}}_h^1\right\|_{\mathcal{I}_h^1}^2.\end{aligned}$$

For I^7,

$$\begin{aligned}I^7 &= \sum_{F\in\mathcal{I}_h^2} -\langle\sigma_h^2\boldsymbol{n}^2, \boldsymbol{T}_1\circ\boldsymbol{\varphi}\rangle_F + \nu\langle\tau(\boldsymbol{u}_h^2 - \hat{\boldsymbol{u}}_h^2), \boldsymbol{T}_1\circ\boldsymbol{\varphi}\rangle_F \\ &\leq \frac{\nu}{4}\max_{F\in\mathcal{I}_h^2}\delta_F(C_F^{\mathrm{tr}})^2\left(\left\|\mathrm{L}_h^2\right\|_{\Omega_h^2}^2 + \left\|\tilde{p}_h^2\right\|_{\Omega_h^2}^2\right) + \frac{1}{\nu}\left\|\delta_e^{-1/2}h_e^{-1}\boldsymbol{T}_1\right\|_{\mathcal{I}_h^1}^2 \\ &\quad + \nu\max_{F\in\mathcal{I}_h^2}\delta_F\left\|\tau^{1/2}(\boldsymbol{u}_h^2 - \hat{\boldsymbol{u}}_h^2)\right\|_{\mathcal{I}_h^2}^2 + \frac{\nu}{4}\left\|\delta_e^{-1/2}\boldsymbol{T}_1\right\|_{\mathcal{I}_h^1}^2.\end{aligned}$$

For I^8,

$$I^8 \le \sum_{F \in \mathcal{I}_h^2} \left\{ 2\nu^{-1} \left\| |\ell|^{1/2} \tilde{p}_h^2 \boldsymbol{n}^2 \right\|_F^2 + \frac{\nu}{8} \left\| |\ell|^{-1/2} \left(\tilde{u}_h^2 \circ \phi - \widehat{\boldsymbol{u}}_h^2 \right) \right\|_F^2 \right\}$$
$$\le \left[\max_{F \in \mathcal{I}_h^2} 2\nu^{-1} (\delta_F h_F^{-1} C_F^{\mathrm{tr}}) \right] \left\| \tilde{p}_h^2 \right\|_{\Omega_h^2}^2 + \frac{\nu}{8} \left\| |\ell|^{-1/2} \left(\tilde{u}_h^2 \circ \phi - \widehat{\boldsymbol{u}}_h^2 \right) \right\|_{\mathcal{I}_h^2}^2 .$$

For the source terms, we have

$$\sum_{i=1}^2 \nu(\mathrm{H}, \mathrm{L}_h^i)_{\Omega_h^i} \le 16\nu \sum_{i=1}^2 \|\mathrm{H}\|_{\Omega_h^i}^2 + \frac{\nu}{64} \sum_{i=1}^2 \left\| \mathrm{L}_h^i \right\|_{\Omega_h^i}^2 ,$$
$$\sum_{i=1}^2 (\boldsymbol{f}, \boldsymbol{u}_h^i)_{\Omega_h^i} \le \frac{2}{\nu} \|\boldsymbol{f}\|_{\Omega}^2 + \frac{\nu}{4} \sum_{i=1}^2 \left\| \boldsymbol{u}_h^i \right\|_{\Omega_h^i}^2 .$$

We decompose

$$\sum_{i=1}^2 \langle \boldsymbol{g}, \widehat{\sigma} \boldsymbol{n}_h^i \rangle_{\Gamma_h^i \setminus \mathcal{I}_h^i} = \sum_{i=1}^2 \langle \boldsymbol{g}, \nu \mathrm{L}_h^i \boldsymbol{n}^i - \tilde{p}_h^i \boldsymbol{n}^i - \tau\nu (\boldsymbol{u}_h^i - \widehat{\boldsymbol{u}}_h^i) \rangle_{\Gamma_h^i \setminus \mathcal{I}_h^i}$$
$$= \sum_{i=1}^2 \langle h_e^{-1/2} \boldsymbol{g}, h_e^{1/2} \left(\nu \mathrm{L}_h^i \boldsymbol{n}^i - \tilde{p}_h^i \boldsymbol{n}^i \right) \rangle_{\Gamma_h^i \setminus \mathcal{I}_h^i} - \nu \sum_{i=1}^2 \langle \boldsymbol{g}, \tau (\boldsymbol{u}_h^i - \widehat{\boldsymbol{u}}_h^i) \rangle_{\Gamma_h^i \setminus \mathcal{I}_h^i}$$

and use Young's inequality and a discrete trace inequality to obtain

$$\langle h_e^{-1/2} \boldsymbol{g}, h_e^{1/2} \left(\nu \mathrm{L}_h^i \boldsymbol{n}^i - \tilde{p}_h^i \boldsymbol{n}^i \right) \rangle_{\Gamma_h^i \setminus \mathcal{I}_h^i} \le \sum_{e \in \Gamma_h^i \setminus \mathcal{I}_h^i} \left\{ 16\nu (C_e^{\mathrm{tr}})^2 h_e^{-1} \|\boldsymbol{g}\|_e^2 + \frac{\nu}{64} \left\| \mathrm{L}_h^i \right\|_{K_e}^2 + \frac{1}{16\nu} \left\| \tilde{p}_h^i \right\|_{K_e}^2 \right\}$$

for $i \in \{1, 2\}$. From this, it follows that

$$\sum_{i=1}^2 \langle h_e^{-1/2} \boldsymbol{g}, h_e^{1/2} \left(\nu \mathrm{L}_h^i \boldsymbol{n}^i - \tilde{p}_h^i \boldsymbol{n}^i \right) \rangle_{\Gamma_h^i \setminus \mathcal{I}_h^i} \le \max_{e \in \Gamma_h^1 \setminus \mathcal{I}_h^1 \cup \Gamma_h^2 \setminus \mathcal{I}_h^2} 32\nu (C_e^{\mathrm{tr}}) h_e^{-1} \|\boldsymbol{g}\|_{\Gamma}^2 + \frac{\nu}{8} \sum_{i=1}^2 \left\| \mathrm{L}_h^i \right\|_{\Omega_h^i}^2 + \frac{1}{8\nu} \sum_{i=1}^2 \left\| \tilde{p}_h^i \right\|_{\Omega_h^i}^2 .$$

For the second term,

$$-\nu \sum_{i=1}^2 \langle \boldsymbol{g}, \tau (\boldsymbol{u}_h^i - \widehat{\boldsymbol{u}}_h^i) \rangle_{\Gamma_h^i \setminus \mathcal{I}_h^i} \le \nu \sum_{i=1}^2 \sum_{e \in \Gamma_h^i \setminus \mathcal{I}_h^i} 4 \left\| \tau^{1/2} \boldsymbol{g} \right\|_e^2 + \nu \sum_{i=1}^2 \sum_{e \in \Gamma_h^i \setminus \mathcal{I}_h^i} \frac{1}{16} \left\| \tau^{1/2} (\boldsymbol{u}_h^i - \widehat{\boldsymbol{u}}_h^i) \right\|_e^2$$
$$\le 8\nu \left(\max_{e \in \Gamma_h^1 \setminus \mathcal{I}_h^1 \cup \Gamma_h^2 \setminus \mathcal{I}_h^2} \tau \right) \|\boldsymbol{g}\|_{\Gamma}^2 + \frac{\nu}{16} \sum_{i=1}^2 \left\| \tau^{1/2} (\boldsymbol{u}_h^i - \widehat{\boldsymbol{u}}_h^i) \right\|_{\partial\Omega_h^i}^2 .$$

Putting everything together and dividing by $\nu > 0$, we have

$$
\begin{aligned}
\mathcal{S}(\mathrm{L}_h, \boldsymbol{u}_h, \widehat{\boldsymbol{u}}_h, \tilde{\boldsymbol{u}}_h)^2 \leq & \left(4 \max_{e\in\mathcal{I}_h^1}(C_e^1 C_e^{\mathrm{ext}})^2 \delta_e^{12/7} h_e^{-3}\tau^{-1} + \max_{e\in\mathcal{I}_h^2} \frac{8}{3} r_e^3 (C_e^{\mathrm{ext}} C_e^{\mathrm{inv}})^2 + \frac{1}{4}\max_{e\in\mathcal{I}_h^2} \delta_e (C_e^{\mathrm{tr}})^2 \right.\\
& \left. + \frac{3}{64}\right) \sum_{i=1}^2 \left\|\mathrm{L}_h^i\right\|_{\Omega_h^i}^2 + \left(8\max_{e\in\mathcal{I}_h^2}\delta_e\tau + \max_{e\in\mathcal{I}_h^1}\delta_e^{2/7} + \max_{e\in\mathcal{I}_h^2}\delta_e + \frac{1}{16}\right)\sum_{i=1}^2 \left\|\tau^{1/2}(\boldsymbol{u}_h^i - \widehat{\boldsymbol{u}}_h^i)\right\|_{\partial\Omega_h^i}^2\\
& + \frac{1}{16}\left\||\ell|^{-1/2}\left(\tilde{\boldsymbol{u}}_h^2\circ\boldsymbol{\varphi} - \widehat{\boldsymbol{u}}_h^2\right)\right\|_{\mathcal{I}_h^2}^2 + \frac{3}{4}\left\|\delta_e^{1/7}\tau^{1/2}\widehat{\boldsymbol{u}}_h^1\right\|_{\mathcal{I}_h^1}^2\\
& + \left(\frac{1}{4} + \max_{e\in\mathcal{I}_h^1}(C_e^{\mathrm{tr}})^2\delta_e^{2/7}h_e^{-1}\tau\right)\sum_{i=1}^2\left\|\boldsymbol{u}_h^i\right\|_{\Omega_h^i}^2\\
& + \left(4\nu^{-2}\max_{e\in\mathcal{I}_h^1}(C_e^1 C_e^{\mathrm{ext}})^2\delta_e^{12/7}h_e^{-3}\tau^{-1} + \frac{1}{4}\max_{e\in\mathcal{I}_h^2}\delta_e(C_e^{\mathrm{tr}})^2\right.\\
& \left. + 2\nu^{-2}\max_{e\in\mathcal{I}_h^2}\delta_e h_e^{-1}C_e^{\mathrm{tr}} + \frac{\nu^{-2}}{8}\right)\sum_{i=1}^2\left\|\tilde{p}_h^i\right\|_{\Omega_h^i}^2\\
& + 16\sum_{i=1}^2\left\|\mathrm{H}\right\|_{\Omega_h^i}^2 + 2\nu^{-2}\left\|\boldsymbol{f}\right\|_\Omega^2 + \max_{e\in\Gamma_h^1\setminus\mathcal{I}_h^1\cup\Gamma_h^2\setminus\mathcal{I}_h^2}\left[32(C_e^{\mathrm{tr}})^2h_e^{-1} + 8\tau\right]\left\|\boldsymbol{g}\right\|_\Gamma^2\\
& + \left\|\sqrt{2}\nu^{-1/2}\delta_e^{-1/7}\tau^{-1/2}\boldsymbol{T}_2\right\|_{\mathcal{I}_h^2}^2 + \left\|(2^{-1}\delta_e^{-1/2} + \nu^{-1}\delta_e^{-1/2}h_e^{-1}\delta_e^{-1/2})\boldsymbol{T}_1\right\|_{\mathcal{I}_h^1}^2.
\end{aligned}
$$

Due to our assumptions some of the terms on the right hand side as follows. For the first term we employ (A.5), whereas for the second one we use (A.6). The definition of $\mathcal{S}$ (cf. (13)) is used for the third and fourth terms. Finally, for the fifth and sixth terms, we just consider the definition of $C_{\boldsymbol{u}}^{\mathcal{S}}$ and $C_{\tilde{p}}^{\mathcal{S}}$ Assumption (A.9):

$$
\begin{aligned}
\mathcal{S}(\mathrm{L}_h, \boldsymbol{u}_h, \widehat{\boldsymbol{u}}_h, \tilde{\boldsymbol{u}}_h)^2 \leq & \frac{61}{64}\mathcal{S}(\mathrm{L}_h, \boldsymbol{u}_h, \widehat{\boldsymbol{u}}_h, \tilde{\boldsymbol{u}}_h)^2 + C_{\boldsymbol{u}}^{\mathcal{S}}\sum_{i=1}^2\left\|\boldsymbol{u}_h^i\right\|_{\Omega_h^i}^2 + C_{\tilde{p}}^{\mathcal{S}}\sum_{i=1}^2\left\|\tilde{p}_h^i\right\|_{\Omega_h^i}^2\\
& + 16\sum_{i=1}^2\left\|\mathrm{H}\right\|_{\Omega_h^i}^2 + 2\nu^{-2}\left\|\boldsymbol{f}\right\|_\Omega^2 + \max_{e\in\Gamma_h^1\setminus\mathcal{I}_h^1\cup\Gamma_h^2\setminus\mathcal{I}_h^2}\left[32(C_e^{\mathrm{tr}})^2h_e^{-1} + 8\tau\right]\left\|\boldsymbol{g}\right\|_\Gamma^2\\
& + \left\|\sqrt{2}\nu^{-1/2}\delta_e^{-1/7}\tau^{-1/2}\boldsymbol{T}_2\right\|_{\mathcal{I}_h^2}^2 + \left\|(2^{-1}\delta_e^{-1/2} + \nu^{-1}\delta_e^{-1/2}h_e^{-1})\boldsymbol{T}_1\right\|_{\mathcal{I}_h^1}^2.
\end{aligned}
$$

and the result follows. □

A.2 Proof of Lemma 9

Proof. As we have done before, we will deal with these terms by expressing them in terms of the mismatch between $\mathcal{I}_h^1$ and $\mathcal{I}_h^2$.

Using (5h), (5k) and (5f), we can obtain that

$$
\mathbb{T}_{\boldsymbol{u}}^1 = \langle\sigma_h^1\boldsymbol{n}^1 + \boldsymbol{E}_{\sigma_h^1\boldsymbol{n}^2}\circ\boldsymbol{\varphi}^{-1} + \tilde{\boldsymbol{\sigma}}_h^1\circ\boldsymbol{\varphi}^{-1}, \boldsymbol{\phi}\rangle_{\mathcal{I}_h^1} + \langle\tilde{\boldsymbol{u}}_h^2, \mathrm{P}_{\boldsymbol{M}_h^1}(\nu\boldsymbol{\Phi}\boldsymbol{n}^1 - \phi\boldsymbol{n}^1)\rangle_{\mathcal{I}_h^1} + \langle\boldsymbol{T}_1, \mathrm{P}_{\boldsymbol{M}_h^1}(\nu\boldsymbol{\Phi}\boldsymbol{n}^1 - \phi\boldsymbol{n}^1)\rangle_{\mathcal{I}_h^1}.
$$

Mapping these integrals from $\mathcal{I}_h^1$ to $\mathcal{I}_h^2$,

$$
\begin{aligned}
\mathbb{T}_{\boldsymbol{u}}^1 = & \langle\tilde{\boldsymbol{u}}_h^2\circ\boldsymbol{\varphi}, \mathrm{P}_{\boldsymbol{M}_h^1}(\nu\boldsymbol{\Phi}\boldsymbol{n}^1 - \phi\boldsymbol{n}^1)\circ\boldsymbol{\varphi}\rangle_{\mathcal{I}_h^2} + \langle\tilde{\boldsymbol{\sigma}}_h^1, \boldsymbol{\phi}\circ\boldsymbol{\varphi}\rangle_{\mathcal{I}_h^2}\\
& + \langle\sigma_h^1\boldsymbol{n}^1\circ\boldsymbol{\varphi} + \boldsymbol{E}_{\sigma_h^1\boldsymbol{n}^2}, \boldsymbol{\phi}\rangle_{\mathcal{I}_h^2} + \langle\boldsymbol{T}_1, \mathrm{P}_{\boldsymbol{M}_h^1}(\nu\boldsymbol{\Phi}\boldsymbol{n}^1 - \phi\boldsymbol{n}^1)\rangle_{\mathcal{I}_h^1}.
\end{aligned}
$$

Since we're omitting hanging nodes from our analysis, we have that $\tilde{\boldsymbol{\sigma}}_h^1 \in \boldsymbol{M}_h(\mathcal{I}_h^2)$ and so we can use (5i) to obtain $\langle\tilde{\boldsymbol{\sigma}}_h^1, \boldsymbol{\phi}\circ\boldsymbol{\varphi}\rangle_{\mathcal{I}_h^2} = -\langle\widehat{\sigma}_h^2\boldsymbol{n}^2, \boldsymbol{\phi}\circ\boldsymbol{\varphi}\rangle_{\mathcal{I}_h^2} + \langle\boldsymbol{T}_2, \mathrm{P}_{\boldsymbol{M}_h^2}(\boldsymbol{\phi}\circ\boldsymbol{\varphi})\rangle_{\mathcal{I}_h^2}$. Thus, using that

$$
\langle\tilde{\boldsymbol{u}}_h^2\circ\boldsymbol{\varphi}, \mathrm{P}_{\boldsymbol{M}_h^1}(\nu\boldsymbol{\Phi}\boldsymbol{n}^1 - \phi\boldsymbol{n}^1)\circ\boldsymbol{\varphi}\rangle_{\mathcal{I}_h^2} = \langle\tilde{\boldsymbol{u}}_h^2, \mathrm{P}_{\boldsymbol{M}_h^1}(\nu\boldsymbol{\Phi}\boldsymbol{n}^1 - \phi\boldsymbol{n}^1)\rangle_{\mathcal{I}_h^1} = \langle\tilde{\boldsymbol{u}}_h^2\circ\boldsymbol{\varphi}, (\nu\boldsymbol{\Phi}\boldsymbol{n}^1 - \phi\boldsymbol{n}^1)\circ\boldsymbol{\varphi}\rangle_{\mathcal{I}_h^2},
$$

the fact that $\boldsymbol{n}^1 \circ \boldsymbol{\varphi} = -\boldsymbol{n}^2$, and adding and substracting $\langle \widehat{\boldsymbol{u}}_h^2, (\nu \boldsymbol{\Phi} \boldsymbol{n}^2 - \phi \boldsymbol{n}^2) \circ \boldsymbol{\varphi} \rangle_{\mathcal{I}_h^2}$, we have

$$\begin{aligned}\mathbb{T}_{\boldsymbol{u}}^1 = &- \langle \tilde{\boldsymbol{u}}_h^2 \circ \boldsymbol{\varphi} - \widehat{\boldsymbol{u}}_h^2, (\nu \boldsymbol{\Phi} \boldsymbol{n}^2 - \phi \boldsymbol{n}^2) \circ \boldsymbol{\varphi} \rangle_{\mathcal{I}_h^2} - \langle \widehat{\sigma}_h^2 \boldsymbol{n}^2, \boldsymbol{\phi} \circ \boldsymbol{\varphi} \rangle_{\mathcal{I}_h^2} - \langle \widehat{\boldsymbol{u}}_h^2, (\nu \boldsymbol{\Phi} \boldsymbol{n}^2 - \phi \boldsymbol{n}^2) \circ \boldsymbol{\varphi} \rangle_{\mathcal{I}_h^2} \\ &- \langle \sigma_h^1 \boldsymbol{n}^2 \circ \boldsymbol{\varphi} - \boldsymbol{E}_{\sigma_h^1 \boldsymbol{n}^2}, \boldsymbol{\phi} \rangle_{\mathcal{I}_h^2} + \langle \boldsymbol{T}_1, \mathrm{P}_{\boldsymbol{M}_h^1}(\nu \boldsymbol{\Phi} \boldsymbol{n}^1 - \phi \boldsymbol{n}^1) + \langle \boldsymbol{T}_2, \mathrm{P}_{\boldsymbol{M}_h^2}(\boldsymbol{\phi} \circ \boldsymbol{\varphi}) \rangle_{\mathcal{I}_h^2} \rangle_{\mathcal{I}_h^1}.\end{aligned}$$

Adding $\mathbb{T}_{\boldsymbol{u}}^2$, we have

$$\begin{aligned}\mathbb{T}_{\boldsymbol{u}}^1 + \mathbb{T}_{\boldsymbol{u}}^2 = &- \langle \tilde{\boldsymbol{u}}_h^2 \circ \boldsymbol{\varphi} - \widehat{\boldsymbol{u}}_h^2, (\nu \boldsymbol{\Phi} \boldsymbol{n}^2 - \phi \boldsymbol{n}^2) \circ \boldsymbol{\varphi} \rangle_{\mathcal{I}_h^2} + \langle \widehat{\sigma}_h^2 \boldsymbol{n}^2, \boldsymbol{\phi} - \boldsymbol{\phi} \circ \boldsymbol{\varphi} \rangle_{\mathcal{I}_h^2} - \langle \sigma_h^1 \boldsymbol{n}^2 \circ \boldsymbol{\varphi} - \boldsymbol{E}_{\sigma_h^1 \boldsymbol{n}^2}, \boldsymbol{\phi} \rangle_{\mathcal{I}_h^2} \\ &- \langle \boldsymbol{u}_h^2 - \widehat{\boldsymbol{u}}_h^2, (\nu \boldsymbol{\Phi} \boldsymbol{n}^2 - \phi \boldsymbol{n}^2) - (\nu \boldsymbol{\Phi} \boldsymbol{n}^2 - \phi \boldsymbol{n}^2) \circ \boldsymbol{\varphi} \rangle_{\mathcal{I}_h^2} + \langle \boldsymbol{u}_h^2, (\nu \boldsymbol{\Phi} \boldsymbol{n}^2 - \phi \boldsymbol{n}^2) - (\nu \boldsymbol{\Phi} \boldsymbol{n}^2 - \phi \boldsymbol{n}^2) \circ \boldsymbol{\varphi} \rangle_{\mathcal{I}_h^2} \\ &+ \langle \boldsymbol{T}_1, \mathrm{P}_{\boldsymbol{M}_h^1}(\nu \boldsymbol{\Phi} \boldsymbol{n}^1 - \phi \boldsymbol{n}^1) \rangle_{\mathcal{I}_h^1} + \langle \boldsymbol{T}_2, \mathrm{P}_{\boldsymbol{M}_h^2}(\boldsymbol{\phi} \circ \boldsymbol{\varphi}) \rangle_{\mathcal{I}_h^2}.\end{aligned}$$

Using (18), we decompose $\mathbb{T}_{\boldsymbol{u}}^1 + \mathbb{T}_{\boldsymbol{u}}^2 = \sum_{i=1}^9 \mathbb{S}^i$, where

$$\begin{aligned}
\mathbb{S}^1 &:= - \left\langle \tau^{1/2}(\boldsymbol{u}_h^2 - \widehat{\boldsymbol{u}}_h^2), \nu \tau^{1/2}(\boldsymbol{\phi} - \boldsymbol{\phi} \circ \boldsymbol{\phi}) + \tau^{-1/2} \left((\nu \boldsymbol{\Phi} \boldsymbol{n}^2 - \phi \boldsymbol{n}^2) - (\nu \boldsymbol{\Phi} \boldsymbol{n}^2 - \phi \boldsymbol{n}^2) \circ \boldsymbol{\varphi} \right) \right\rangle_{\mathcal{I}_h^2} \\
\mathbb{S}^2 &:= \langle |\ell|^{1/2} \boldsymbol{u}_h^2, |\ell|^{-1/2} \left((\nu \boldsymbol{\Phi} \boldsymbol{n}^2 - \phi \boldsymbol{n}^2) - (\nu \boldsymbol{\Phi} \boldsymbol{n}^2 - \phi \boldsymbol{n}^2) \circ \boldsymbol{\varphi} \right) \rangle_{\mathcal{I}_h^2} \\
\mathbb{S}^3 &:= \nu \langle |\ell|^{1/2} \Lambda_{\mathrm{L}_h^2}^2, |\ell|^{-1/2} (\boldsymbol{\phi} - \boldsymbol{\phi} \circ \boldsymbol{\varphi}) \rangle_{\mathcal{I}_h^2} \\
\mathbb{S}^4 &:= \nu \left\langle |\ell|^{-1/2} \left(\tilde{\boldsymbol{u}}_h^2 \circ \boldsymbol{\varphi} - \widehat{\boldsymbol{u}}_h^2 \right), |\ell|^{-1/2} (\boldsymbol{\phi} - \boldsymbol{\phi} \circ \boldsymbol{\varphi}) - |\ell|^{1/2} (\boldsymbol{\Phi} \circ \boldsymbol{\varphi}) \boldsymbol{n}^2 \right\rangle_{\mathcal{I}_h^2} \\
\mathbb{S}^5 &:= \left\langle |\ell|^{-1/2} \left(\tilde{\boldsymbol{u}}_h^2 \circ \boldsymbol{\varphi} - \widehat{\boldsymbol{u}}_h^2 \right), |\ell|^{1/2} (\phi \circ \boldsymbol{\varphi}) \boldsymbol{n}^2 \right\rangle_{\mathcal{I}_h^2} \\
\mathbb{S}^6 &:= - \left\langle |\ell|^{1/2} \tilde{p}_h^2 \boldsymbol{n}^2, |\ell|^{-1/2} (\boldsymbol{\phi} - \boldsymbol{\phi} \circ \boldsymbol{\varphi}) \right\rangle_{\mathcal{I}_h^2} \\
\mathbb{S}^7 &:= \left\langle \boldsymbol{E}_{\sigma_h^1 \boldsymbol{n}^2} - \sigma_h^1 \boldsymbol{n}^2 \circ \boldsymbol{\varphi}, \boldsymbol{\phi} \circ \boldsymbol{\varphi} \right\rangle_{\mathcal{I}_h^2} \\
\mathbb{S}^8 &:= \left\langle \boldsymbol{T}_1, \mathrm{P}_{\boldsymbol{M}_h^1}(\nu \boldsymbol{\Phi} \boldsymbol{n}^1 - \phi \boldsymbol{n}^1) \right\rangle_{\mathcal{I}_h^1} \\
\mathbb{S}^9 &:= \left\langle \boldsymbol{T}_2, \mathrm{P}_{\boldsymbol{M}_h^2}(\boldsymbol{\phi} \circ \boldsymbol{\varphi}) \right\rangle_{\mathcal{I}_h^2}
\end{aligned}$$

Using the Cauchy-Schwartz inequality, the estimates from Lemma 2, discrete trace inequalities and the regularity assumption (22), we have

$$\begin{aligned}
\mathbb{S}^1 &\lesssim \left\| \tau^{1/2}(\boldsymbol{u}_h^2 - \widehat{\boldsymbol{u}}_h^2) \right\|_{\mathcal{I}_h^2} \left(\tau^{1/2} \delta \|\boldsymbol{\phi}\|_{\boldsymbol{H}^2(\Omega)} + \tau^{-1/2} \delta^{1/2} \|\nu \boldsymbol{\Phi} - \phi \mathbb{I}\|_{\mathrm{H}^1(\Omega)} \right) \\
&\lesssim (\delta \tau^{1/2} + \delta^{1/2} \tau^{-1/2}) \left\| \tau^{1/2}(\boldsymbol{u}_h^2 - \widehat{\boldsymbol{u}}_h^2) \right\|_{\mathcal{I}_h^2} \|\boldsymbol{\theta}\|_{\Omega} \\
\mathbb{S}^2 &\lesssim \left\| |\ell|^{1/2} \boldsymbol{u}_h^2 \right\|_{\mathcal{I}_h^2} \|\nu \boldsymbol{\Phi} - \phi \mathbb{I}\|_{\mathrm{H}^1(\Omega)} \lesssim \max_{e \in \mathcal{I}_h^2} h_e^{-1/2} C_e^{\mathrm{tr}} \left\| \boldsymbol{u}_h^2 \right\|_{\Omega_h^2} \|\boldsymbol{\theta}\|_{\Omega_h^2} \\
\mathbb{S}^3 &\lesssim \delta^{1/2} \left\| |\ell|^{1/2} \Lambda_{\mathrm{L}_h^2}^2 \right\| \|\boldsymbol{\phi}\|_{\boldsymbol{H}^2(\Omega)} \lesssim \delta^{1/2} \max_{e \in \mathcal{I}_h^2} r_e^{3/2} C_e^{\mathrm{ext}} C_e^{\mathrm{inv}} \left\| \mathrm{L}_h^2 \right\|_{\Omega_h^2} \|\boldsymbol{\theta}\|_{\Omega} \\
\mathbb{S}^4 &\lesssim \nu \delta \left\| |\ell|^{-1/2} (\tilde{\boldsymbol{u}}_h^2 \circ \boldsymbol{\varphi} - \widehat{\boldsymbol{u}}_h^2) \right\|_{\mathcal{I}_h^2} \|\boldsymbol{\phi}\|_{\boldsymbol{H}^2(\Omega)} \lesssim \nu \delta \left\| |\ell|^{-1/2} (\tilde{\boldsymbol{u}}_h^2 \circ \boldsymbol{\varphi} - \widehat{\boldsymbol{u}}_h^2) \right\|_{\mathcal{I}_h^2} \|\boldsymbol{\theta}\|_{\Omega}
\end{aligned}$$

$$\begin{aligned}
\mathbb{S}^5 &\lesssim \delta^{1/2} \left\| |\ell|^{-1/2} (\tilde{\boldsymbol{u}}_h^2 \circ \boldsymbol{\varphi} - \widehat{\boldsymbol{u}}_h^2) \right\|_{\mathcal{I}_h^2} \|\phi \circ \boldsymbol{\varphi}\|_{\mathcal{I}_h^2} \lesssim \delta^{1/2} \left\| |\ell|^{-1/2} (\tilde{\boldsymbol{u}}_h^2 \circ \boldsymbol{\varphi} - \widehat{\boldsymbol{u}}_h^2) \right\|_{\mathcal{I}_h^2} \|\boldsymbol{\theta}\|_{\Omega} \\
\mathbb{S}^6 &\lesssim \delta^{1/2} \left\| |\ell|^{1/2} \tilde{p}_h^2 \right\|_{\mathcal{I}_h^2} \|\boldsymbol{\phi}\|_{\boldsymbol{H}^2(\Omega)} \lesssim \delta^{1/2} \max_{e \in \mathcal{I}_h^2} h_e^{-1/2} C_e^{\mathrm{tr}} \left\| \tilde{p}_h^2 \right\|_{\Omega_h^2} \|\boldsymbol{\theta}\|_{\Omega} \\
\mathbb{S}^7 &\lesssim \left\| \boldsymbol{E}_{\sigma_h^1 \boldsymbol{n}^2} - \sigma_h^1 \boldsymbol{n}^2 \circ \boldsymbol{\varphi} \right\|_{\mathcal{I}_h^2} \|\boldsymbol{\phi} \circ \boldsymbol{\varphi}\|_{\mathcal{I}_h^2} \lesssim \max_{e \in \mathcal{I}_h^2} (\delta_e h_e^{-3/2} C_e^{\mathrm{ext}}) \left\| \nu \mathrm{L}_h^1 - \tilde{p}_h^1 \mathbb{I} \right\|_{\Omega_h^1} \|\boldsymbol{\theta}\|_{\Omega} \\
\mathbb{S}^8 &\lesssim \|\boldsymbol{T}_1\|_{\mathcal{I}_h^1} \|\nu \boldsymbol{\Phi} - \phi \mathbb{I}\|_{\mathcal{I}_h^1} \lesssim \|\boldsymbol{T}_1\|_{\mathcal{I}_h^1} \|\boldsymbol{\theta}\|_{\Omega} \\
\mathbb{S}^9 &\lesssim \|\boldsymbol{T}_2\|_{\mathcal{I}_h^2} \|\boldsymbol{\phi} \circ \boldsymbol{\varphi}\|_{\mathcal{I}_h^2} \lesssim \|\boldsymbol{T}_2\|_{\mathcal{I}_h^2} \|\boldsymbol{\theta}\|_{\Omega}.
\end{aligned}$$

and (24) follows. □

References

[1] R. Araya, M. Solano, and P. Vega, *Analysis of an adaptive HDG method for the Brinkman problem*, IMA Journal of Numerical Analysis, 39 (2018), pp. 1502–1528.

[2] G. Bfer, *An isoparametric joint/interface element for finite element analysis*, International Journal for Numerical Methods in Engineering, 21 (1985), pp. 585–600.

[3] J. H. Bramble and J. T. King, *A robust finite element method for nonhomogeneous Dirichlet problems in domains with curved boundaries*, Mathematics of Computation, 63 (1994), pp. 1–17.

[4] ——, *A finite element method for interface problems in domains with smooth boundaries and interfaces*, Advances in Computational Mathematics, 6 (1996), pp. 109–138.

[5] E. Burman, S. Claus, P. Hansbo, M. G. Larson, and A. Massing, *Cutfem: Discretizing geometry and partial differential equations*, International Journal for Numerical Methods in Engineering, 104 (2015), pp. 472–501.

[6] Burman, Erik and Hansbo, Peter, *Fictitious domain methods using cut elements: III. A stabilized Nitsche method for Stokes' problem*, ESAIM: M2AN, 48 (2014), pp. 859–874.

[7] J. Carrero, B. Cockburn, and D. Schötzau, *Hybridized globally divergence-free LDG methods. Part i: The Stokes problem*, Mathematics of Computation, 75 (2005), pp. 533–564.

[8] A. Cesmelioglu, B. Cockburn, and W. Qiu, *Analysis of a hybridizable discontinuous Galerkin method for the steady-state incompressible Navier-Stokes equations*, Mathematics of Computation, 86 (2016), pp. 1643–1670.

[9] Y. Chen and B. Cockburn, *Analysis of variable-degree HDG methods for convection-diffusion equations. Part I: general nonconforming meshes*, IMA Journal of Numerical Analysis, 32 (2012), pp. 1267–1293.

[10] Y. Chen and B. Cockburn, *Analysis of variable-degree HDG methods for convection-diffusion equations. part II: Semimatching nonconforming meshes*, Mathematics of Computation, 83 (2013), pp. 87–111.

[11] J. Cheung, M. Gunzburger, P. Bochev, and M. Perego, *An optimally convergent higher-order finite element coupling method for interface and domain decomposition problems*, Results in Applied Mathematics, 6 (2020), p. 100094.

[12] J. Cheung, M. Perego, P. Bochev, and M. Gunzburger, *Optimally accurate higher-order finite element methods for polytopial approximations of domains with smooth boundaries*, Mathematics of Computation, 88 (2019), pp. 2187–2219.

[13] B. Cockburn and J. Gopalakrishnan, *Incompressible finite elements via hybridization. Part I: The Stokes system in two space dimensions*, SIAM Journal on Numerical Analysis, 43 (2005), pp. 1627–1650.

[14] ——, *Incompressible finite elements via hybridization. Part II: The Stokes system in three space dimensions*, SIAM Journal on Numerical Analysis, 43 (2005), pp. 1651–1672.

[15] ——, *The derivation of Hybridizable Discontinuous Galerkin methods for Stokes flow*, SIAM Journal on Numerical Analysis, 47 (2009), pp. 1092–1125.

[16] B. Cockburn, J. Gopalakrishnan, and R. Lazarov, *Unified hybridization of discontinuous Galerkin, mixed, and continuous Galerkin methods for second order elliptic problems*, SIAM Journal on Numerical Analysis, 47 (2009), pp. 1319–1365.

[17] B. Cockburn, J. Gopalakrishnan, N. Nguyen, J. Peraire, and F.-J. Sayas, *Analysis of HDG methods for Stokes flow.*, Math. Comput., 80 (2011), pp. 723–760.

[18] B. Cockburn, D. Gupta, and F. Reitich, *Boundary-conforming discontinuous Galerkin methods via extensions from subdomains*, J. Sci. Comput., 42 (2010), pp. 144–184.

[19] B. Cockburn, N. C. Nguyen, and J. Peraire, *A comparison of HDG methods for Stokes flow*, Journal of Scientific Computing, 45 (2010), pp. 215–237.

[20] B. Cockburn, W. Qiu, and M. Solano, *A priori error analysis for HDG methods using extensions from subdomains to achieve boundary conformity*, Mathematics of Computation, 83 (2014).

[21] B. Cockburn and F.-J. Sayas, *Divergence-conforming HDG methods for Stokes flows*, Mathematics of Computation, 83 (2014), pp. 1571–1598.

[22] B. Cockburn, F.-J. Sayas, and M. Solano, *Coupling at a distance HDG and BEM*, SIAM Journal on Scientific Computing, 34 (2012), pp. A28–A47.

[23] B. Cockburn and M. Solano, *Solving Dirichlet boundary-value problems on curved domains by extensions from subdomains*, SIAM J. Sci. Comput., 34 (2012), pp. A497–A519.

[24] ——, *Solving convection-diffusion problems on curved domains by extensions from subdomains*, J. Sci. Comput., 59 (2014), pp. 512–543.

[25] M. Dauge, *Stationary Stokes and Navier–Stokes systems on two- or three-dimensional domains with corners. Part I. Linearized equations*, SIAM Journal on Mathematical Analysis, 20 (1989), pp. 74–97.

[26] M. Dittmann, S. Schuss, B. Wohlmuth, and C. Hesch, *Weak c^n coupling for multipatch isogeometric analysis in solid mechanics*, International Journal for Numerical Methods in Engineering, 118 (2019), pp. 678–699.

[27] C. R. Dohrmann, S. W. Key, and M. W. Heinstein, *A method for connecting dissimilar finite element meshes in two dimensions*, International Journal for Numerical Methods in Engineering, 48 (2000), pp. 655–678.

[28] B. Flemisch, J. Melenk, and B. Wohlmuth, *Mortar methods with curved interfaces*, Applied Numerical Mathematics, 54 (2005), pp. 339–361. Selected papers from the 16th Chemnitz Finite Element Symposium 2003.

[29] B. Flemisch, M. A. Puso, and B. I. Wohlmuth, *A new dual mortar method for curved interfaces: 2d elasticity*, International Journal for Numerical Methods in Engineering, 63 (2005), pp. 813–832.

[30] G. Fu, Y. Jin, and W. Qiu, *Parameter-free superconvergent H(div)-conforming HDG methods for the Brinkman equations*, IMA Journal of Numerical Analysis, 39 (2018), pp. 957–982.

[31] G. N. Gatica and F. A. Sequeira, *Analysis of an augmented HDG method for a class of quasi-Newtonian Stokes flows*, Journal of Scientific Computing, 65 (2015), pp. 1270–1308.

[32] ——, *A priori and a posteriori error analyses of an augmented HDG method for a class of quasi-Newtonian Stokes flows*, Journal of Scientific Computing, 69 (2016), pp. 1192–1250.

[33] ——, *Analysis of the HDG method for the Stokes-Darcy coupling*, Numerical Methods for Partial Differential Equations, 33 (2017), pp. 885–917.

[34] L. N. T. Huynh, N. C. Nguyen, J. Peraire, and B. C. Khoo, *A high-order hybridizable discontinuous Galerkin method for elliptic interface problems*, International Journal for Numerical Methods in Engineering, 93 (2013), pp. 183–200.

[35] R. Kellogg and J. Osborn, *A regularity result for the Stokes problem in a convex polygon*, Journal of Functional Analysis, 21 (1976), pp. 397–431.

[36] Y. Mori, *Convergence proof of the velocity field for a Stokes flow immersed boundary method*, Commun. Pure Appl. Math., 61 (2008), pp. 1213–1263.

[37] N. Nguyen, J. Peraire, and B. Cockburn, *A hybridizable discontinuous Galerkin method for Stokes flow*, Computer Methods in Applied Mechanics and Engineering, 199 (2010), pp. 582–597.

[38] ——, *An implicit high-order hybridizable discontinuous Galerkin method for the incompressible Navier–Stokes equations*, Journal of Computational Physics, 230 (2011), pp. 1147–1170.

[39] D. A. D. Pietro and A. Ern, *Mathematical Aspects of Discontinuous Galerkin Methods*, Springer Berlin Heidelberg, 2012.

[40] W. Qiu and K. Shi, *A superconvergent HDG method for the incompressible Navier–Stokes equations on general polyhedral meshes*, IMA Journal of Numerical Analysis, 36 (2016), pp. 1943–1967.

[41] W. Qiu, M. Solano, and P. Vega, *A high order HDG method for curved-interface problems via approximations from straight triangulations*, J. Sci. Comput., 69 (2016), pp. 1384–1407.

[42] S. Rhebergen and G. N. Wells, *A hybridizable discontinuous Galerkin method for the Navier–Stokes equations with pointwise divergence-free velocity field*, (2017).

[43] M. Solano, S. Terrana, N.-C. Nguyen, and J. Peraire, *An HDG method for dissimilar meshes*, IMA Journal of Numerical Analysis, (2021). drab059.

[44] M. Solano and F. Vargas, *A high order HDG method for Stokes flow in curved domains*, Journal of Scientific Computing, 79 (2019), pp. 1505–1533.

[45] M. Solano and F. Vargas M., *An unfitted hdg method for oseen equations*, Journal of Computational and Applied Mathematics, 399 (2022), p. 113721.

[46] O. Steinbach, *A natural domain decomposition method with non-matching grids*, Applied Numerical Mathematics, 54 (2005), pp. 362–377.

[47] B. Wang and B. C. Khoo, *Hybridizable discontinuous Galerkin method (HDG) for Stokes interface flow*, Journal of Computational Physics, 247 (2013), pp. 262–278.